กลไกการตกผลึกของเซอร์โคเนียภายใต้ภาวะไกลโคเทอร์มอลและผลของซิลิกาต่อความเสถียรทางความร้อนและพื้นที่ผิวของเซอร์โคเนียที่ดัดแปร

น.ส. ศิรรัตน์ คงวุฒิติ

วิทยานิพนธ์นี้เป็นส่วนหนึ่งของการศึกษาตามหลักสูตรปริญญาวิศวกรรมศาสตรดุษฎีบัณฑิต

สาขาวิชาวิศวกรรมเคมี ภาควิชาวิศวกรรมเคมี

คณะวิศวกรรมศาสตร์ จุฬาลงกรณ์มหาวิทยาลัย

ปีการศึกษา 2545

ISBN 974-17-2679-1

CRYSTALLIZATION MECHANISM OF ZIRCONIA UNDER THE GLYCOTHERMAL CONDITION AND THE EFFECT OF SILICA ON THE THERMAL STABILITY AND SURFACE AREA OF MODIFIED ZIRCONIA

Miss Sirarat Kongwudthiti

A Dissertation Submitted in Partial Fulfillment of the Requirements
for the Degree of Doctor of Engineering in Chemical Engineering
Department of Chemical Engineering
Chulalongkorn University
Academic Year 2002

ISBN 974-17-2679-1

Thesis Title	CRYSTALLIZATION MECHANISM OF ZIRCONIA UNDER THE GLYCOTHERMAL CONDITION AND THE EFFECT OF SILICA ON THE THERMAL STABILITY AND SURFACE AREA OF MODIFIED ZIRCONIA
By	Miss Sirarat Kongwudthiti
Field of Study	Chemical Engineering
Thesis Advisor	Professor Piyasan Praserthdam, Dr.Ing.
Thesis Co-advisor	Professor Masashi Inoue, D.Eng.

Accepted by the Faculty of Engineering, Chulalongkorn University in Partial Fulfillment of the Requirements for the Doctor's Degree

..... Dean of Faculty of Engineering
(Professor Somsak Panyakeow, D.Eng.)

THESIS COMMITTEE

..... Chairman
(Associate Professor Ura Pancharoen, D.Eng.Sc.)
..... Thesis Advisor
(Professor Piyasan Praserthdam, Dr.Ing.)
..... Thesis Co-advisor
(Professor Masashi Inoue, D.Eng.)
..... Member
(Suphot Phatanasri, D.Eng.)
..... Member
(Waraporn Tanakulrungsank, D.Eng.)
..... Member
(Assistant Professor Siriporn Damrongsakkul, Ph.D.)

ศิรรัตน์ คงวุฒิติ : กลไกการตกผลึกของเซอร์โคเนียภายใต้ภาวะไกลโคเทอร์มอลและผลของซิลิกาต่อความเสถียรทางความร้อนและพื้นที่ผิวของเซอร์โคเนียที่ดัดแปร (CRYSTALLIZATION MECHANISM OF ZIRCONIA UNDER THE GLYCOTHERMAL CONDITION AND THE EFFECT OF SILICA ON THE THERMAL STABILITY AND SURFACE AREA OF MODIFIED ZIRCONIA) อ.ที่ปรึกษา : ศ.ดร.ปิยะสาร ประเสริฐธรรม, อ.ที่ปรึกษาร่วม : PROFESSOR MASASHI INOUE, 115 หน้า, ISBN 974-17-2679-1

การศึกษากลไกการตกผลึกของเซอร์โคเนียภายใต้ภาวะไกลโคเทอร์มอล โดยเซอร์โคเนียที่เตรียมขึ้นจากปฏิกิริยาของเซอร์โคเนียมเตตระนอร์มอลโพรพอกไซด์ในสารละลายไกลคอล พบว่า รูปแบบการตกผลึกขึ้นกับจำนวนคาร์บอนของสารละลายไกลคอลที่ใช้ ปฏิกิริยาที่ใช้เอทิลีนไกลคอลให้ผลิตภัณฑ์เป็นเฟสอสัณฐาน (amorphous) การใช้ 1,3-โพรเพนไดออลให้ผลิตภัณฑ์เป็นสารประกอบไกลคอลที่เป็นผลึกแต่ไม่พบผลึกของเซอร์โคเนียถึงแม้ว่าปฏิกิริยาจะเกิดที่อุณหภูมิ 300 องศาเซลเซียส กรณีที่ใช้ 1,4-บิวเทนไดออลพบว่าในตอนเริ่มต้นเกิดสารประกอบไกลคอลที่เป็นผลึกขึ้นก่อนแล้วจึงเกิดการเปลี่ยนเป็นเฟสที่ไร้รูปร่าง หลังจากนั้นเตตระโกนอลเซอร์โคเนียจึงเกิดผลึกจากเฟสที่ไร้รูปร่างในสภาวะของแข็ง (solid state transformation) แต่การสังเคราะห์ใน 1,5-เพนเทนไดออลและ1,6-เฮกเซนไดออล พบว่า ผลึกเซอร์โคเนียเกิดจากสารประกอบที่ละลายได้ ซึ่งก็คือ ไกลคอกไซด์ (glycoxides)

การศึกษาผลของภาวะในการสังเคราะห์ต่อสมบัติของเซอร์โคเนีย ซึ่งได้แก่ ความเข้มข้นของเซอร์โคเนียมนอร์มอลโพรพอกไซด์และกระบวนการทำให้แห้ง พบว่า กรณีที่ใช้ 1,4-บิวเทนไดออล ขนาดผลึก ขนาดอนุภาคทรงกลมของเซอร์โคเนียและพื้นที่ผิว BET เพิ่มขึ้นเมื่อเพิ่มความเข้มข้นของเซอร์โคเนียมนอร์มอลโพรพอกไซด์ และการดึงไกลคอลออกที่อุณหภูมิของปฏิกิริยาไม่ทำให้โครงสร้างรูพรุนของอนุภาคเปลี่ยนแปลงเนื่องจากการเกาะกันระหว่างอนุภาคเกิดขึ้นระหว่างการเกิดปฏิกริยา แต่ในทางตรงกันข้าม การเปลี่ยนแปลงความเข้มข้นของเซอร์โคเนียมนอร์มอลโพรพอกไซด์ไม่ทำให้สมบัติทางกายภาพของเซอร์โคเนียที่สังเคราะห์ได้ใน 1,5–เพนเทนไดออล เปลี่ยนแปลงไป แต่การดึงไกลคอลออกที่อุณหภูมิของปฏิกิริยาโดยการระเหยที่จุดเดือดช่วยปรับปรุงโครงสร้างรูพรุนของอนุภาคเนื่องจากการลดลงของการเกาะรวมตัวกันระหว่างอนุภาคขนาดเล็กในขั้นตอนการทำให้แห้ง

การศึกษาผลของซิลิกาต่อพื้นที่ผิว BET และความเสถียรทางความร้อน โดยเซอร์โคเนียที่ดัดแปรด้วยซิลิกาที่อัตราส่วนซิลิกอนต่อเซอร์โคเนียมเป็น 0.01 ถึง 0.15 ซึ่งสังเคราะห์ขึ้นจากปฏิกิริยาของเซอร์โคเนียมนอร์มอลโพรพอกไซด์และเตตระเอทิลออร์โทซิลิเกตใน 1,4-บิวเทนไดออล พบว่า เมื่อเพิ่มปริมาณเตตระเอทิลออร์โทซิลิเกตจะได้ผลิตภัณฑ์ที่มีพื้นที่ผิว BET เพิ่มขึ้นอย่างมากและอุณหภูมิของการเปลี่ยนเฟสจากเตตระโกนอลไปเป็นโมโนคลินิกเพิ่มสูงขึ้น การวิเคราะห์ด้วยเครื่องอินฟราเรดสเปกโตรสโครปีบ่งชี้การมีอยู่ของพันธะ Si-O-Zr ในสารตัวอย่างซึ่งจะมีผลต่อการช่วยลดอัตราการเติบโตของขนาดผลึกในระหว่างกระบวนการเผา

ภาควิชา……..วิศวกรรมเคมี……. ลายมือชื่อนิสิต…….

สาขาวิชา…….วิศวกรรมเคมี……. ลายมือชื่ออาจารย์ที่ปรึกษา……

ปีการศึกษา…..2545……. ลายมือชื่ออาจารย์ที่ปรึกษาร่วม……..

4271821921 : MAJOR CHEMICAL ENGINEERING
KEY WORD: ZIRCONIA / SILICA-MODIFIED ZIRCONIA / GLYCOTHERMAL METHOD / CRYSTALLIZATION

SIRARAT KONGWUDTHITI: CRYSTALLIZATION MECHANISM OF ZIRCONIA UNDER THE GLYCOTHERMAL CONDITION AND THE EFFECT OF SILICA ON THE THERMAL STABILITY AND SURFACE AREA OF MODIFIED ZIRCONIA. THESIS ADVISOR: PROFESSOR PIYASAN PRASERTHDAM, Dr.Ing., THESIS CO-ADVISOR: PROFESSOR MASASHI INOUE, D.Eng. 115 pp. ISBN 974-17-2679-1

To study the crystallization mechanism of zirconia under the glycothermal condition, zirconia powders were produced by the reaction of zirconium tetra *n*-propoxide (ZNP) in glycol. It was found that the crystallization behavior depended on the carbon number of glycol used. Amorphous product was obtained for the reaction in ethylene glycol. The use of 1,3-propanediol resulted in crystalline glycol complex and zirconia was not formed even by the reaction at 300^{o}C. When 1,4-butanediol was employed, crystalline glycol complex was initially formed, which then transformed to amorphous phase and the tetragonal zirconia subsequently crystallized from the amorphous phase through the solid-state transformation mechanism. However, the formation of crystalline zirconia in 1,5-pentanediol and 1,6-hexanediol proceeded via a soluble intermediate (i.e., glycoxides).

Synthesis conditions, i.e., ZNP concentration and drying method, affected the properties of zirconia powders. For the use of 1,4-butanediol, crystallite size, microsphere particle size of zirconia and BET surface area increased with increasing the ZNP concentration. Glycol removal at reaction temperature did not change the pore system of the powders because the aggregation of primary particles probably occurred during the reaction process. In contrast, physical properties of zirconia obtained in 1,5-pentanediol were not affected by ZNP concentration, whereas the pore system of the powders was improved when the glycol was removed from the autoclave by flash evaporation due to the reduction of aggregation among the ultrafine particles during drying.

The effect of silica on the BET surface area of tetragonal zirconia and its thermal stability was studied. Silica-modified zirconia with the Si/Zr ratios of 0.01-0.15 were prepared by the reaction of ZNP and tetraethyl orthosilicate (TEOS) in 1,4-butanediol. With increasing TEOS amount, the BET surface area drastically increased and tetragonal-to-monoclinic transformation temperature shifted toward higher temperatures. Infrared spectroscopy indicated the presence of Si-O-Zr bonds in the samples, resulting in the retardation of crystallite growth during calcination.

Department ... Chemical Engineering… Student's signature……..
Field of study...Chemical Engineering… Advisor's signature……..
Academic year…….2002…… Co-advisor's signature…….

ACKNOWLEDGEMENTS

The author would like to express her greatest gratitude to her advisor, Professor Piyasan Praserthdam, for his invaluable guidance and suggestion throughout the study.

Her sincere gratitude is expressed to Professor Masashi Inoue, her co-advisor, for his precious suggestion and kind supervision during her doing research in Japan. Her grateful thanks are also given to Dr. Shinji Iwamoto for his kind instruction, and all members in Professor Inoue's laboratory for their help and good relationships.

The author is grateful to Associate Professor Ura Pancharoen as the chairman, Dr. Suphot Patanasri, Dr. Waraporn Tanakulrungsank and Assistant Professor Sirriporn Damrongsakkul, members of the thesis committee for their kind cooperation.

Best regards are expressed to all her friends in the laboratory for their encouragement. Her deep appreciation is also given to Mr. Sarit Chotchakornpant for being so supportive with sincerity throughout the study.

The author acknowledges to The Thailand Research Fund (TRF) for the financial support of this doctoral course.

Finally, she also would like to dedicate this thesis to her parents for their worthy support at all times.

CONTENTS

PAGE

CONTENTS (CONT.)

PAGE

LIST OF TABLES

LIST OF FIGURES

FIGURE PAGE

LIST OF FIGURES (CONT.)

FIGURE PAGE

LIST OF FIGURES (CONT.)

FIGURE PAGE

LIST OF FIGURES (CONT.)

FIGURE PAGE

LIST OF FIGURES (CONT.)

FIGURE PAGE

LIST OF FIGURES (CONT.)

FIGURE PAGE

CHAPTER I

INTRODUCTION

During recent years zirconia has attracted much attention from researchers in the field of heterogeneous catalysis as a support material as well as a catalyst. Generally, the interest in zirconia as a support materials can be ascribed to at least one of the following three properties: (i) as a carrier, it gives rise to a unique kind of interaction between the active phase and support, this being manifested in both the catalytic activity and the selectivity pattern of the system (Prokhorenko *et al.*, 1988 and Fujii *et al.*, 1987); (ii) it can be more chemically inert than the classical supports (e.g., γ-alumina or silica) (Gavalas *et al.*, 1984); and (iii) it is the only single-metal oxide which may possess four chemical properties, namely acidity or basicity as well as reducing or oxidizing ability (Tanabe, 1985).

Zirconia as a support showed promising results in environmental catalysis, such as CO_2 hydrogenation (Bitter *et al.*, 1997), nitrous oxide decomposition (Miller and Grassian, 1995) and CO oxidation (Dow and Huang, 1994). Various reactions such as hydrodesulphurization, methanol synthesis, and the Fischer-Tropsch reaction to give higher hydrocarbons were reported to show higher activity and selectivity with zirconia than with conventional supports (Chuah, 1999). For example, copper supported on zirconia gives a higher yield of methanol from CO_2 and H_2 than oxides such as alumina, silica, titania, chromium oxide, and zinc oxide (Amenomiya, 1987). Chromium oxide supported on zirconia has very high activity for CO oxidation by molecular oxygen and nitrous oxide. Compared with traditional supports, zirconia-supported nickel is a good catalyst for Fischer-Tropsch synthesis and it exhibits a greater selectivity for higher hydrocarbons, especially olefins (Bruce and Mathews, 1982). Zirconia can also function as a catalyst by itself. For instance, it catalyzes the hydrogenation of CO (He and Ekerdt, 1984 and Johnson *et al.*, 1990), olefin (Domen *et al.*, 1992) and dienes (Nakano *et al.*, 1983).

It has become well established that the performance of a heterogeneous catalyst not only depends on the intrinsic catalytic activity of the components but also on its texture and stability. The important criterion that any catalytic support must meet is high accessible surface area with well-developed porous texture, good thermal and chemical stabilities and high strength that remain stable under process conditions. Mesoporosity (pore radius of 20-500 Å) is preferable for various applications since it provides a balance between good diffusion rates of reactants and useful in-pore effects. Common supports like silica and alumina can be prepared with surface areas of 100-600 m^2/g. Unfortunately, commercially available zirconia has surface area typically less than 50 m^2/g. Moreover, silica and alumina maintained their high surface area up to temperature around 1000^oC while the surface area of zirconia decreased rapidly when the material was heated above 500^oC (Chuah *et al.*, 1998). One of the reasons for the instability of zirconia materials is the polymorphism, which gives rise to phase transitions. It was reported that stability of tetragonal phase of zirconia is important for applications as a catalyst or catalyst support. Centi *et al.* (1996) studied the decomposition of N_2O over copper/zirconia catalysts. The tetragonal form was found to be twice as active as the monoclinic zirconia. Therefore, zirconia with the tetragonal structure is preferred for the reactions. Although tetragonal to monoclinic transformation inevitably occurred, higher transformation temperature is required for the zirconia catalysts.

The factor controlling the textural properties of the materials is the preparation method. In order to obtain the useful zirconia, extensive preparation studies have been made by many researchers. The thermal stability of the predominantly tetragonal zirconia sample prepared by a gel precipitation method was not satisfactory. The initial surface area decreased and particle sizes increased abruptly at above 450^oC due to crystallization of the monoclinic and/or tetragonal phases, phase transformation (from the tetragonal into the monoclinic phase) and inter-crystallite sintering (i.e., agglomeration, neck-formation and growth) (Mercera *et al.*, 1990). In addition, many other preparation methods such as gel-precipitation of various zirconium salts at specific pH followed by calcination, hydrothermal treatment of amorphous hydrous zirconia employing different mineralizers as well as refluxing either $ZrOCl_2$ solutions or amorphous hydrous zirconia in different media, only yield monoclinic zirconia

having a relatively low surface area (Yamaguchi and Tanabe, 1986; Srinivasan *et al.*, 1988; Nishisawa *et al.*, 1982 and Tani *et al.*, 1981).

Several approaches have been developed to improve the textural properties and thermal stability of zirconia. These methods include doping zirconia with rare earth ions (Mercera *et al.*, 1991: 71, 78; Morterra *et al.*, 1994; Frankin *et al.*, 1991) and the other transition metal ions (Valigi *et al.*, 1996 and Beck *et al.*, 1990). The roles of anions such as carbonates, sulfates and heptamolybdates on the stabilization of surface areas have also reported (Norman *et al.*, 1994; Afanasiev *et al.*, 1994 and R. Srinivasan *et al.*, 1991). Depending on the dopants, an improvement in the thermal stability up to 900^{o}C was observed. It has been noted that the amount of dopants needed to markedly improve the thermal stability will be in the range of 20-50%. However, for many catalytic purposes, the incorporation of some of these oxides or dopants may not be desired as they may lead to side reactions or reduced activity.

The modification of zirconia by the stable oxide such as silica has been reported to improve the textural and thermal stabilities of zirconia. The surface area of zirconia is enlarged by the presence of silica in the sol-gel process (Soled and Mcvicker, 1992 and Miller *et al.*, 1994). Zirconia-silica mixed oxides were employed for various acid-catalyzed reactions such as cyclohexanol dehydrogenation (Bosman et al., 1994), dehydrogenation and dealkylation reactions (Sohn and Jang, 1991), CO hydrogenation to isobutene (Feng *et al.*, 1994), and alkene isomerization (Contescu *et. al.*, 1995). Most of the previous works focused on the preparation of ZrO_2-SiO_2 binary oxides with high SiO_2 content (>30%). In this study, we will report the stabilization of the ZrO_2 with low SiO_2 molar content (as low as 1%).

Recently, Inoue found that the thermal treatment of zirconium alkoxides in organic solvents like glycols (i.e., glycothermal method) directly yielded tetragonal zirconia having a large surface area and a fairly high thermal stability. In addition, the glycothermal reaction does not require any precaution for handling alkoxides, and reproducible results are obtained even without the purification of the starting materials (Inoue *et al.*, 1993 and Inoue *et al.*, 2000: 65). Previous studies on the use of organic media have demonstrated that various oxides such as yttrium aluminum garnet, lithium niobate and zinc aluminate can be directly crystallized by the

glycothermal reaction (Inoue *et al.*, 1995:121; 1995:226; 1998; 2000:79; and Iwamoto *et al.*, 2000). The observation of these products revealed that each particle, although some of the products showed apparently polycrystalline outline, was a single crystal. The glycothermal reaction of zirconium alkoxides was also examined. However, it was found that the product was composed of spherical secondary particles made of primary nanocrystals. This result shows a sharp contrast against that for other glycothermal products such as rare earth gallium garnets (Inoue *et al.*, 2000:65 and 2000:29). Therefore, it was proposed that the crystallization mechanism of zirconia under glycothermal method is different from that of other compounds.

In this research, the study will focus on the crystallization mechanism of zirconia under glycothermal method and the effect of synthesis parameters (i.e., drying condition, the concentration of starting solution) on the properties of zirconia. The effect of the addition of silica on the surface area and the thermal stability of modified zirconia derived from the glycothermal method was also investigated.

The present study is arranged as follows:

Chapter II presents literature reviews of the previous works related to this research.

Chapter III explains the basic theory about zirconia such as the general properties of zirconia and the various preparation methods to obtain the ultrafine zirconia.

Chapter IV shows the experimental equipment and systems, and the preparation method of zirconia by the glycothermal method.

Chapter V exhibits the experimental results.

In the last chapter, the overall conclusions of this research are given.

Finally, examples for calculation of the required amount of the starting materials and crystallite size are included in appendices at the end of this thesis.

CHAPTER II

LITERATURE REVIEWS

There have been several studies on the hydrothermal synthesis of zirconia. The hydrothermal method is a very useful for preparing nanosized zirconia powders and the formation of zirconia under hydrothermal conditions was exclusively investigated. Mitsuhashi *et al.* (1974) found that tetragonal zirconia could not be obtained hydrothermally as the only phase; a small amount of monoclinic zirconia was always present. For the crystallization of zirconia under hydrothermal reaction, the crystallization of monoclinic zirconia proceeded by dissolution/precipitation and structural rearrangement. Since the interatomic Zr-Zr and Zr-O distances in the amorphous products were similar to the corresponding ones in the tetragonal structure, the formation of tetragonal zirconia occurred as a result of the structural similarity between the amorphous and tetragonal forms (i.e., topotactic crystallization on nuclei in the amorphous zirconia), and the particle size and anionic impurities were not primary factors in stabilization of tetragonal zirconia under hydrothermal conditions (Tani *et al.*, 1981; Tani *et al.*, 1983 and Livage *et al.*, 1968).

Osendi *et al.* (1985) believed that the nucleation of the tetragonal zirconia was associated with lattice defects and anionic vacancies, which are produced upon crystallization. The pH of the medium used in the hydrothermal reaction was found to be the factor controlling the crystallization and a model of m-ZrO_2 and t-ZrO_2 crystallization was proposed. According to this model, there are three control regimes for the crystallization of ZrO_2: At low pH the solubility is high, so that the hydrothermal crystallization occurred via dissolution/precipitation mechanism producing m-ZrO_2. In a neutral or mild acidic medium, the solubility is very low, so that the crystallization occurred in situ by structural (topotactic) rearrangement of zirconium hydroxide, and the product in this region will be predominantly t-ZrO_2. At high pH the solubility of zirconium hydroxide is very high; yet, the obtained product is predominantly metastable t-ZrO_2. The topotactic crystallization prevails at high pH, because of a higher energy state of the obtained zirconium hydroxide gel (Denkewicz *et al.*, 1990). It was reported later that the strong base OH^- favored the formation of

Zr-O-Zr bridges between the non-bridging structural hydroxyl groups present in the gel so favouring its arrangement, its nucleation and its consequent crystallization (Dell *et al.*, 1999).

Miroslaw *et al.* (1995) reported that the ZrO_2 crystallites changes with the time of the hydrothermal process performed in the two environments, water and water solution of NaOH. The rates of these changes are much higher in the NaOH solution. Two mechanisms of crystal growth seem to operate: coalescence of the primary crystallites in a highly oriented way, and filling the contacts and faceting of the particles by the dissolution-precipitation process.

The influences of mineralizers on the morphology of hydrothermally synthesized zirconia has been investigated. Mottet *et al.* (1992) demonstrated that the morphology of zirconia crystallized from zirconium oxychloride can be controlled by the synthesis conditions and type of additives present in the hydrothermal medium. For given synthesis conditions, isometric, platelike, and elongated morphologies were obtained by varying the additives present in the hydrothermal medium. Both spherulitic and isolated textures were encountered with H_2SO_4. The structure of Zr soluble complexes is different when the H_2SO_4 was used as an additive. The sulfate complexes form the polymerized units with bridging sulfate groups, structurally close to the basic zirconium sulfates. The presence of such complexes may change the viscosity of the hydrothermal fluid, hence promoting spherulitic growth. Isometric zirconia crystallized in NaOH or Na_2CO_3. They proposed the growth mechanism of isometric zirconia crystal as follows: (1) dissolution of the starting zirconium oxychloride, (2) transport of Zr in the hydrothermal fluid, (3) nucleation of zirconia followed by isotropic growth. Pyda *et al.* (1991) found that zirconia powders crystallized in an aqueous solution of Na, K and Li hydroxides show elongated particles of much larger sizes than those obtained in pure water or an aqueous solution of Na, K or Li chloride. The shapes of the latter particles are isometric. They suggested that sticking of the elementary units in an ordered manner is plausible mechanism of the elongated particle growth and the dissolution-precipitation process is responsible for filling up the grooves between the sticking crystallites.

Comparison studies of different synthesis processes have been done by Hu *et al.* (1999). Forced hydrolysis of $ZrOCl_2$ in aqueous solution yielded nearly cubic-shaped, nanosize zirconia particles with a narrow distribution (~ 50 nm average size). Each of particles was an aggregate of many needle-like, small primary particles measuring ~3 nm (rod diameter) by 5 nm (rod length). As the initial Zr concentration was increased, the particle size and hydrolysis reaction kinetics increased and the shape of particles became more cubelike. In contrast, hydrous zirconia particles obtained from the homogeneous precipitation of $ZrOCl_2$ in water-isopropyl alcohol solutions are perfectly dispersed microspheres, which sizes ranging from nanometers to a few micrometers. The lower the initial zirconium concentration in the solution, the smaller the microsphere size. Since the presence of the isopropyl alcohol reduced the dielectric constant of the solution, the solubility of the zirconium species becomes lower, and therefore particle formation could be attributed to the salting-out phenomenon instead of hydrolytic condensation.

Matsui and Ohgai (1997) investigated the effects of H^+ and Cl^- ion concentrations on the formation of secondary particles. Hydrous-zirconia particles were produced by the hydrolysis of various $ZrOCl_2$ solutions. The average secondary particle size of hydrous zirconia increased as the H^+ ion concentration increased, attaining a maximum of 200 nm. Further increases in the H^+ ion concentration then caused a decrease in the average particle size. The primary particle size of hydrous zirconia, under a constant $ZrOCl_2$ concentration, decreased monotonously with increasing Cl^- ion concentration (Matsui and Ohgai, 2000). The formation behavior of primary particles is explained by the interference action on crystal growth of the Cl^- ions attracted to the particle surface. On the contrary, the secondary particle size increased monotonously with increasing Cl^- ions concentration. The dependence of secondary particle size on the Cl^- ion concentration can be explained qualitatively using homocoagulation and heterocoagulation models

There have been recent reports on the effect of drying agent (alcohol versus carbon dioxide) on the textural properties and crystallization behavior of silica and titania aerogel (Beghi *et al.*, 1992). The removal of solvent from a gel by supercritical drying is an example of an effective approach in preserving the gel structure. The resultant products, known as aerogel, are of interest as catalysts because of their open

pore structure and high surface area. Typically, drying is done at high temperature because alcohols, which have high critical temperatures, are used as solvents in sol-gel chemistry involving metal alkoxides. However, drying at a lower temperature is possible by displacing the alcohol with, for example, supercritical carbon dioxide.

Brodsky and Ko (1995) prepared aerogel of zirconia, niobia and titania-silica by supercritical drying of the corresponding alcogels with carbon dioxide at 343 and 473 K. They found that supercritical drying temperature significantly affects the physical properties. Higher drying temperature of 473 K increased the pore volume of all three oxides but affected their pore size distributions differently. There was an increase in pore diameter for zirconia and titania-silica but nor for niobia. Bedilo and Klabunde (1997) studied effects of synthesis parameters on the properties of the zirconia aerogels. Aerogels sample possessed high surface areas and pore volumes than samples prepared by the conventional precipitation method. Pore size distributions could be controlled by varying precursors and acid concentrations. Increasing in aging time of the gel resulted in an increase in surface area but had little effect on pore structure.

Iwamoto *et al.* (2000) produced nanocrystalline silica-modified titania by the reaction in 1,4-butanediol, followed by the removal of the organic phase from the autoclave at the reaction temperature by flash evaporation. The products exhibited significant volume of pores in the macropore range, which also suggests that the primary particles were loosely packed in the samples. The products also exhibited extremely high thermal stability on calcination at high temperatures and showed improved photocatalytic activities.

Chuah *et al.* (1996) showed that digestion (i.e., hydrothermal treatment for a period of time) in basic conditions had an important effect on the synthesis of ZrO_2. The digested samples had larger surface area at elevated temperatures than the samples without digestion. These results are attributed to the stronger structure of digested sample. Also, tetragonal zirconia which has high thermal stability can be obtained by digesting the samples for longer than 24 h. Chuah *et al.* (1998) further showed that the mean pore size and pore wall thickness at elevated temperature increased as digestion progressed.

To stabilize the tetragonal phase of zirconia, Li and Chen (1994) and Aronne (1996) doped yttria, ceria or magnesia in zirconia. Mercera *et al.* (1991:78) recently reported doping yttria or lanthana in zirconia. In both studies the doped zirconia was synthesized by the co-precipitation method which gives a solid solution of zirconia and dopant. They found doping reduces the sintering and grain-growth rates. Doping yttria or lanthana substantially stabilizes the tetragonal phase of zirconia. They proposed that doping reduced the sintering and grain-growth rates by either lowering the surface energy of the zirconia grain or decreasing the concentration of species on the grain surface (Mercera *et al.*, 1991:78).

Gopalan *et al.* (1995) prepared zirconia sol by hydrolysis and condensation of zirconium *n*-propoxide in a water/propanol solution. The sol-gel derived undoped and 2 and 3 mol% yttria-doped zirconia samples after calcination at 450^{o}C are in the tetragonal phase. Undoped zirconia starts to transform to thermodynamically stable monoclinic phase at 600^{o}C. The yttria-doped zirconia samples remain in the metastable phase after heat treatment in air at 900^{o}C for 30 h. Doping yttria also retards the sintering and grain-growth rates of the sol-gel derived zirconia. Doping with 2 mol% yttria gives the most effective results with respect to retarding the surface area loss of zirconia at high temperatures. The improvement of the thermal stability of zirconia by coating yttria is explained in terms of the effects of dopant on the mobility and concentration of the surface defects.

Inoue *et al.* (2000: 65) reported the formation of large surface area zirconia rare-earth oxide solid solution by the glycothermal method. The products maintained large surface area even after calcination at high temperature. When the rare earth content in the product was small, the product partly transformed into the monoclinic phase, but the products with large rare earth contents maintained the tetragonal phase.

Lin and Duh (1997) produced ultrafine 5.5 mol% CeO_2-2 mol% $YO_{1.5}$-ZrO_2 powders with controllable crystallite size by two methods, ammonia coprecipitation and hydrolysis method. The amorphous gel produced by ammonia coprecipitation can transform into fully tetragonal phase by hydrothermal crystallization, while no tetragonal phase is obtained by calcination of the gel alone. The hydrothermal

treatment at 200^{o}C for 3.5 h results in an ultrafine powder with a surface area of 206 m^2/g and a crystallite size of 4.8 nm. They found that the surface area of the powders decreases and the crystallite size increases with increasing stock solution concentration. The powder produced by urea hydrolysis and calcination exhibits a pure tetragonal phase.

The effects of Mg^{2+}, Ca^{2+} and Sr^{2+} ions on the formation of zirconia under hydrothermal conditions were also investigated. The presence of these divalent M^{2+} ions favored the formation of tetragonal (or cubic) zirconia (Cheng *et al.*, 1999). Powder obtained from mixture with CaO content up to 8 mol% contain solid-solutions of both monoclinic and tetragonal zirconia. Mixtures of monoclinic and cubic zirconia have been detected in the composition range between 8 mol and 15 mol% while the amount of the cubic form increased by increasing CaO content (Dell and Mascolo, 2000).

In the above CaO-, MgO-, Y_2O_3-doped zirconia system, the improvement of the tetragonal phase stability may be attributed to the appearance of the oxygen vacancies, resulting as a consequence of the incorporation of divalent and trivalent cations. In doped zirconia system, metastable tetragonal zirconia is stable in a larger range of temperature than that observed for pure zirconia. Some researchers believe that it is due to lattice strains formed in the crystalline tetragonal structure by incorporation of the oxygen vacancies. However, Zhu *et al*. (1997) argued that oxygen vacancies produced in an oxygen-deficient atmosphere facilitate the tetragonal-to-monoclinic phase transformation.

Chang and Shady (2000) studied the effects of Na^+ on the surface area of ZrO_2 at elevated temperatures. ZrO_2 powders were produced by a precipitation method. They found that the properties of the powders at elevated temperatures were sensitive to the sodium content. The surface area decreased while the crystallite size and pore size of the samples increased with increased sodium content. Zheng *et al.* (1998) dispersed sodium nitrate on tetragonal zirconia. The dispersed Na^+ ion species can effectively hinder the sintering of zirconia and prevent its transformation from tetragonal to monoclinic phase.

Another approach reported for retarding the metastable to stable phase transformation is to coat a second oxide on the ceramic grain surface in order to reduce the nucleation sites on the grain boundary and/or to increase the nucleation activation energy (Gopalan *et al.*, 1995). Coating a second oxide could also reduce the sintering rate. In these coating processes, the solid oxide particles are brought into contact with liquid solution or solid containing the dopant. The dopant coated by these methods was present as a monolayer on the grain surface of the support. They theorized that the formation of a monolayer of a dopant on the surface of the support is a thermodynamically favorable process if the dopant, with a metal ion larger than the size of the metal ion of ceramic oxide, can form a strong surface bond with the oxide particles. Several other investigators also suggested that dopant is present as a two-dimensional layer covering the grain surface of the ceramic oxide (Tigburg *et al.*, 1991).

The addition of small percentages of silica in the preparation of zirconia was found to play an important role in tetragonal zirconia stabilization; i.e., the tetragonal zirconia is stable for temperatures ranging from 600^{o}C to 1100^{o}C, a larger range of temperature than that observed for pure zirconia (the polymorphic transformation to the monoclinic phase begins at 500^{o}C in pure zirconia). Contrary to Y_2O_3-ZrO_2, CaO-ZrO_2, or MgO-ZrO_2 system, lattice deformation in ZrO_2-SiO_2 oxides cannot be due to the formation of oxygen vacancies because of the strong covalent nature of oxygen bonded to the silicon atoms. Thus, the improvement of the tetragonal phase stability is due to the lattice deformation resulting from the chemical interactions at the silica-zirconia interface. Formation of Si-O-Zr bonds have been identified through FT-IR spectroscopy (del Monte *et al.*, 2000).

Wang *et al.* (1996) prepared ZrO_2-SiO_2 composite powder with ZrO_2 in the range of 10-40 vol% by a co-precipitation approach using fumed silica and zirconium oxychloride octahydrate as raw materials. They found that tetragonal zirconia grains were stabilized after calcination at elevated temperatures. With increasing temperature, Si-O-Si bonds were formed among different SiO_2 particles indicating the growth of SiO_2 particles. Therefore, the stability of tetragonal zirconia is attributed to its smaller particle size than the critical size for tetragonal-to-monoclinic transformation. Based on the particle size effect reported by Garvie; i.e., the smaller

the particle size of the tetragonal zirconia phase, the more stable it is at low temperature. When the SiO_2 grains grow, ZrO_2 were encased in silica grains. Since the ZrO_2 particles were embedded in the silica matrix, grain growth of ZrO_2 was impeded.

A catalyst-free approach for sol-gel synthesis of mixed ZrO_2-SiO_2 oxides was carried out by Zhan and Zeng (1999). ZrO_2-SiO_2 mixed oxides with Zr-content up to 50 mol% were obtained. By monitoring FTIR absorption, the formation of Zr-O-Si in low Zr-content gels was observed and a linear shift of peak position as a function of Zr content has been found, indicating a high degree of mixing for ZrO_2-SiO_2 oxides.

In addition to stabilize the tetragonal phase, the presence of a small amount of silica in the sol-gel process enlarged the surface area of zirconia (Soled and Mcvicker, 1992; Miller *et al.*, 1994 and Contescu *et al.*, 1995). In the bulk-substituted SiO_2-ZrO_2 prepared using a mixture of silicon and zirconium alkoxides in a sol-gel process, the surface area monotonically increased with silica content from 19 m^2/g of pure zirconia to 558 m^2/g of pure silica (Miller *et al.*, 1994). Sato *et al.* (2000) prepared SiO_2-ZrO_2 by depositing silica in the hydrothermal process. The specific surface area of samples varied with the hydrothermal period. Specific surface area of the SiO_2-ZrO_2 with the hydrothermal period longer than 96 h were unchanged as high as 230 m^2/g after calcination at 500^oC, while that of pure zirconia was at most 45 m^2/g.

Inoue *et al.* has developed the new synthesis method of inorganic materials in organic media at elevated temperature (200-300^oC) under autogeneous pressure of organics and found that many oxides and mixed oxides can be crystallized in organic media at temperatures lower than that required by the hydrothermal reaction (Inoue *et al.*, 1993; 1995:121; 1995:226; 1989, 1991). Titania nanocrystals was synthesized by the glycothermal reaction and it was found that the crystallite size observed by transmission electron microscopy was close to that calculated by X-ray line broadening technique, suggesting that each particle was a single crystal. The BET surface area was inversely proportional to the crystallite size of the product, which suggested that the particle expose its entire surface area to the adsorbate molecules (Iwamoto *et al.*, 2000). Some of the glycothermal products such as rare earth gallium garnets (RE = Nd-Gd) were spherical particles with smooth surface. Electron

diffraction revealed that each spherical particle was a single crystal grown from one nucleus (Inoue *et al.*, 1998). Some other products such as rare earth aluminum garnets with smaller rare earth ions are composed of apparently agglomerates of spherical particles. However, electron diffraction exhibited the single-crystal pattern (Inoue *et al.*, 1995:226 and 1998). The glycothermal reaction of zirconium *n*-propoxide in glycol also yielded tetragonal zirconia having quite large surface area. The images observed by transmission electron microscopy revealed that the products were comprised of the aggregates of fine primary particles and electron diffraction indicated that these primary particles were randomly oriented. This result is different from that of the other glycothermal products (Inoue, 2000:29 and Inoue *et al*., 2000:65).

From the list of literatures, the objective of this study is, hence, to study the crystallization of zirconia in various organic media under glycothermal condition and the effect of synthesis conditions on zirconia properties, for examples effect of drying condition and concentration of starting solution. The effect of the presence of silica on the surface area and thermal stability of the modified zirconia was also investigated.

CHAPTER III

THEORY

3.1 Properties of metal alkoxides and organic solvents

Metal alkoxides are compounds in which a metal is attached to one or more alkyl groups by an oxygen atom. Alkoxides are derived from alcohols by the replacement of the hydroxyl hydrogen by metal (Othmer, 1978).

3.1.1 Physical properties

The metal alkoxides exhibit great differences in physical properties, depending on the position of the metal in the periodic table, and secondarily on the alkyl group. Many alkoxides are strongly associated by intermolecular forces, which depend on the size and shape of the alkyl groups.

Many metal alkoxides are soluble in the corresponding alcohols, but magnesium alkoxides are practically insoluble.

In recent decades, much work has been done on the structure of the metal alkoxides. The simple alkali alkoxides have an ionic lattice and a layer-like structure, but alkaline earth alkoxides show more covalent character.

Structures are highly varied among the transition metals. Metal alkoxides are colored when the corresponding metal ions are colored, otherwise not.

3.1.2 Chemical properties

The most outstanding property of the metal alkoxides is ease of hydrolysis. Uranium hexa-tert-butoxide is an exception and does not react with water.

Zirconium tetra *n*-propoxide $Zr(OC_3H_7)_4$, molecular weight of 327.6, is a yellow-brown liquid; density, d_4^{20} = 1.05 g/ml; solidification point below –70°C; flammable, flash point below 21°C; soluble in hydrocarbons. Usually, zirconium alkoxides hydrolyze in moist air.

Table 3.1 Physical properties of glycols and solvent (Lide, 2000-2001)

glycol or solvent	chemical formula	boiling point (°C)	density (g/ml)
ethylene glycol	$HO(CH_2)_2OH$	197	1.113
1,3-propanediol	$HO(CH_2)_3OH$	215	1.053
1,4-butanediol	$HO(CH_2)_4OH$	235	1.016
1,5-pentanediol	$HO(CH_2)_5OH$	239	0.994
1,6-hexanediol	$HO(CH_2)_6OH$	243-50	0.995
monoethanolamine	$H_2N(CH_2)_2OH$	171	1.018
diethanolamine	$(HOCH_2CH_2)_2NH$	269	1.088
triethanolamine	$(HOCH_2CH_2)_3N$	335	1.124
N-methylethanolamine	$CH_3NHC_2H_4OH$	159.5	0.941
N,*N*-dimethylethanolamine	$(CH_3)_2NC_2H_4OH$	134.6	0.888

3.2 General feature of zirconia

Zirconia exhibits three polymorphs, the monoclinic, tetragonal, and cubic phases. Figure 3.1 shows the typical crystal systems; cubic, tetragonal and monoclinic ones. Crystal structures of cubic, tetragonal and monoclinic zirconia are shown in Figure 3.2. The monoclinic is stable up to ~1170°C, at which temperature it transforms into the tetragonal phase, which is stable up to 2370°C (Cormack and Parker, 1990). The stabilization of the tetragonal phase below 1100°C is important in the use of zirconia as a catalyst in some reactions. Above 2370°C, the cubic phase is stable and it exists up to the melting point of 2680°C. Due to the martensitic nature of the transformations, neither the high temperature tetragonal nor cubic phase can be quenched in rapid cooling to room temperature. However, at low temperature, a

metastable tetragonal zirconia phase is usually observed when zirconia is prepared by certain methods, for example by precipitation from aqueous salt solutions or by thermal decomposition of zirconium salts. This is not the expected behavior according to the phase diagram of zirconia (i.e., monoclinic phase is the stable phase at low temperatures). The presence of the tetragonal phase at low temperatures can be attributed to several factors such as chemical effects, (the presence of anionic impurities) (Srinivasan *et al.*, 1990 and Tani *et al.*, 1982) structural similarities between the tetragonal phase and the precursor amorphous phase (Osendi *et al.*, 1985; Tani, 1982 and Livage, 1968) as well as particle size effects based on the lower surface energy in the tetragonal phase compared to the monoclinic phase (Garvie, 1978; Osendi *et al.*, 1985 and Tani 1982). The transformation of the metastable tetragonal form into the monoclinic form is generally complete by 650-700 ^{o}C.

3.3 Crystallization (West, 1997)

3.3.1 Oriented reactions or transformations

3.3.1.1 Epitactic reactions require a structural relationship between the two phases but it is restricted to the actual interface between the two crystals. Hence, the two structures may have a common arrangement of oxide ions at the interface but the oxide arrangement to either side develops in a different way. Epitactic reactions, therefore require only a two-dimensional structural similarity at the crystal interface.

3.3.1.2 Topotactic reactions are more specific than epitactic reactions, not only because they requires the structural similarity at the interface but also because this similarity should continue into the bulk of both phases.

Topotactic and Epitactic reactions are of common occurrence since their nucleation step is usually easier than that for reaction in which there is no structural or orientation relationship between reactant and product.

Crystal system	Unit cell shape
Cubic	$a = b = c, \alpha = \beta = \gamma = 90^o$
Tetragonal	$a = b \neq c, \alpha = \beta = \gamma = 90^o$
Monoclinic	$a \neq b \neq c, \alpha = \gamma = 90^o, \beta \neq 90^o$
Triclinic	$a \neq b \neq c, \alpha \neq \beta \neq \gamma$

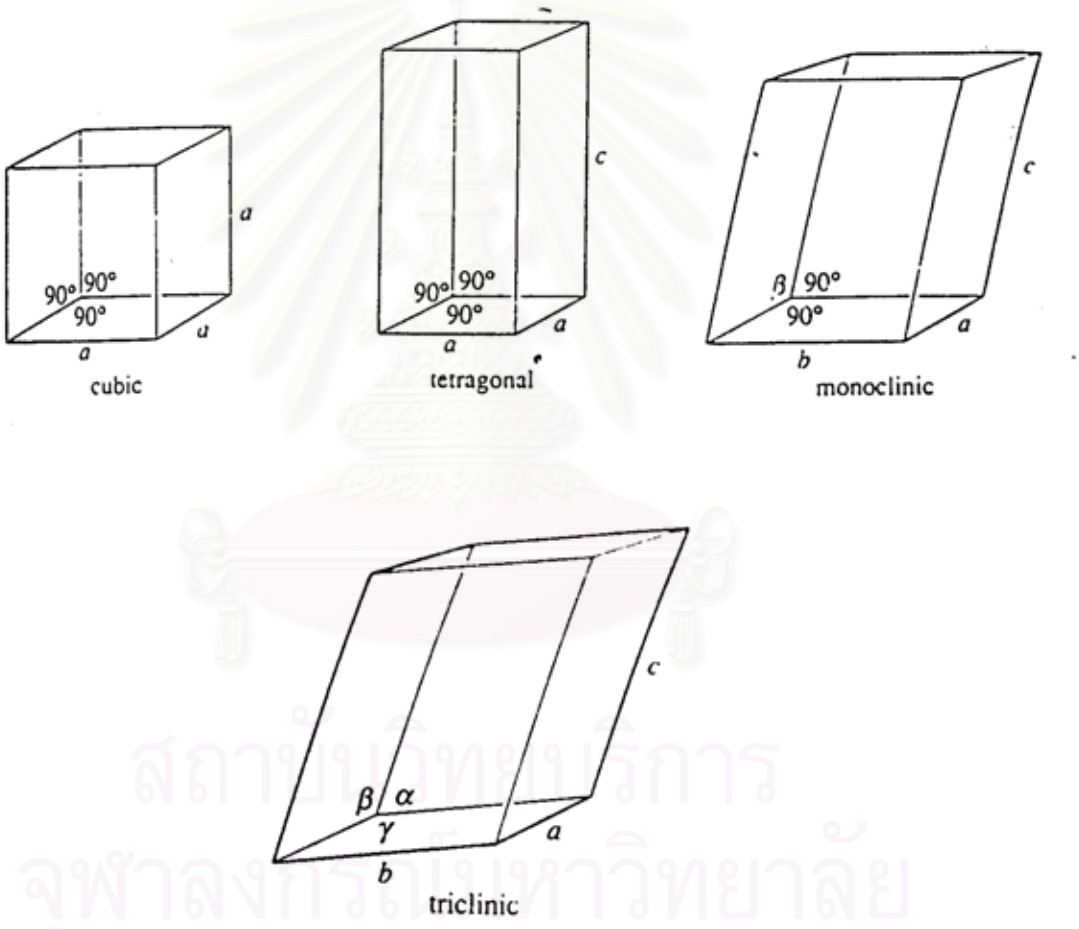

Figure 3.1 The unit cells of the crystal systems (West, 1997)

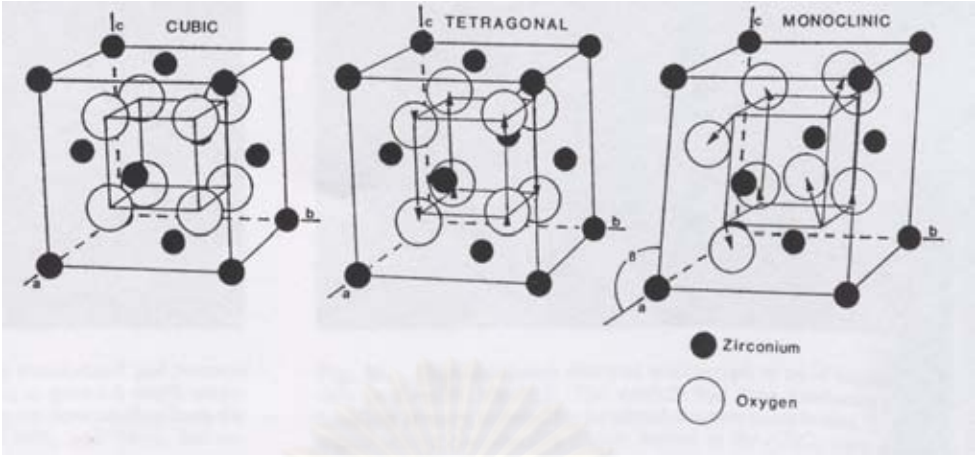

Figure 3.2 Crystal structures of cubic, tetragonal and monoclinic zirconia (Heuer, 1987).

3.3.2 Crystallization in solutions

This crystallization method hasone feature, which makes them particularly useful for preparation: the starting material for crystallization (i.e. aqueous solution) is usually homogeneous. This may greatly facilitate formation of the crystalline product, since long range diffusion of ions may not be necessary and the product may form at much lower temperatures. A high degree of supersaturation of the components is desirable leading to the nucleation of crystals. A nucleus that has formed from a supersaturated liquid phase can grow by transport of solute species to the particle surface.

3.4 Preparation of zirconia

The main conventional synthesis for multicomponent ceramic powders is a solid state reactions between oxide and/or carbonate powder precursors. Thus, repeated cycle of milling and calcination at high temperatures are required to achieve the solid-state reaction. Disadvantages of this method are large grain sizes due to the high firing temperatures and poor chemical homogeneity. In addition, undesirable phase can form. Therefore, chemical routes are attracting much attention because they allow production of powders in an unaggregated form. This route also uses lower

reaction temperatures for producing the required crystalline phases. In addition, chemical routes have the potential for achieving improved chemical homogeneity on the molecular scale. Major chemical routes, which are under intensive worldwide investigation for powder preparation, are described below.

3.4.1 Precipitation method

It is possible to control precipitation reactions to such a degree that the concentration of the solute exceeds that for nucleation for only a brief period. This is achieved by bringing the solution into supersaturation, either by changing the temperature, the salt concentration, the pH, or by exploiting the slow release of some hydrolysis products in a water solution.

Zirconia was prepared by adding a solution of zirconium chloride to the well-stirred precipitating solution (e.g. NH_4OH, KOH, or NaOH) at room temperature. The pH of the solution was controlled. The resulting precipitate was recoverd, and then washed with an ammonium nitrate solution. When no more chloride was detected in the washings (silver nitrate test), the precipitate was rinsed with deionized water. The obtained sample was then dried overnight at 100^{o}C. The obtained product was amorphous hydrous oxide and the crystalline material was obtained after calcination at 500^{o}C. The resulting zirconia was predominantly monoclinic, 84%. After heat treatment at 500^{o}C for 1 h, the surface area was only 65 m^2/g and decreased further to 40 m^2/g when calcined for 12 h (Chuah *et al.*, 1998).

3.4.2 Sol-gel method

To prepare a solids using the sol-gel method, a sol is first prepared from a suitable reactants in a suitable liquid. Sol preparation can either be simply the dispersal of an insoluble solid or addition of a precursor which reacts with the solvent to form a colloid product. A typical example of the first is the dispersal of oxides or hydroxides in water with the pH adjusted so that the solid particles remain in suspension rather than precipitate out. A typical example of the second method is the addition of metal alkoxides to water. The alkoxides are hydrolyzed giving the oxide as

a colloidal product. The sol is then either treated or simply left to form a gel. To obtain a final product, the gel is heated. This heating serves several purposes: it removes the solvent, it decomposes anions such as alkoxides or carbonates to give oxides, it allows rearrangement of the structure of the solid and it allows crystallization to occur.

Zirconia was obtained from hydrolysis of zirconium *n*-propoxide with ethanol in an argon atmosphere to avoid precipitation. The mixture was kept at 50^{o}C for 1 h under constant agitation. Gellation was induced by adding distilled water dropwise. The fresh gel was amorphous and tetragonal zirconia was crystallized between 300^{o}C to 500^{o}C (Aguilar, 2001).

3.4.3 Hydrothermal method

The hydrothermal reaction is suitable for the preparation of powders; from nano-particles to single crystals. High-temperature, high-pressure aqueous solution, vapors and/or fluids in hydrothermal processing can act on materials as (a) transfer medium of pressure, temperature, and mechanical energy, (b) adsorbate, which plays a role of catalyzer or reaction accelerator, (c) solvent which dissolves or reprecipitates the solid materials, (d) reagent which forms hydroxides, oxides, oxyhydroxides and/or salts. The substances which act as (b) and/or (c) are called mineralizer. The mineralizer can be distilled water or ions such as F^- or OH^-. This synthesis system can assure the homogeneity of the particles in molecular or atomic scale when the process was ideally controlled (Yoshimura and Somiya, 1999).

Wet gel hydrous zirconia obtained from the precipitation method described above was washed and then encapsulated in an autoclave filled with distilled water or mineralizer solution. The wet gel was subjected to hydrothermal treatment as the autoclave was heated. Pressure inside the autoclave was not controlled.

3.4.4 Glycothermal and solvothermal method

Glycothermal method and solvothermal method have been developed for synthesis of metal oxide and binary metal oxide by using glycol and organic solvent

as the reaction medium, respectively. The use of glycol or solvents other than water in the hydrothermal method produced the different form of intermediate phase. The preparation method is described in the experimental section, Chapter IV.

3.5 Basic chemistry (Smith and March, 2001 and Morrison and Boyd, 1992)

3.5.1 Steric effect is an effect on relative rates caused by the space-filling properties of those parts of molecule attached at or near the reacting site. One important kind of steric effect is called *steric hindrance*. By this we mean that the spatial arrangement of the atoms or groups at or near the reacting site of the molecule hinders or retards a reaction.

For particles (molecules and ions) to react, their reactive centers must be able to come within bonding distance of each other. Although most molecules are reasonably flexible, very large and bulky groups can often hinder the formation of the required transition state. In some cases they can prevent its formation altogether.

3.5.2 Inductive effect depends upon the intrinsic tendency of the substituent to release or withdraw electron, by definition, its electronegativity acting either through the molecular chain or through space. The effect weakens steadily with increasing distance from the substituent.

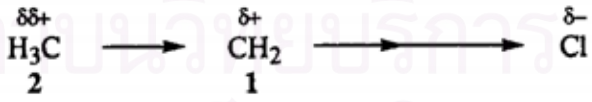

For example, the C-C bond in ethane has no polarity because it connects two equivalent atoms. However, the C-C bond in chroloethane is polarlized by the presence of the electronegative chlorine atom. The C-1 atom, having been deprived of some of its electron density by the greater electronegativity of Cl, is partially compensated by drawing the C-C electrons closer to itself, resulting in a polarization of this bond and a slightly positive charge on the C-2 atom. This polarization of one bond caused by the polarization of an adjacent bond is called the *inductive effect*. The

effect is greatest for adjacent bonds but may also be felt farther away; thus the polarization of the C-C bond causes a (slight) polarization of the three methyl C-H bonds.

3.5.3 Stabilization of carbocations

The characteristic feature of a carbocation is, by definition, the electron deficient carbon and the attendant positive charge. The relative stability of a carbocation is determined chiefly by how well it accommodates that charge.

According to the laws of electrostatics, the stability of a charged system is increased by dispersal of the charge. Any factor, therefore, that tends to spread out the positive charge of the electron-deficient carbon and distribute it over the rest of the ion must stabilize a carbocation.

Considering a substituent, G, attached to an electron-deficient carbon in place of a hydrogen atom. Compared with hydrogen, G may either release electrons or withdraw electrons.

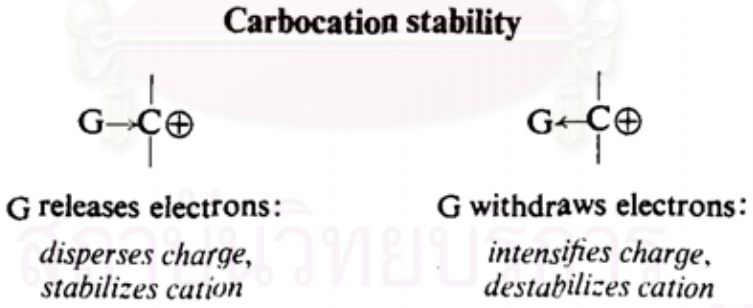

An electron-releasing substituent tends to reduce the positive charge at the electron-deficient carbon; in doing this, the substituent itself becomes somewhat positive. This dispersal of the charge stabilizes the carbocations.

An electron-withdrawing substituent tends to intensify the positive charge on the electron-deficient carbon, and hence makes the carbocation less stable.

3.5.4 S_N1 reaction

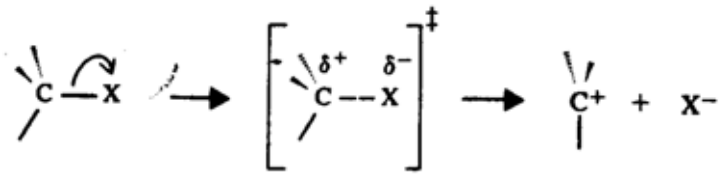

Transition state

The primary factor that determined the reactivity of organic substrates in an S_N1 reaction is the relative stability of the carbocation that is formed. Except for those reactions that take place in strong acids, the only organic compounds that undergo reaction by an S_N1 path at a reasonable rate are those that are capable of forming relatively stable carbocations. Formation of a relatively stable carbocation is important in S_N1 reaction because it means that the free energy of activation for the slow step for the reaction will be low enough for the reaction to take place at a reasonable rate.

For instances, in S_N1 reaction of an alkyl halide, the carbocation is formed by heterolysis of the substrate molecule, that is, by breaking of the carbon-halogen bond. In the reactant, an electron pair is shared by carbon and halogen. In the products, halogen has taken away the electron pair, and carbon is left with only a sextet; halide carries a full negative charge, and the carbocation carries a full positive charge centered on carbon. In the transition state, the C-X bond must be partly broken, halogen having partly pulled the electron pair away from carbon. Halogen has partly gained the negative charge it is to carry in the halide ion. Most important, carbon has partly gained the positive charge it is to carry in the carbocation. Electron releasing groups tend to disperse the partial positive charge developing on carbon, and in this way stabilize the transition state. Stabilization of the transition state lowers the activation energy and permits a faster reaction. Of the simple alkyl halides, this means that tertiary halides react relatively easily by an S_N1 mechanism because they can form relatively stable carbocation. Tertiary cabocation is stabilized because three alkyl groups release electrons to the positive carbon atom and thereby disperse its charge.

3.5.5 Neighboring group effects: intramolecular nucleophile attack

Carbocations can rearrange through migration of an organic group or a hydrogen atom, with its pair of electrons, to the electron-deficient carbon. Indeed, when carbocations were first postulated as reactive intermediates, it was to account for rearrangement of a particular kind.

The driving force behind all carbocation reactions is the need to provide electrons to the electron-deficient carbon. When an electron-deficient carbon is generated, a nearby group may help to relieve this deficiency. It may remain in place and release electrons through space or through the molecular framework, inductively or by resonance, or it may actually carry the electrons to where they needed. This give rise to what are called “neighboring group effects: intramolecular effects exerted on a reaction through direct participation by a group near the reaction center.

If a neighboring group is to form a bridged cation, it must have electrons to form the extra bond. These may be unshared pairs on atoms like sulfur, nitrogen, oxygen, or bromine; π electrons of a double bond or aromatic ring. In making its nucleophilic attack, a neighboring group competes with outside molecules that are often intrinsically much stronger nucleophiles. Yet the evidence clearly shows that the neighboring group enjoys very great advantages over these outside nucleophiles because it is in the same molecule, the proper position to attack.

3.5.6 S_N2 reaction

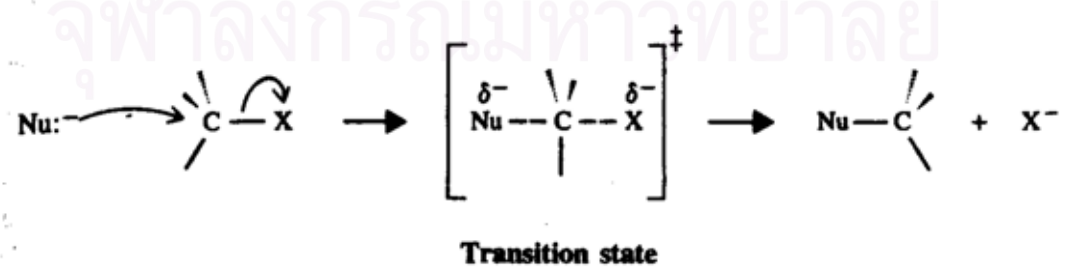

Transition state

According to this mechanism, the nucleophile approaches the carbon bearing the leaving group from the backside, that is, from the side directly opposite the leaving group. As the reaction progresses the bond between the nucleophile and the carbon atom grows, and the bond between the carbon atom and the leaving group weakens. As this happens, the carbon atom has its configuration turned inside out, it becomes inverted, and the leaving group is pushed away.

An S_N2 reaction required an approach by the nucleophile to a distance within bonding range of the carbon atom bearing the leaving group. Because of this, bulky substituents on or near that carbon atom have a dramatic inhibiting effect. They cause the potential energy of the required transition state to be increased and, consequently they increase the free energy of activation for the reaction. Of the simple alkyl halides, methyl halides react most rapidly in S_N2 reactions because only three small hydrogen atoms interfere with the approaching nucleophile. Tertiary halides are the least reactive because bulky groups present a strong hindrance to the approaching nucleophile.

3.5.7 Transesterification

One alcohol is capable of displacing another alcohol from an ester. This alcoholysis (cleavage by an alcohol) of an ester is called *transesterification*

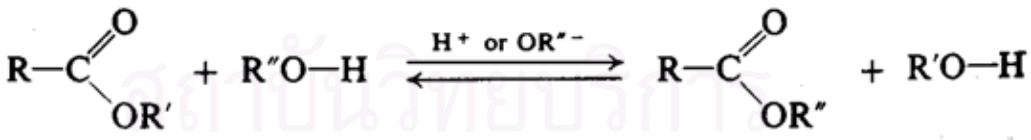

CHAPTER IV

EXPERIMENTAL

The experimental system and procedures in the synthesis of zirconia are presented in this chapter. The chemicals and experimental equipment are shown in sections 4.1 and 4.2, respectively. In section 4.3, the preparation and characterization of products are explained.

4.1 Chemicals

Zirconia powders were synthesized with the following reagents:

1. Zirconium tetra-*n*-propoxide (ZNP, $Zr(OC_3H_7)_4$) available from Mitsuwa pure Chemicals.
2. Tetraethyl orthosiliocate (TEOS, $(C_2H_5O)_4Si$) available from Aldrich.
3. Glycol and aminoalcohols available from Aldrich (for the experiments in Thailand) and from Wako (for the experiments in Japan). The glycol and aminoalcohols used for the experiments include ethylene glycol, 1,3-propanediol, 1,4-butanediol, 1,5-pentanediol, 1,6-hexanediol, monoethanolamine, dimethanolamine, trimethanolamine, N-methylethanolamine and N, N-dimethylethanolamine

The calculation of the amount of reagents required in the reaction is shown in Appendix A.

4.2 Equipment

The equipment for the synthesis of zirconia consisted of:

4.2.1 Autoclave reactor

- Made from stainless steel
- Maximum temperature of 350^{o}C

- Pressure gauge
- Relief valve used to prevent runaway reaction
- Test tube was used to contain the reagent and glycol

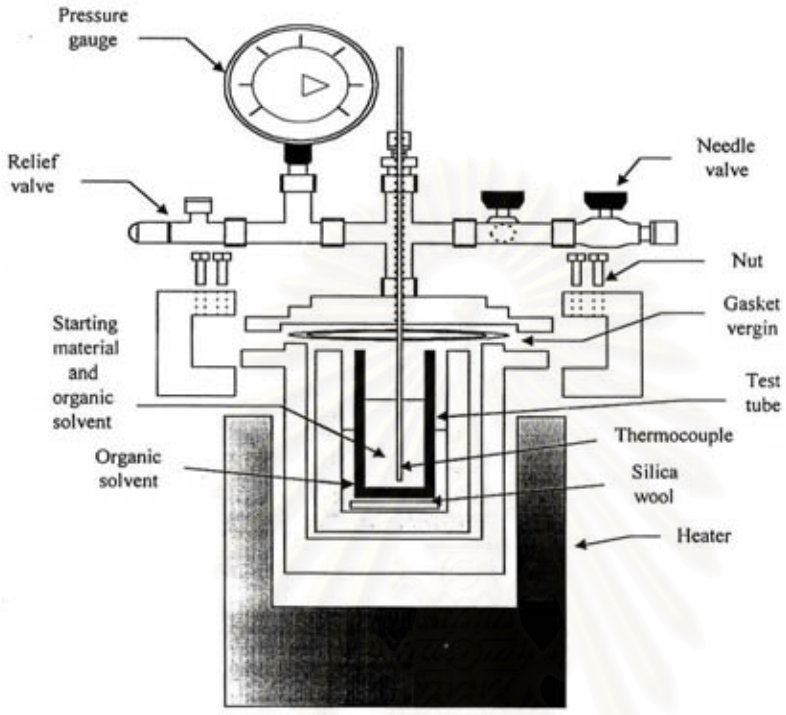

Figure 4.1 Autoclave reactor used in Thailand

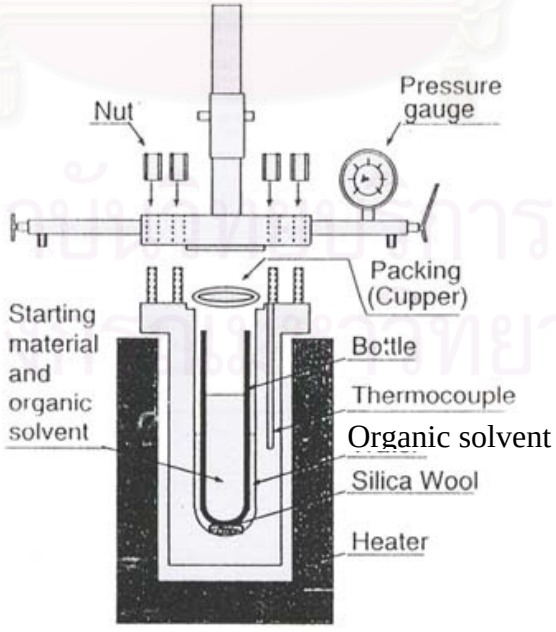

Figure 4.2 Autoclave reactor used in Japan

Autoclave reactors used for the experiments in Thailand and in Japan are shown in Figure 4.1 and Figure 4.2, respectively. There are some differences of synthesis parameters between the experiments in Thailand and in Japan as follows:

Experiments in Thailand

- Autoclave volume of 1000 cm^3 and an iron jacket was used to reduce the volume of autoclave to be 300 cm^3.
- Thermocouple is attached to the reagent in the autoclave.
- Amount of starting material = 15 g
- Amount of organic solvent in the test tube = 100 cm^3
  and amount of organic solvent in the gap between test tube and autoclave wall = 30 cm^3

Experiments in Japan

- Autoclave volume of 200 cm^3
- Thermocouple is inserted into the autoclave wall; therefore the thermocouple is not attached to the reagent directly.
- Amount of starting material = 10 g
- Amount of organic solvent in the test tube = 60 cm^3
  and amount of organic solvent in the gap between test tube and autoclave wall = 40 cm^3

4.2.2 Temperature program controller

A temperature program controller was connected to a thermocouple attached to the autoclave.

4.2.3 Electrical furnace (Heater)

Electrical furnace supplied the required heat to the autoclave for the reaction.

4.2.4 Gas controlling system

Nitrogen was set with a pressure regulator (0-150 bar) and needle valves were used to release gas from autoclave.

The diagram of the reaction equipment for the synthesis of zirconia is shown in Figure 4.3

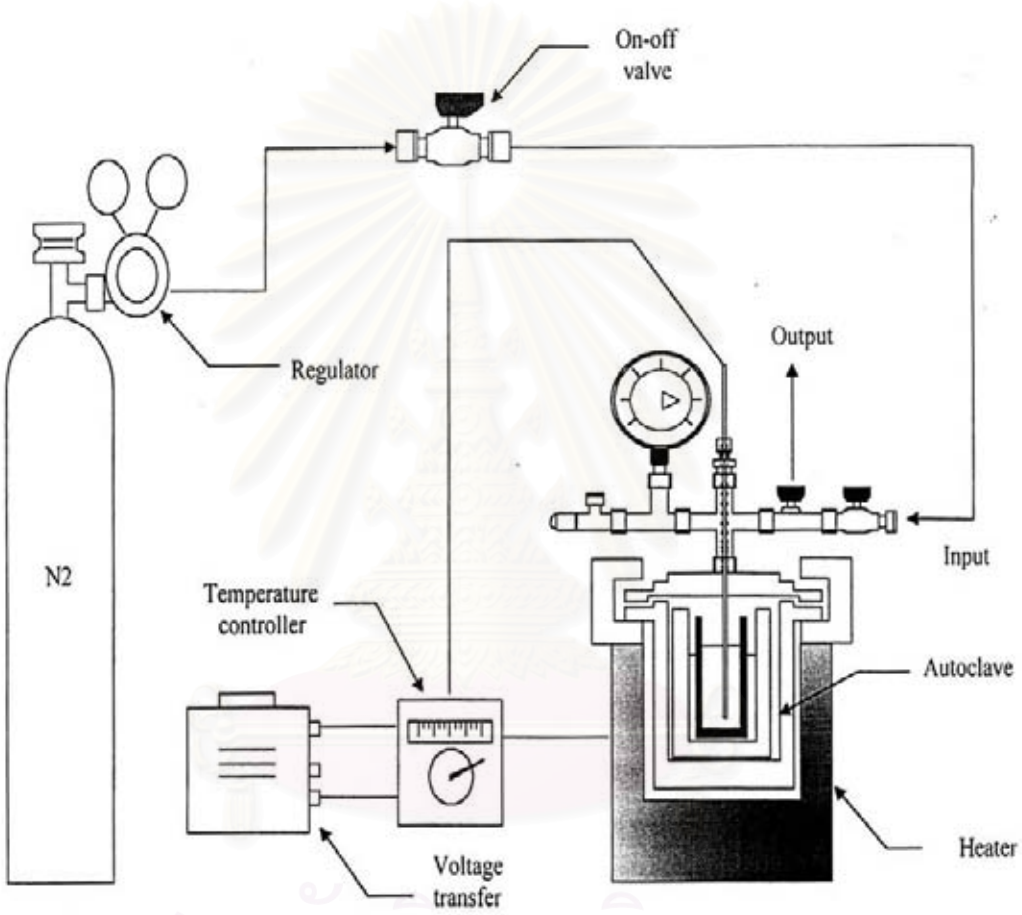

Figure 4.3 Diagram of the reaction equipment for the synthesis of zirconia

4.3 Preparation of zirconia

Zirconia was prepared by using zirconium *n*-propoxide 15 g as a starting material. The starting material were suspended in 100 ml of a solvent (glycol) in the test tube, and then set up in the autoclave. In the gap between the test tube and

autoclave wall, 30 ml of the glycol was added. After the autoclave was completely purged with nitrogen, the autoclave was heated to a desired temperature (200^{o}C-300^{o}C) at a rate of 2.5^{o}C min^{-1} and held at that temperature for 2 hours. In this study, beside the reaction temperature, the reaction time was also varied from 0-8 hours. Autogeneous pressure during the reaction gradually increased as the temperature was raised. After the reaction, the autoclave was cooled to room temperature. The resulting powders were collected after repeated washing with methanol by centrifugation. They were then air-dried.

For the synthesis of silica-modified zirconia, the method is the same as that for pure zirconia synthesis except the starting material, i.e. the mixture of zirconium *n*-propoxide 15 g and an amount of tetraethyl orthosilicate (TEOS) at Si/Zr ratio of 0.01-0.15 was used as the starting material (see Appendix A).

For some experiments, a different drying process was applied as follows. After the reaction for 2 hours, the valve of the autoclave was slightly opened to release the organic vapor from the autoclave by flash evaporation while keeping the temperature at 300^{o}C. The valve was opened until the pressure inside the autoclave was decreased to atmospheric level. The dried products were obtained directly after the assembly was cooled down without the step of washing by methanol and centrifugation.

The calcination of the thus-obtained product was carried out in a box furnace. The product was heated at a rate of 10^{o}C min^{-1} to a desired temperature and held at that temperature for 1 hour.

4.4 Characterization

4.4.1 X-ray diffraction spectroscopy (XRD)

The X-ray powder diffraction (XRD) patterns were obtained on a X-ray diffractometer. The crystallite size was estimated from line broadening according to the Scherrer equation (see Appendix B) and α-Al_2O_3 was used as a standard.

Model of XRD for experiments in Japan: Shimadzu XD-D1 diffractometer using CuKα radiation and a carbon monochromator.
Model of XRD for experiments in Thailand: Siemens D5000 using nickel filtered CuKα radiation at Center of Excellences on Catalysis and Catalytic Reaction Engineering, Chulalongkorn University.

4.4.2 Scanning electron microscopy (SEM)

Morphology and size of secondary particle of the samples were observed by scanning electron microscope (SEM).
Model of SEM for experiments in Japan: Hitachi S-2500CX.
Model of SEM for experiments in Thailand: JSM-5410LV at the Scientific and Technological Research Equipment Center, Chulalongkorn University (STREC).

4.4.3 Transmission electron microscopy (TEM)

Morphology and size of the samples were observed by a transmission electron microscope (TEM), Hitachi H-800 at the laboratory in Japan

4.4.4 Surface area measurement

The specific surface area of the samples was calculated using the Brunauer-Emmett-Teller (BET) equation by both the single point and multipoint method on the basis of nitrogen uptake at liquid-nitrogen temperature.

4.4.4.1 BET apparatus for the single point method

The reaction apparatus of BET surface area measurement consisted of two feed lines for helium and nitrogen. The flow rate of the gas was adjusted by means of fine-metering valve on the gas chromatograph. The sample cell made from pyrex glass. The schematic diagram of the reaction apparatus was shown in Figure 4.3.

The mixture gases of helium and nitrogen flowed through the system at the nitrogen relative pressure of 0.3. The catalyst sample (ca. 0.3 to 0.5 g) was placed in

the sample cell, which was then heated up to 160^{o}C and held at this temperature for 2 h. After the catalyst sample was cooled down to room temperature, nitrogen uptakes were measured as follows.

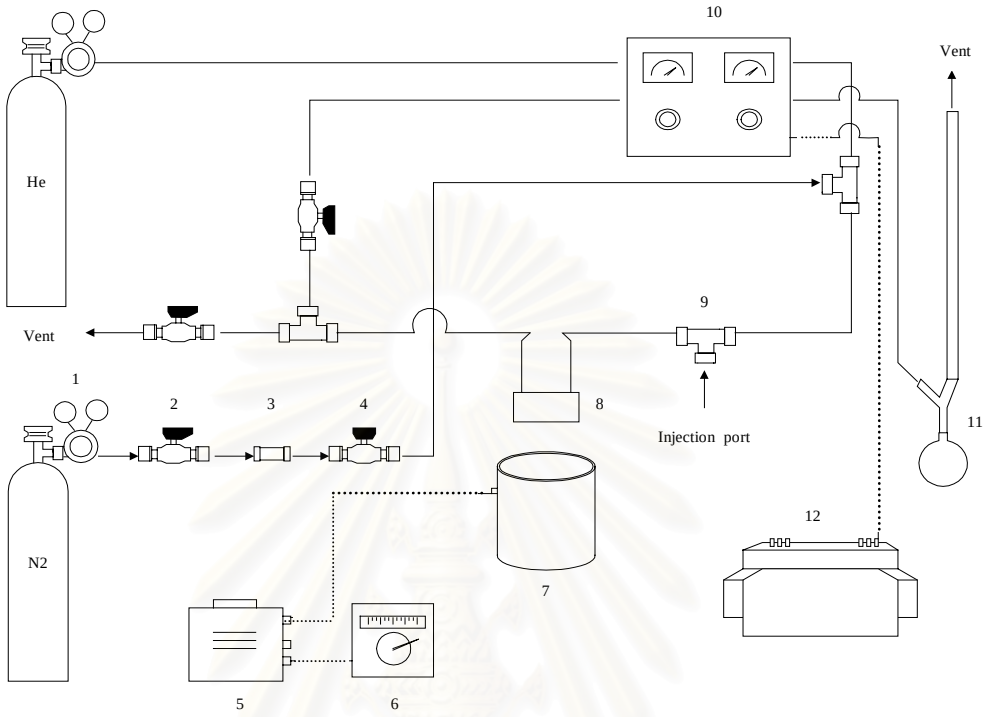

1. Pressure regulator	5. Voltage transformer	9. Three-way valve
2. On-off valve	6. Temperature controller	10. Gas chromatograph with TCD
3. Gas filter	7. Heater	11. Bubble flowmeter
4. Needle valve	8. Sample cell	12. Recorder

Figure 4.4 The schematic diagram of the reaction apparatus of BET surface area measurement.

Step (1) Adsorption step: The sample that set in the sample cell was dipped into liquid nitrogen. Nitrogen gas that flowed through the system was adsorbed on the surface of the sample until equilibrium was reached.

Step (2) Desorption step: The sample cell with nitrogen gas-adsorbed catalyst sample was dipped into the water at room temperature. The adsorbed nitrogen gas was

desorbed from the surface of the sample. This step was completed when the indicator line was in the position of the base line.

Step (3). Calibration step: 1ml of nitrogen gas at atmospheric pressure was injected through the calibration port of the gas chromatograph and the area was measured. The area was the calibration peak. The calculation method is explained in Appendix C.

4.4.4.2 BET apparatus for the multipoint method

The multipoint BET surface area of the samples were measured by a micromeritics medel ASAP 2000 using nitrogen as the adsorbate at the Analysis Center of the Department of Chemical Engineering, Faculty of Engineering, Chulalongkorn University. The operating conditions are as follows:

Sample weight	~ 0.3 g
Degas temperature	200^{o}C for as-synthesized sample
	300^{o}C for calcined sample
Vacuum pressure	< 10 μmHg

4.4.5 Thermogravimetric analysis and differential thermal analysis (TGA&DTA)

The weight loss and thermal behavior of the samples were performed on a Shimadzu TG-50 thermal analyzer at a heating rate of 10^{o}C min^{-1} in a 40 ml min^{-1} flow of dried air. The sample weight used for each analysis is about 20 mg.

4.4.6 Infrared spectroscopy (IR)

The functional group in the samples was determined by using infrared spectroscopy. Before measurement, the sample was mixed with KBr and then was formed into a thin wafer.

Model of IR for experiments in Japan: Shimadzu IR-435 spectrometer.

Model of IR for experiments in Thailand: Nicolet impact 400 at Center of Excellences on Catalysis and Catalytic Reaction Engineering, Chulalongkorn University.

CHAPTER V

RESULTS AND DISCUSSION

In this chapter, the results and discussion are divided into four sections. Section 5.1 explains the formation of zirconia in various solvents. The crystallization mechanisms of zirconia are discussed in section 5.2. The influences of synthesis conditions on the properties of zirconia are included in section 5.3. In section 5.4, the synthesis of silica-modified zirconia and the effect of silica on the properties of modified zirconia are explained. Note that the experiments in section 5.1 and 5.2 were done in Japan and the experiments in section 5.3 and 5.4 were conducted in Thailand.

5.1 The formation of zirconia in various solvents

Ethylene glycol (EG), 1,3-propanediol (1,3-PG), 1,4-butanediol (1,4-BG), 1,5-pentanediol (1,5-PeG) and 1,6-hexanediol (1,6-HG) are the glycol used as the reaction medium in the synthesis of zirconia from zirconium *n*-propoxide (ZNP). The XRD patterns of the products prepared in several glycols at 300^{o}C for 2 h are shown in Figure 5.1.

When ethylene glycol (EG) was used as the reaction medium, the crystalline product was not obtained even at reaction temperature of 300^{o}C. This can be attributed to the difficulty in cleavage of C-O bonds of ethylene glycol moieties due to electron withdrawing effect of the intramolecular hydroxyl group. Such effect causes the formation of relatively unstable carbocation; therefore the C-O bond is difficult to be broken down. The use of 1,3-propanediol (1,3-PG) resulted in the formation of an unidentified phase and zirconia was not formed even by the reaction at 300^{o}C. As demonstrated later, the unidentified phase has glycol moieties in crystal lattice. Similar to the reaction in ethylene glycol, the inability of 1,3-propanediol (1,3-PG) for the formation of crystalline zirconia can also be attributed to the difficulty in heterolytic cleavage of C-O bond in the unidentified phase because electron-withdrawing effect of the intramolecular hydroxyl group disturbs the bond breaking of C-O bonds. Based on the inductive effect (i.e., electron withdrawing effect) of the

hydroxyl group, the cleavage of C-O bond is expected to proceed more easily with increasing carbon number of glycol because the relatively stable carbocation is formed when the carbon number of glycol increases. When 1,4-butanediol (1,4-BG) was used, pure tetragonal zirconia was obtained at 300^{o}C for 2 h. For the reaction in 1,4-butanediol and 1,5-pentanediol, the cleavage of the C-O bond was also accelerated by the participation of the intramolecular hydroxyl group. Neighboring group participation for the reaction in 1,4-BG formed tetrahydrofuran, which was actually detected by gas chromatographic analysis of the supernatant after the reaction in 1,4-BG (Inoue *et al.,* 1993).

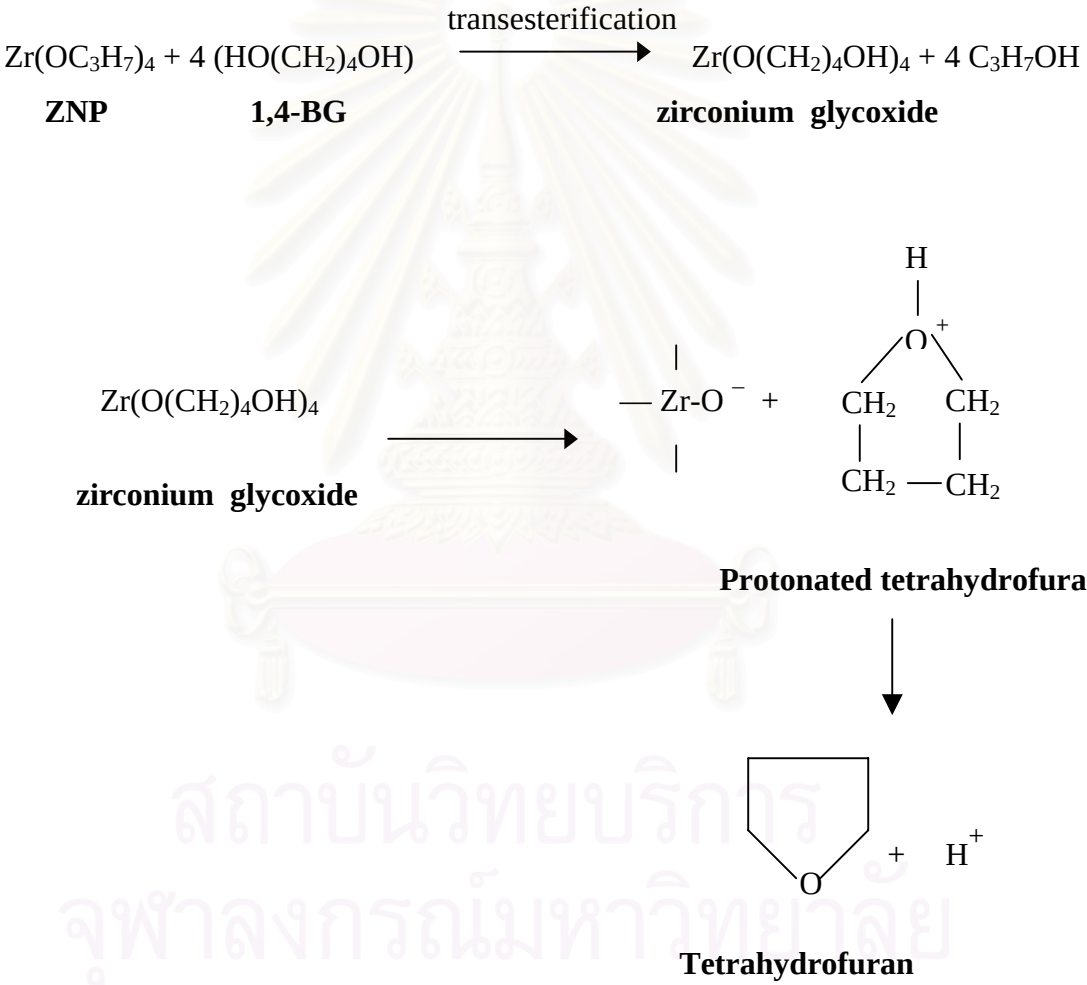

The reaction in 1,6-hexanediol (1,6-HG) also yielded tetragonal zirconia but the use of 1,5-pentanediol (1,5-PeG) resulted in the formation of a mixture of tetragonal and monoclinic phases. It was proposed that the formation of monoclinic phase is due to the presence of water in 1,5-PeG, leading to hydrolysis reaction. Inoue

found that hydrolysis of zirconium alkoxide in toluene yielded monoclinic zirconia (Inoue *et al.*, 1995: 121). However, the formation of monoclinic phase in 1,5-PeG should be studied in detail in the future.

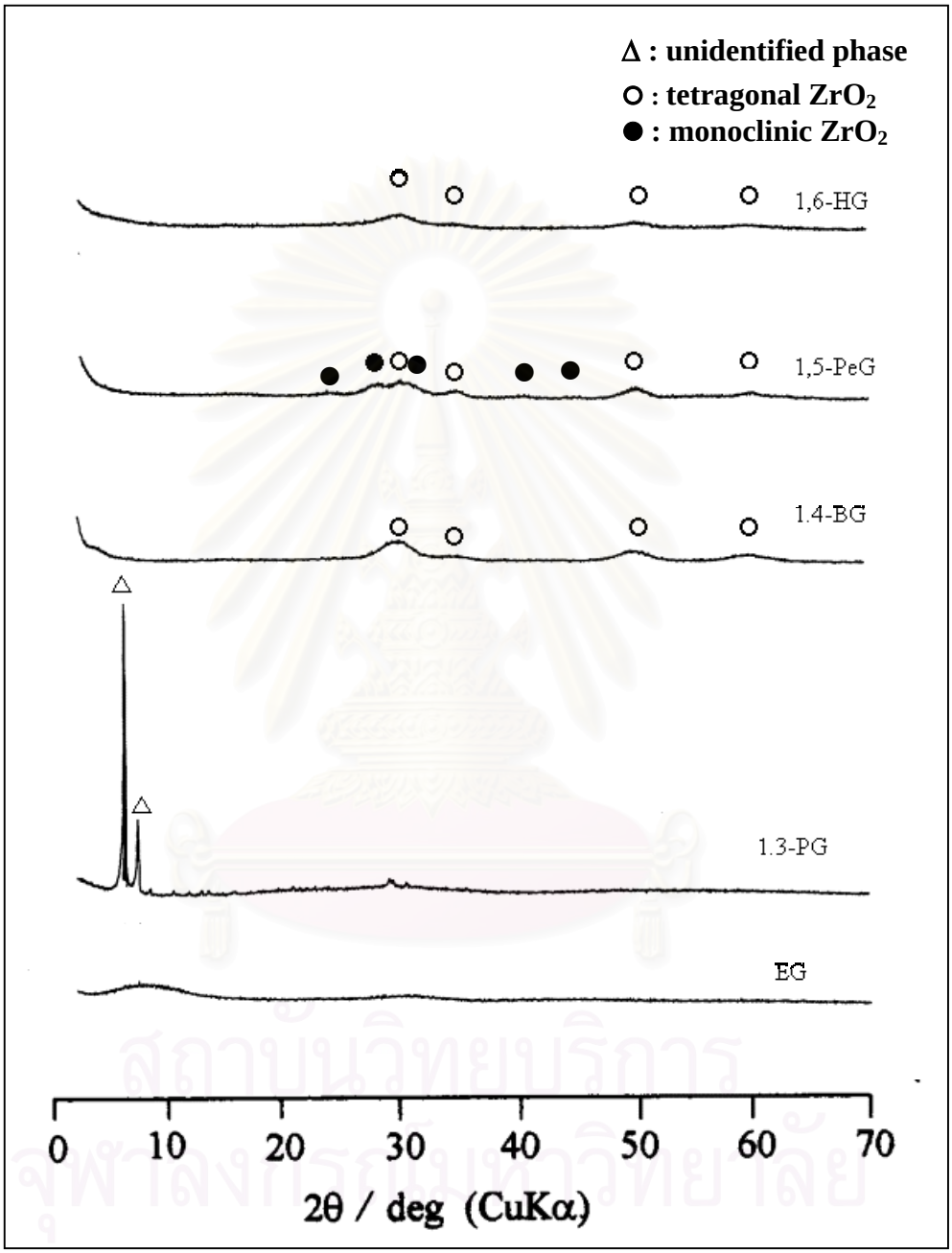

Figure 5.1 XRD patterns of the products obtained by the reaction of zirconium *n*-propoxide in various glycols specified in the figure at 300°C for 2 h.

Besides glycols, the reactions of ZNP in various aminoalcohols were also examined and the XRD patterns are depicted in Figure 5.2. The reaction in ethanol amine (2-aminoethanol) gave a homogeneous solution without formation of any solid product. Alkoxyl exchange reaction of ZNP with the solvent alcohol takes place at lower temperature yielding zirconium 2-aminoethoxide. High coordinating ability of the amino group to zirconium ion stabilizes this intermediate phase. Moreover, inductive effect of the amino group inhibits the cleavage of C-O bonds of the intermediate so that the crystalline zirconia was not formed in 2-aminoethanol. The other aminoalcohols used in this study can be considered to be alkyl (i.e., methyl or 2-hydroxyethyl) derivatives of ethanol amine. The use of these solvents gave crystalline zirconia. Tetragonal phase was formed for the reaction in diethanolamine, triethanolamine and *N*,*N*-dimethylethanolamine, whereas the reaction in *N*-methyl ethanolamine yielded the mixture of tetragonal and monoclinic zirconia. Substitution of hydrogen of the NH_2 group of monoethanolamine with the alkyl group or hydroxyalkyl group decreases both the inductive effect and coordination ability of the amino group. The coordination ability of amino group to zirconium ion decreased due to the steric effect of the alkyl or hydroxyalkyl group. Therefore, the cleavage of C-O bonds of this species takes place yielding crystalline zirconia.

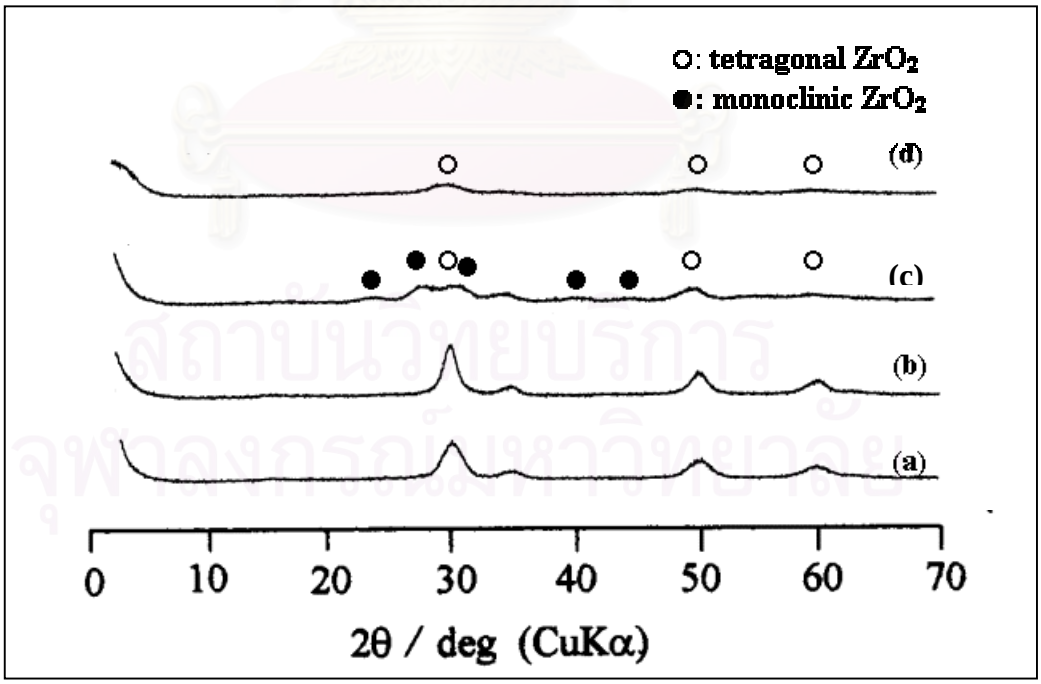

Figure 5.2 XRD patterns of the products obtained by the reaction of zirconium *n*-propoxide in (a) diethanolamine, (b) triethanolamine, (c) *N*-methylethanolamine, (d) *N*,*N*-dimethylethanolamine

5.2 The crystallization mechanism of zirconia

Effect of the reaction medium and reaction temperature on the phase of the products was examined and the results are summarized in Table 5.1.

When the reaction was carried out in 1,4-BG at low temperatures (200-280 ^{o}C), a novel unidentified crystalline phase was obtained and this phase will be called phase A hereafter. The XRD pattern of this phase is shown in Figure 5.3. The XRD data of phase A are given in Table 5.2. Phase A belonged to the triclinic crystal system with the body-centered Bravais lattice. Pure tetragonal zirconia was obtained by the reaction in 1,4-butanediol at 290^{o}C.

Table 5.1. Phases present in the products obtained by the glycothermal reaction of zirconium *n*-propoxide[a]

Reaction medium[b]	Reaction temperature (^{o}C)					
	200	230	250	280	290	300
EG		Am	Am			Am
1,3-PG			A			A
1,4-BG	A		A	A, T	T	T
1,5-PeG	YCS		YCS	T		T, M
1,6-HG		YCS	YCS			T

[a]Am, amorphous; T, tetragonal zirconia; M, monoclinic zirconia; A, unidentified crystalline phase called phase A; YCS, yellow clear homogeneous solution without any solid product.
[b]EG, ethylene glycol; 1,3-PG, 1,3-propanediol; 1,4-BG, 1,4-butanediol; 1,5-PeG, 1,5-pentanediol; 1,6-HG, 1,6-hexanediol.

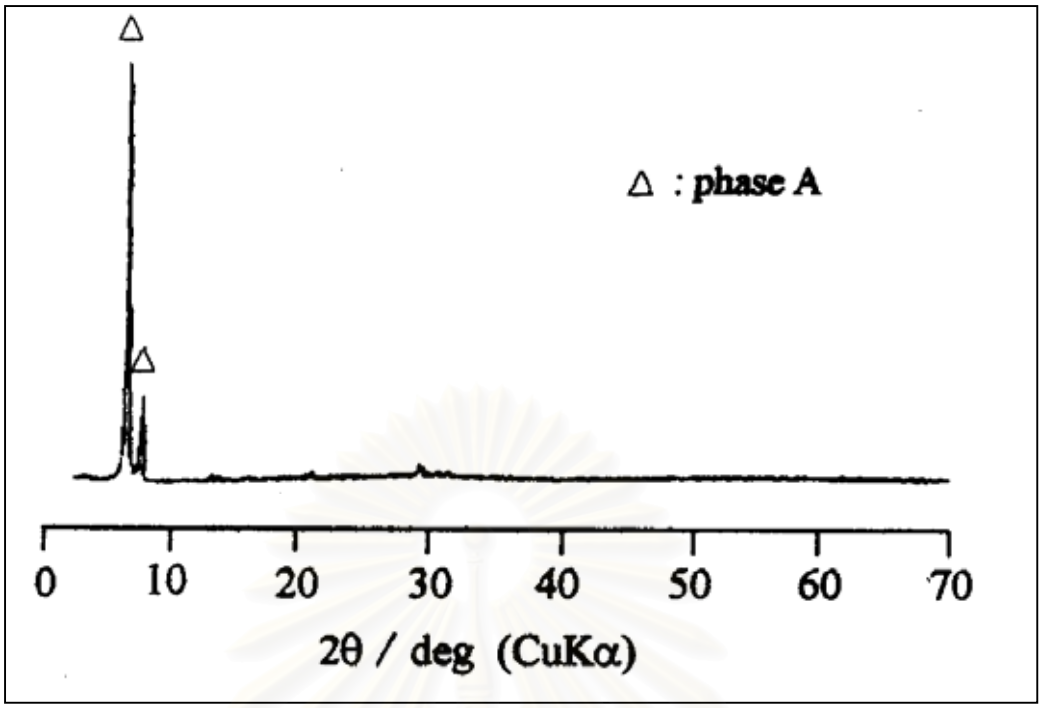

Figure 5.3 The XRD pattern of product obtained from the reaction of zirconium tetra *n*-propoxide in 1,4-butanediol at 250°C for 2 h.

Table 5.2 XRD data for the phase A.

d(Å)	I/I_0	h	k	l
12.1287	100	1	1	0
10.5865	21	0	2	0
6.4631	1	1	3	0
6.1822	1	0	1	1
5.3471	1	0	4	0
4.1469	2	3	3	0
3.0250	4	3	1	-2
2.9940	3	-2	2	2
2.8848	2	1	5	-2
2.8075	2	2	7	-1
2.5436	1	-2	7	1

$a_o = 15.324$ $b_o = 21.734$ $c_o = 6.916$ $\alpha = 98.55$ $\beta = 96.96$ $\gamma = 88.97$

d, interplanar d-spacing; I/Io, relative intensity

h,k,l are Miller indices used to label lattice plane

Figure 5.4 shows the SEM micrographs of products obtained in 1,4-BG and 1,5-PeG at 300°C for 2 h. The products prepared in 1,4-BG were spherical particles, while those obtained in 1,5-PeG were irregularly-shaped particles. These results suggest that the crystallization mechanisms of zirconia in 1,4-BG and 1,5-PeG are completely different.

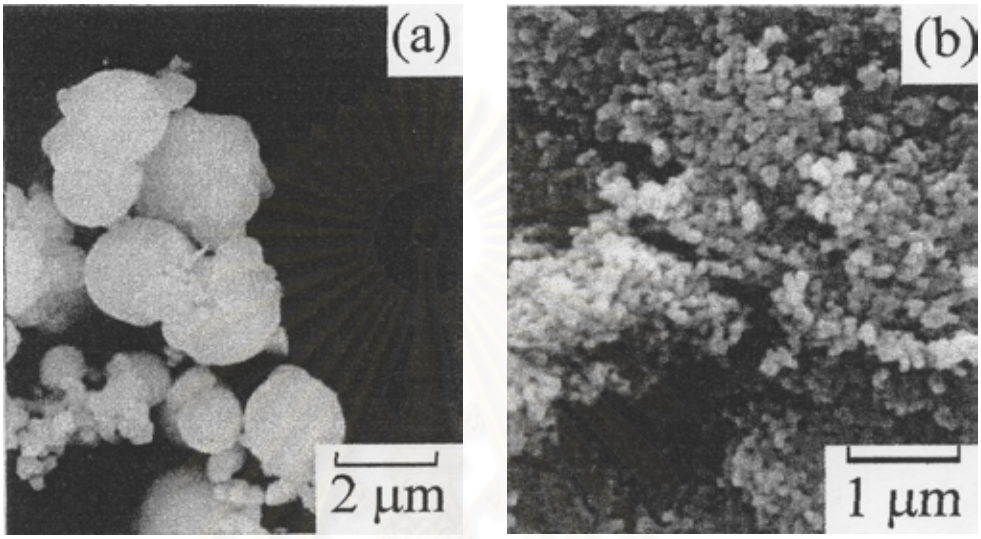

Figure 5.4 Scanning electron micrographs of products obtained by the reaction of zirconium *n*-propoxide at 300°C for 2 h in (a) 1,4-BG, (b) 1,5-PeG

The reaction of ZNP in 1,5-PeG or 1,6-HG at 250°C yielded a yellow clear homogeneous solution without any solid product. On addition of drops of water into the clear homogeneous solution, white precipitates immediately formed, indicating that the solution contained zirconium in the form of alkoxides (zirconium glycoxides). Zirconium glycoxide is formed as an intermediate by transesterification of ZNP and glycol (Inoue *et al.*, 1993). In these two solvents, crystalline zirconia was obtained at relatively high temperatures suggesting that the formation of crystalline zirconia in 1,5-PeG and 1,6-HG proceeded by the decomposition of a soluble intermediate (i.e., glycoxides).

Figure 5.5 shows the XRD patterns of the products obtained by the reaction in 1,4-BG at 280°C for various reaction times. When the reaction was quenched just after the reaction temperature reached 280°C, phase A was the sole crystalline product. The XRD pattern of the 1 h sample (Figure 5.5(b)) shows slight humps at 2

θ 30°, 50° and 60° indicating the presence of a small amount of tetragonal zirconia. With the increase in the reaction time, zirconia peaks became gradually apparent with the expense of the peak intensities of Phase A, and XRD pure tetragonal zirconia was obtained by the reaction for 4 h. Therefore, phase A gradually transformed into tetragonal zirconia at this reaction temperature.

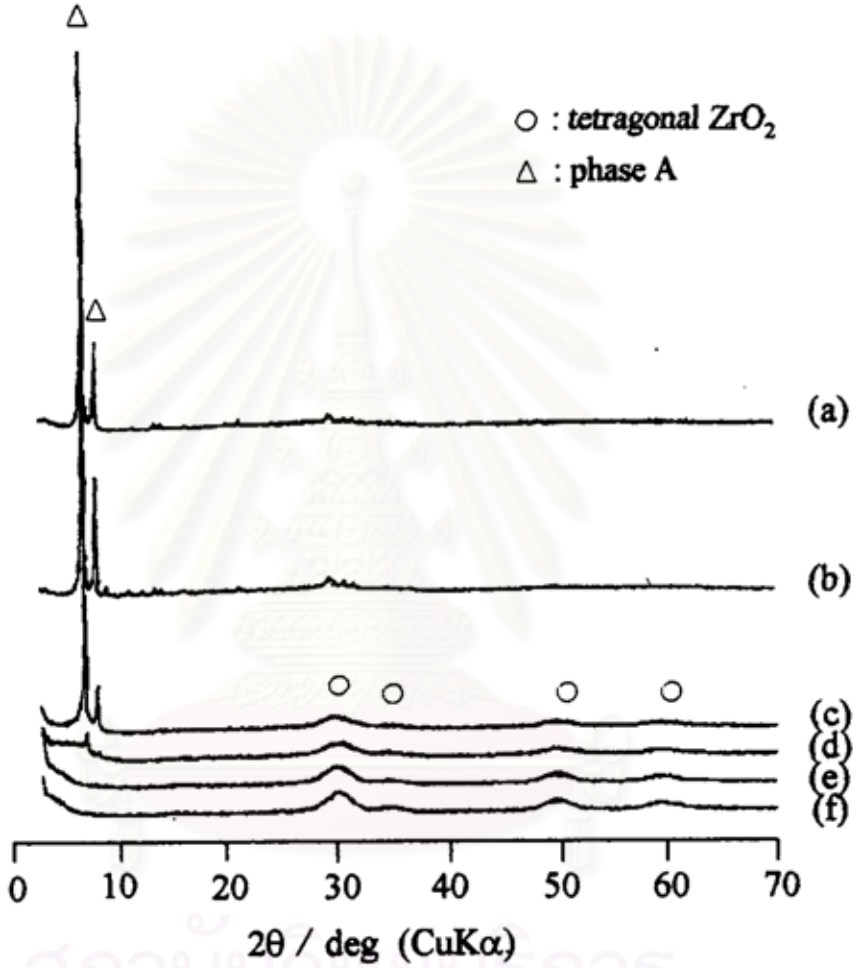

Figure 5.5 XRD patterns of the products obtained by the reaction of zirconium *n*-propoxide in 1,4-BG at 280°C for (a) 0 h, (b) 1 h, (c) 2 h, (d) 3 h, (e) 4 h, (f) 8 h.

In accordance with these results, scanning electron micrographs of the products (Figure 5.6) showed the morphological change of the products with prolonged reaction time at 280°C. The product obtained by quenching the reaction just after the autoclave reached 280°C was composed of two types of particles, hexagonal plate and a small amount of needle-like particles (Figure 5.6(a)). The former seems to be typical morphology of phase A and the latter seems to be another

unidentified phase. In the product of 1 h reaction, the amount of the needle-like particle increased (Figure 5.6(b)), and the XRD pattern of the product showed additional peaks at 2 θ 9.3^{o}, 11.2^{o} and 12.5^{o} besides the peaks due to phase A. The SEM image (Figure 5.6(b)) also showed the presence of the spherical particles, which is the typical morphology of the zirconia obtained by the glycothermal method. With prolonged reaction time, amount of spherical particles (i.e., tetragonal zirconia) gradually increased. Another important change in the product morphology was that particles having well-defined crystal shape disappeared, which was accompanied by formation of the particles with curved surface or irregularly-shaped particles. This result suggests that phase A transformed into an amorphous phase before transformation into zirconia crystal. Figure 5.6(d) shows that a spherical particle is nested in an irregularly-shaped particle, suggesting that solid-phase transformation mechanisms took place for the formation of spherical particles of zirconia. Although the XRD pattern showed the presence of only tetragonal phase for the reaction time of 8 h, a small amount of the irregularly-shaped particles still remained in the product (Figure 5.6(f)). Because of the difference in specific volume of the amorphous phase and tetragonal zirconia, particle should shrunk, and spherical secondary particles are formed to minimize the interface area between tetragonal zirconia and the amorphous phase. In this mechanism, a huge number of nuclei of tetragonal zirconia were formed in the amorphous phase. Because of large surface energy of small primary particles, primary particles are tightly aggregated, forming secondary particles.

These results suggest that phase A initially transformed to amorphous phase and tetragonal zirconia subsequently crystallized from the amorphous phase through the solid state transformation mechanism. The presence of the relatively stable intermediate phases seems to be the reason for the high crystallization temperature of zirconia as compared with other oxides such as titania and zinc oxide where metal glycoxides directly decompose into the oxide phases under the glycothermal conditions.

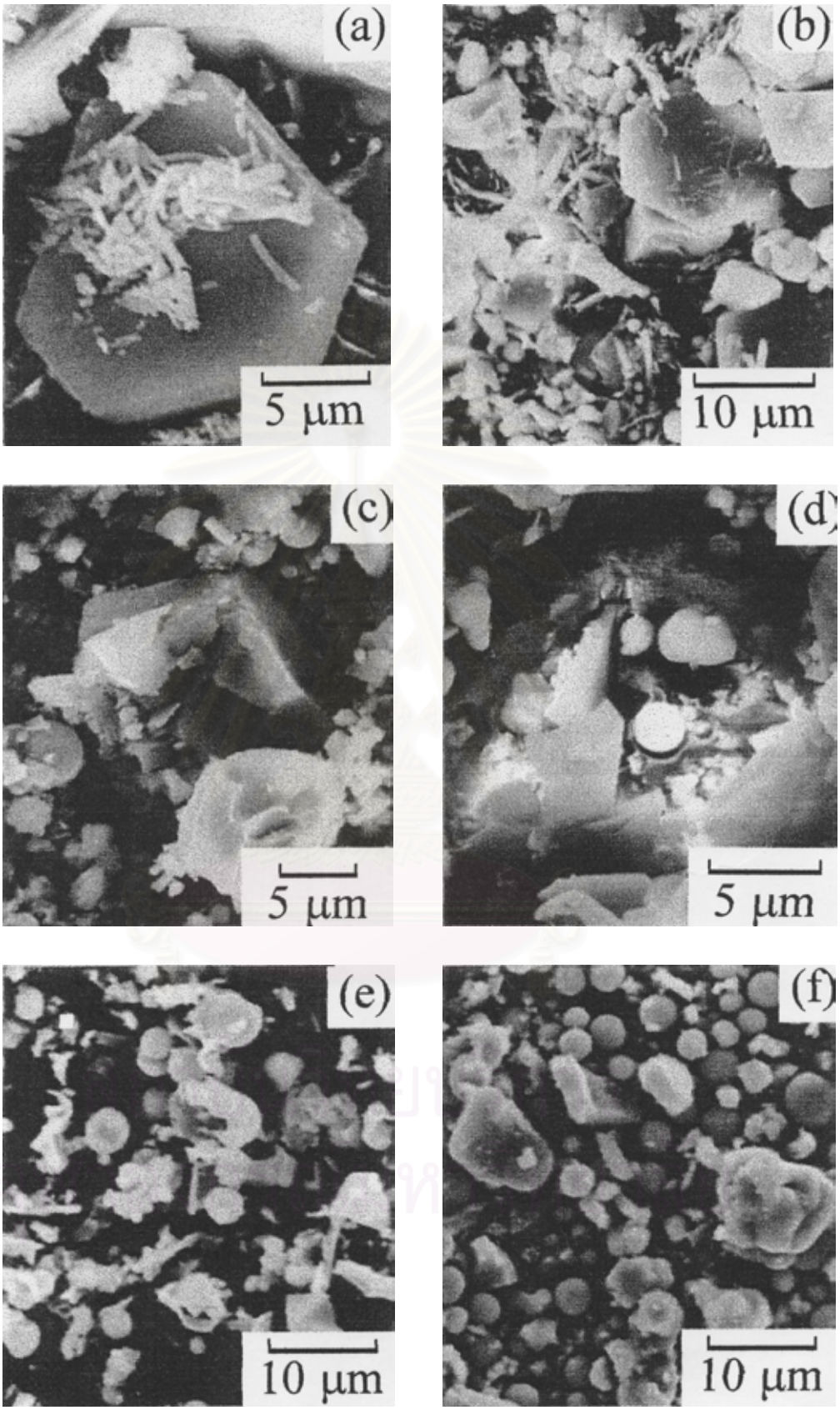

Figure 5.6 Scanning electron micrographs of the products obtained in 1,4-BG at 280 ^{o}C for (a) 0 h, (b) 1 h, (c) 2 h, (d) 3 h, (e) 4 h, (f) 8 h.

Scanning electron micrographs of the products obtained in 1,3-PG and 1,4-BG at 250°C are shown in Figure 5.7 and 5.8, respectively. The reaction in 1,3-PG yielded the product comprised of much smaller particles. On the other hand, the product obtained in 1,4-BG was composed of large crystals together with a small amount of needle-like particles, indicating that the morphologies of the phase A depended on the reaction conditions. More explanation about SEM micrographs will be discussed together with the results from TG&DTA later.

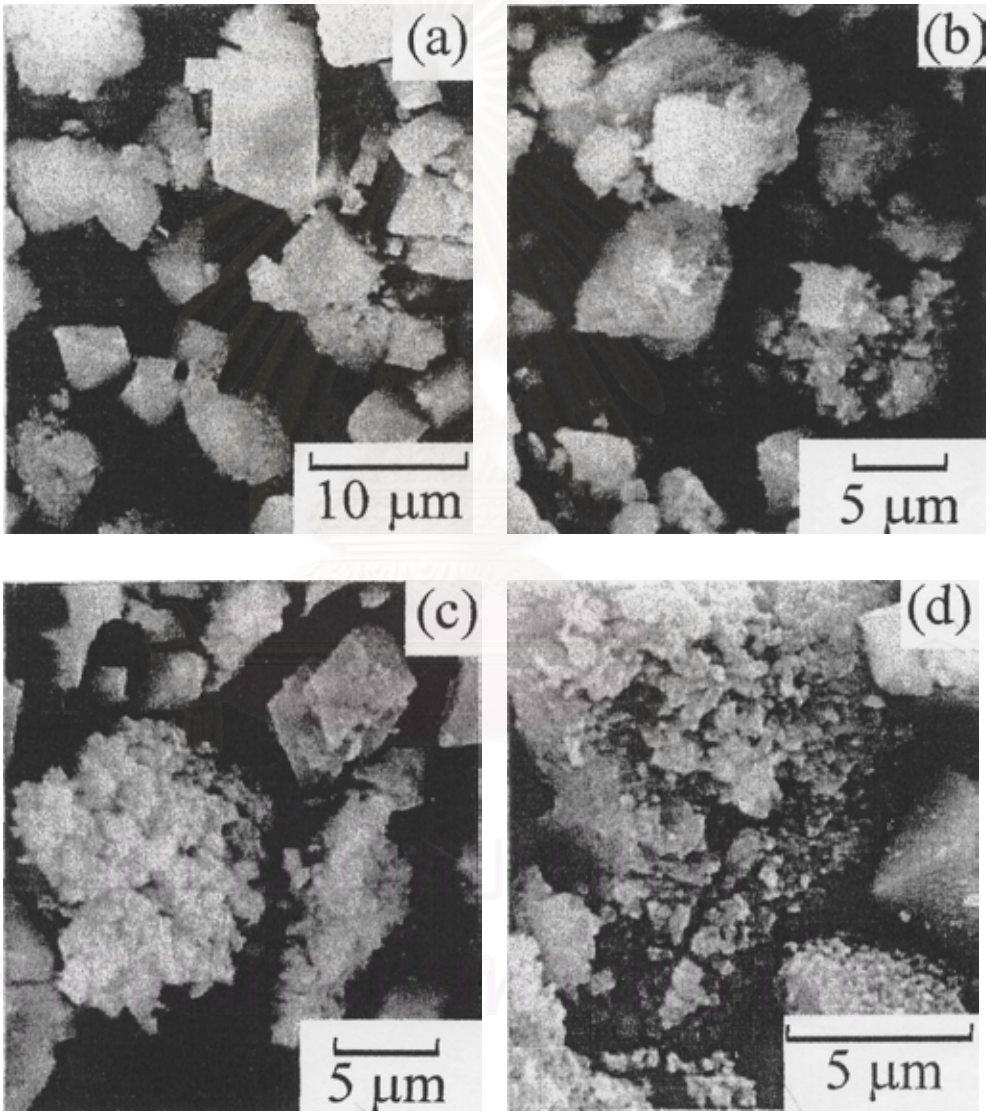

Figure 5.7 Scanning electron micrographs of the products obtained at 250°C for 2 h in 1,3-PG; (a) uncalcined , (b) calcined at 280°C, (c) calcined at 300°C and (d) calcined at 400°C.

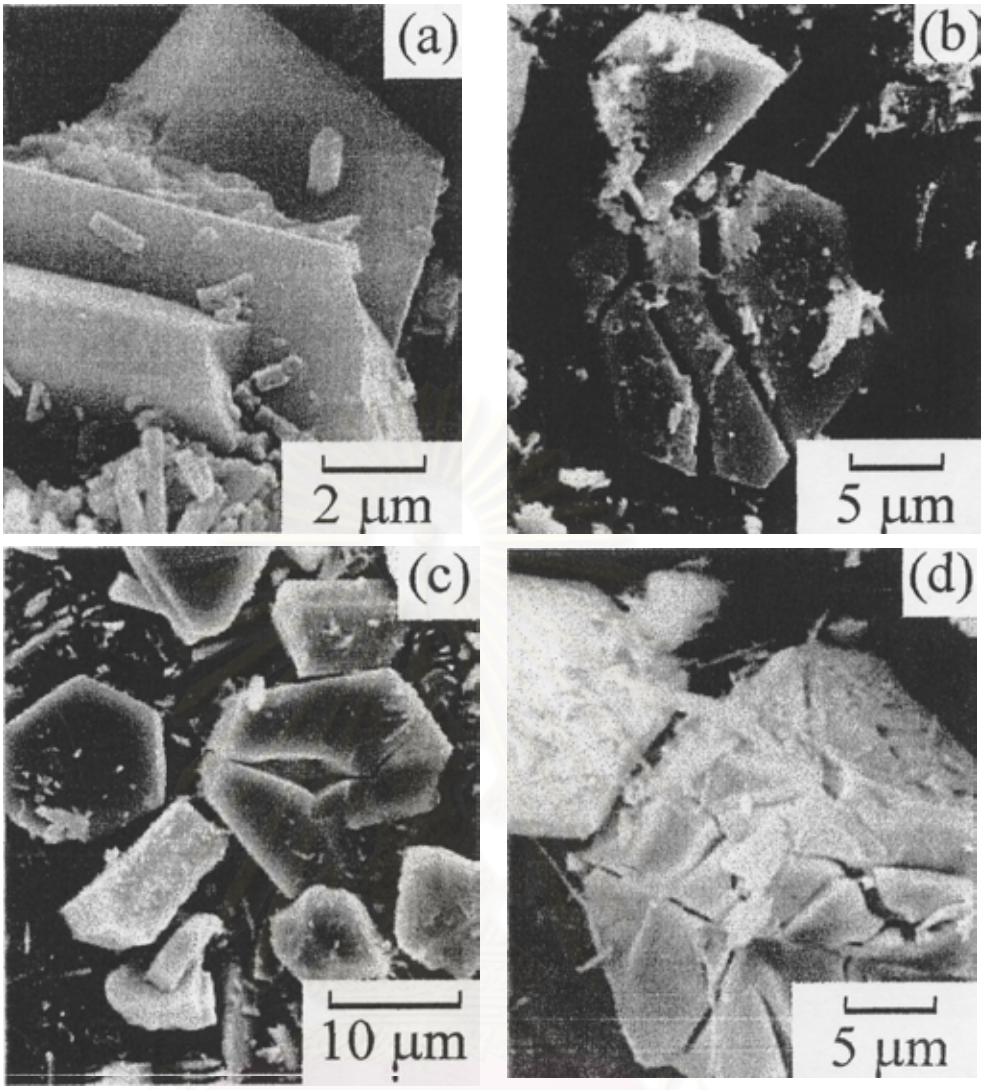

Figure 5.8 Scanning electron micrographs of the products obtained at 250°C for 2 h in 1,4-BG; (a) uncalcined, (b) calcined at 280°C, (c) calcined at 300°C and (d) calcined at 400°C.

The IR spectrum of zirconia obtained in 1,4-BG at 300°C (Figure 5.9) was essentially featureless, although this product contained a small amount of glycol moieties. Figures 5.10 and 5.11 show the IR spectra of phase A products obtained in 1,3-PG and 1,4-BG, respectively. The IR bands observed in the uncalcined sample can be assigned to the glycol moieties since peak positions are in good agreement with those of liquid glycols. No indication of the presence of the propyl group originating from the starting material, ZNP, was obtained. This result suggests that alkoxyl exchange reaction of propoxyl groups of ZNP with glycol took place in the first stage of the reaction and that phase A contains a large amount of glycol moieties in the crystal lattice.

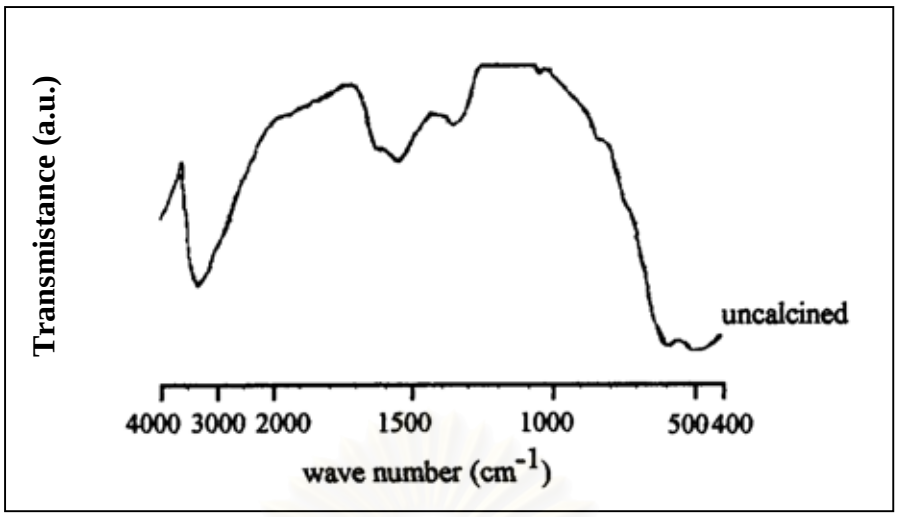

Figure 5.9 IR spectrum of the product obtained in 1,4-butanediol for 2 h at 300°C

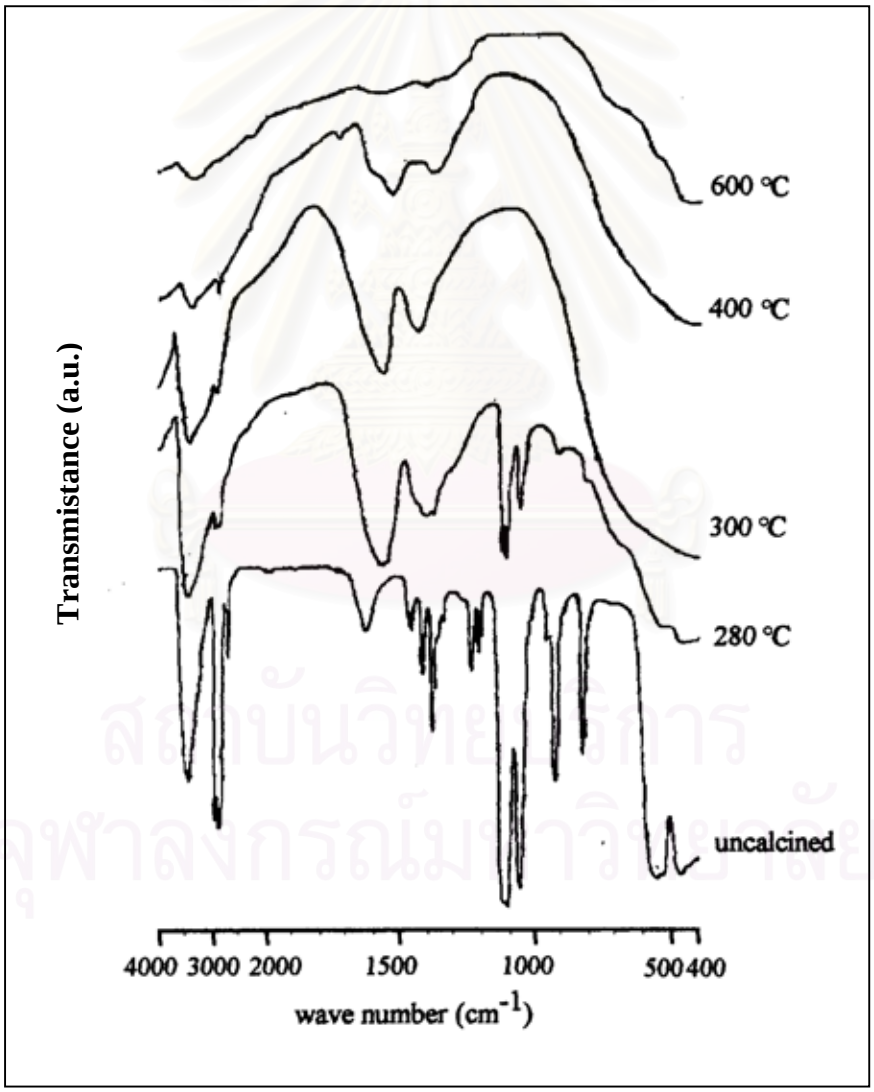

Figure 5.10 IR spectra of the product obtained in 1,3-propanediol for 2 h at 250°C and the samples obtained by calcination thereof at temperature specified in the figure

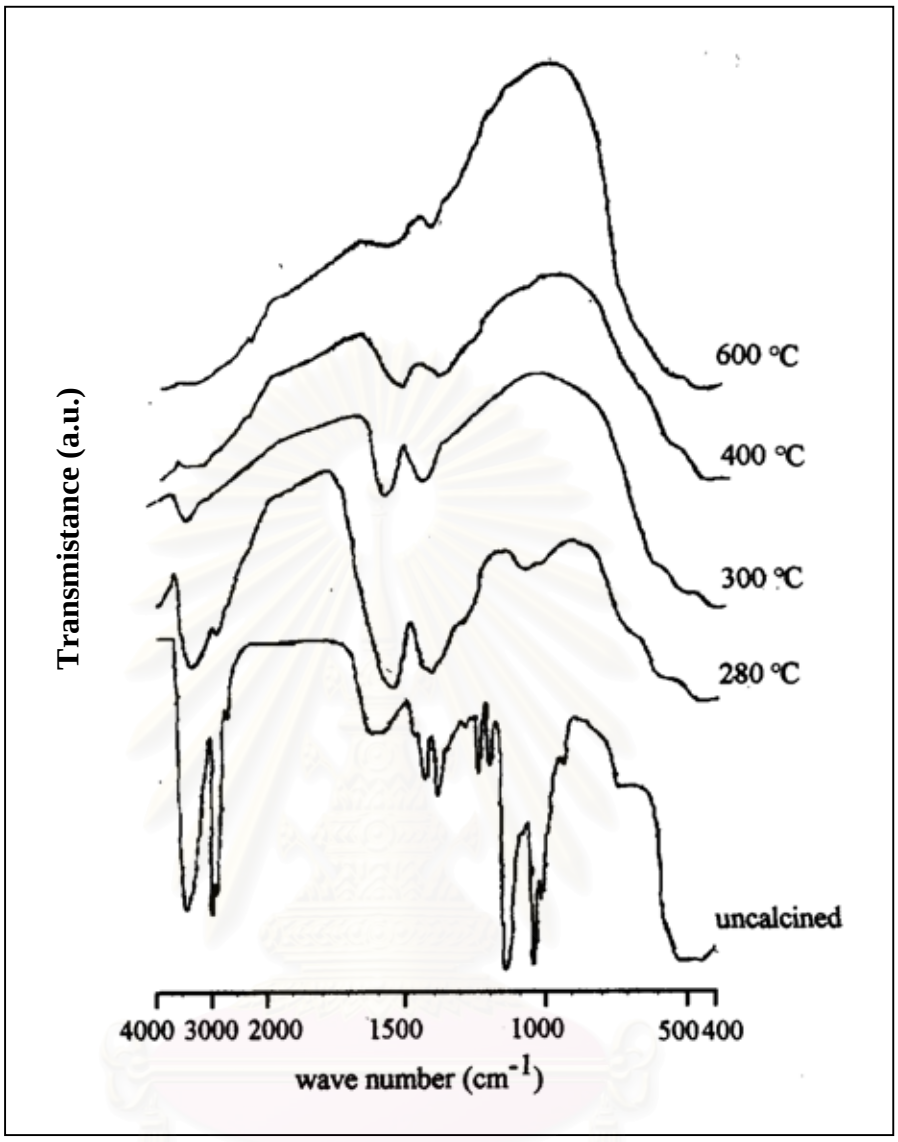

Figure 5.11 IR spectra of the product obtained in 1,4-butanediol for 2 h at 250°C and the samples obtained by calcination thereof at temperature specified in the figure

The thermal analysis for the products obtained in 1,4-BG at 300°C (tetragonal zirconia) is shown in Figure 5.12. The weight decrease at around 80°C was associated with an endothermic response in DTA, and is due to the desorption of physisorbed species such as methanol and water. At the temperature range of 270-310°C, another weight decrease was observed. Since this process was accompanied by an exothermic response in DTA, it is attributed to the combustion of the glycol moieties remaining on the surface of the product.

The thermal analyses for phase A obtained in 1,3-PG and 1,4-BG at 250°C are shown in Figures 5.13 and 5.14, respectively. A small endothermic peak at 132°C for the product obtained in 1,4-BG was ascribed to the desorption of adsorbed glycol molecules. This product exhibited two exothermic peaks at 316°C and 540 °C associated with large weight losses. On the other hand, Phase A obtained in 1,3-PG showed a large weight decrease started at ~300°C. Because the flame leaped from the sample, the temperature could not be controlled at this region. This weight loss can be attributed to the combustion of the glycol moieties incorporated into the crystals. Another small weight decrease was obtained at ~ 615°C.

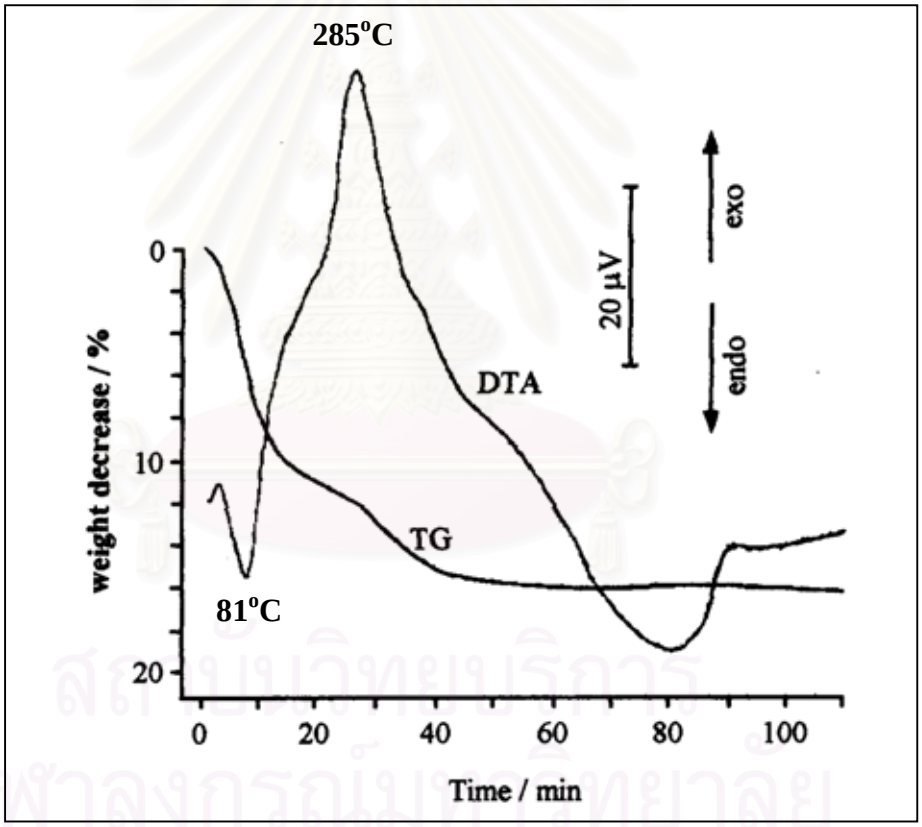

Figure 5.12 Thermal analyses of the product obtained in 1,4-butanediol at 300°C for 2 h: at a heating rate of 10°C min^{-1} in a 40 ml min^{-1} flow of dried air.

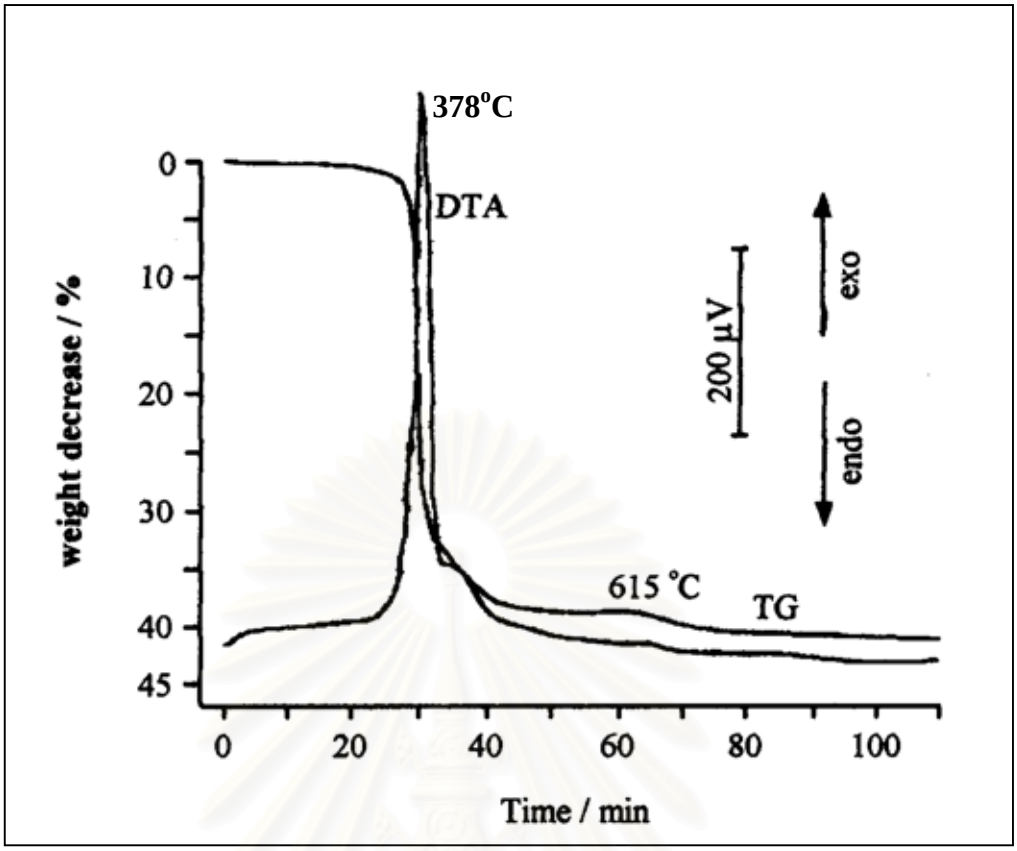

Figure 5.13 Thermal analyses of the product obtained in 1,3-propanediol for 2 h at 250 °C: heating rate of 10°C min^{-1} in a 40 ml min^{-1} flow of dried air.

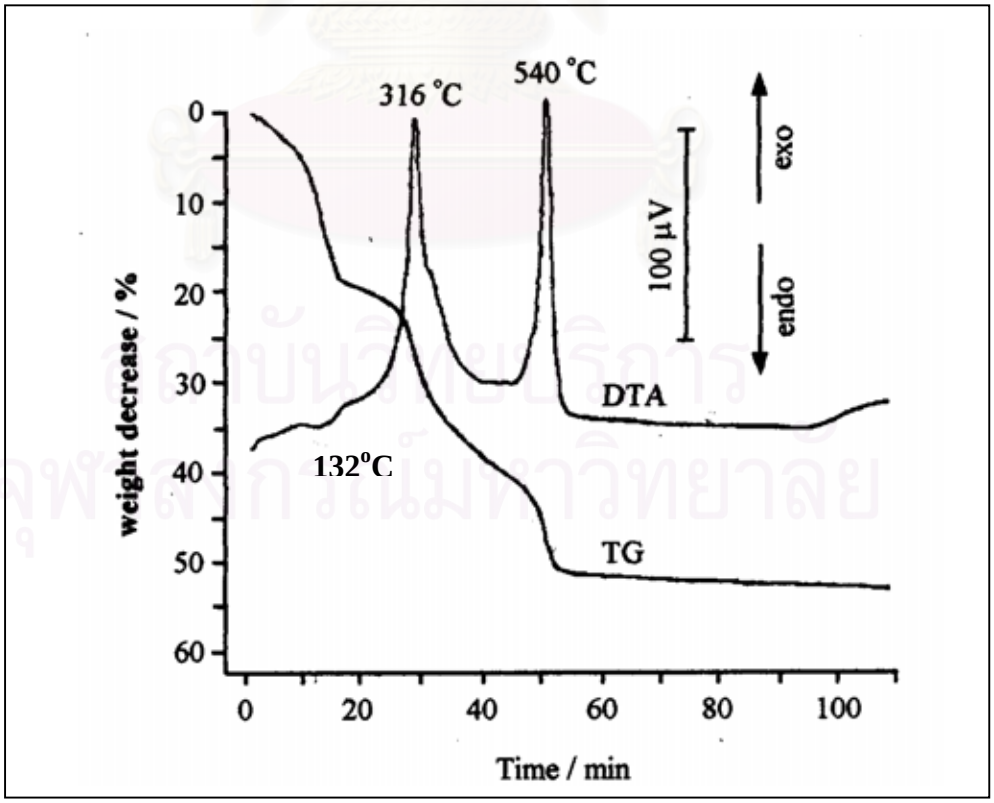

Figure 5.14 Thermal analyses of the product obtained in 1.4-buatnediol at 250°C for 2 h: at a heating rate of 10°C min^{-1} in a 40 ml min^{-1} flow of dried air.

Since phase A products obtained in 1,3-PG and 1,4-BG gave the different TGA and DTA traces, the thermal decomposition behavior of these two samples were examined by XRD and IR. Figures 5.15 and 5.16 show the XRD patterns of Phase A and the products obtained by calcination at various temperatures for 1 h. The XRD patterns of the products obtained by the reaction of ZNP in 1,3-PG and 1,4-BG at 250°C are essentially identical to each other. Partial decomposition of phase A took place by calcination at 280°C yielding an essentially amorphous product. Tetragonal zirconia was detected in the products calcined at 300°C and the intensity gradually increased with an increase in the calcination temperature. This crystallization temperature of the tetragonal zirconia is similar to that required for the reaction of ZNP in 1,4-BG, which leads to an idea that under glycothermal conditions phase A was thermally decomposed into the amorphous phase, from which tetragonal zirconia crystallized.

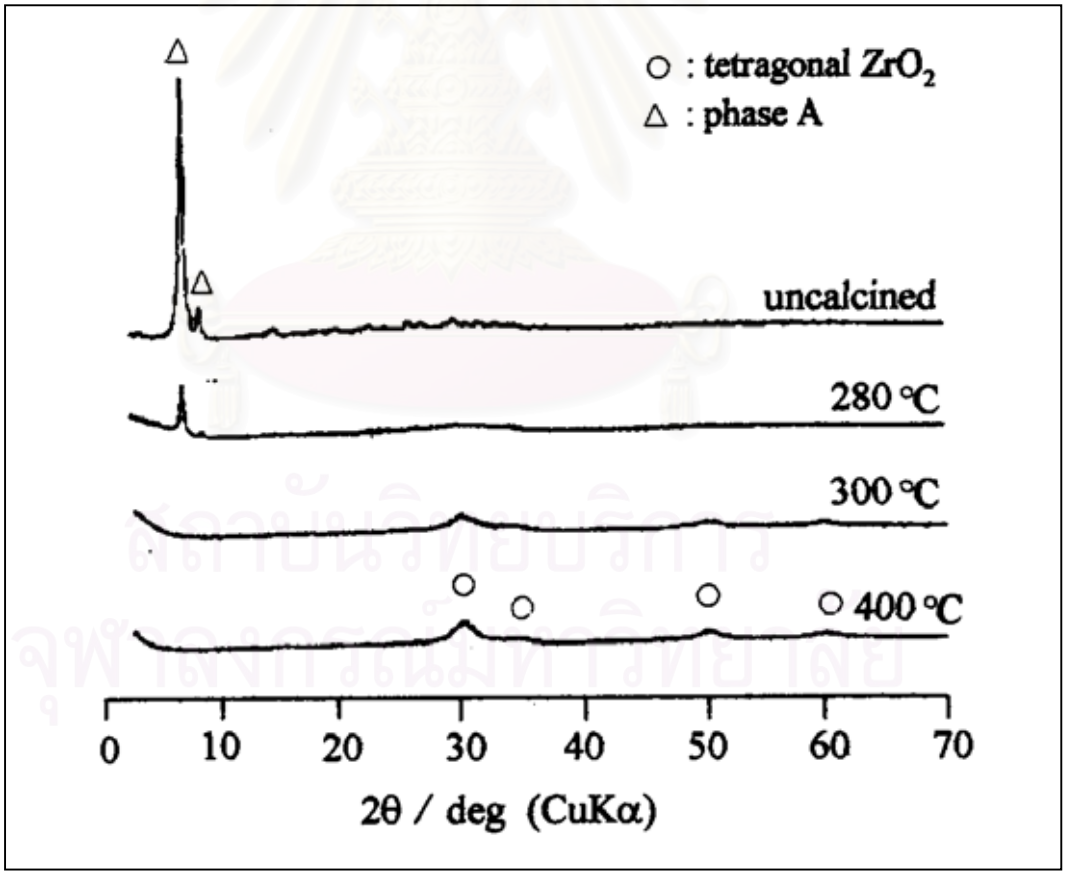

Figure 5.15 XRD patterns for the sample obtained by the reaction at 250°C for 2 h in 1,3-propanediol and the samples obtained by calcination thereof at temperature specified in the figure

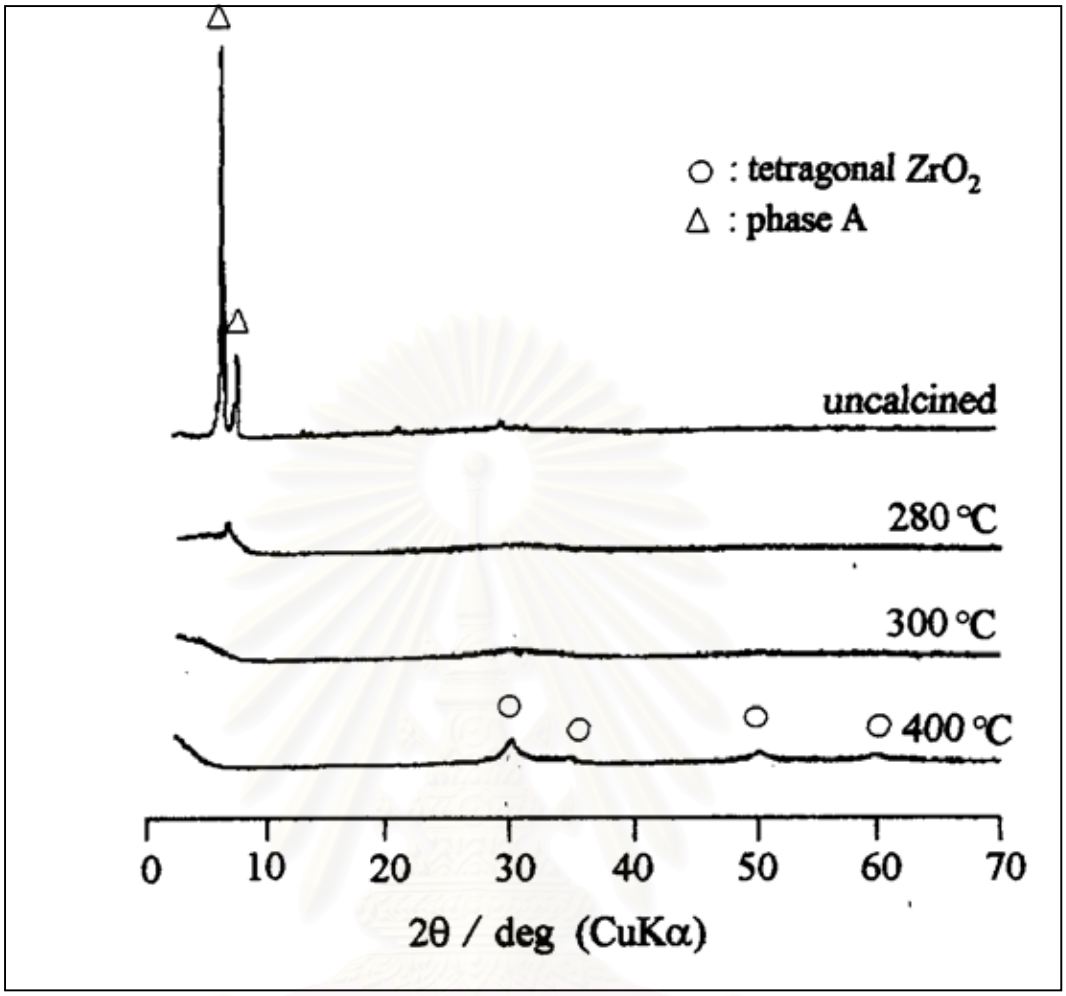

Figure 5.16 XRD patterns for the sample obtained by the reaction at 250°C in 1,4-butanediol and the samples obtained by calcination thereof at temperature specified in the figure

Comparison of the IR spectra of the samples calcined at 280°C in Figure 5.10 and 5.11 clearly shows that 1,4-BG moieties are more easily decomposed than 1,3-PG moieties. This can be attributed to the fact that decomposition of the former species is assisted by participation of the intramolecular hydroxyl group, yielding tetrahydrofuran as the decomposition product (Inoue *et al.*, 1993).

For comparison, the XRD patterns of the samples obtained by quenching at various temperatures during thermal analyses were investigated and shown in Figures 5.17 and 5.18. The sample obtained by quenching at 370°C apparently exhibited an amorphous pattern, while the sample obtained by keeping at 300°C for 1 h (Figure

5.15 and 5.16) showed tetragonal pattern. However, the peaks due to the tetragonal phase gradually became sharp with the increase in heating temperature, suggesting very small crystallites of tetragonal zirconia were formed by thermal decomposition of phase A, and that crystal growth took place with increasing heating temperatures. In accordance with this argument, DTA of phase A did not show the exothermic peak due to crystallization of zirconia at this temperature range (400-600^{o}C). This result gave a sharp contrast against the amorphous products obtained by the precipitation method (Mercera *et al.*, 1990) or the sol-gel method (Bedio and Klabunde, 1997), which exhibit a sharp exothermic peak at the temperature range of 350-450^{o}C due to crystallization of tetragonal zirconia.

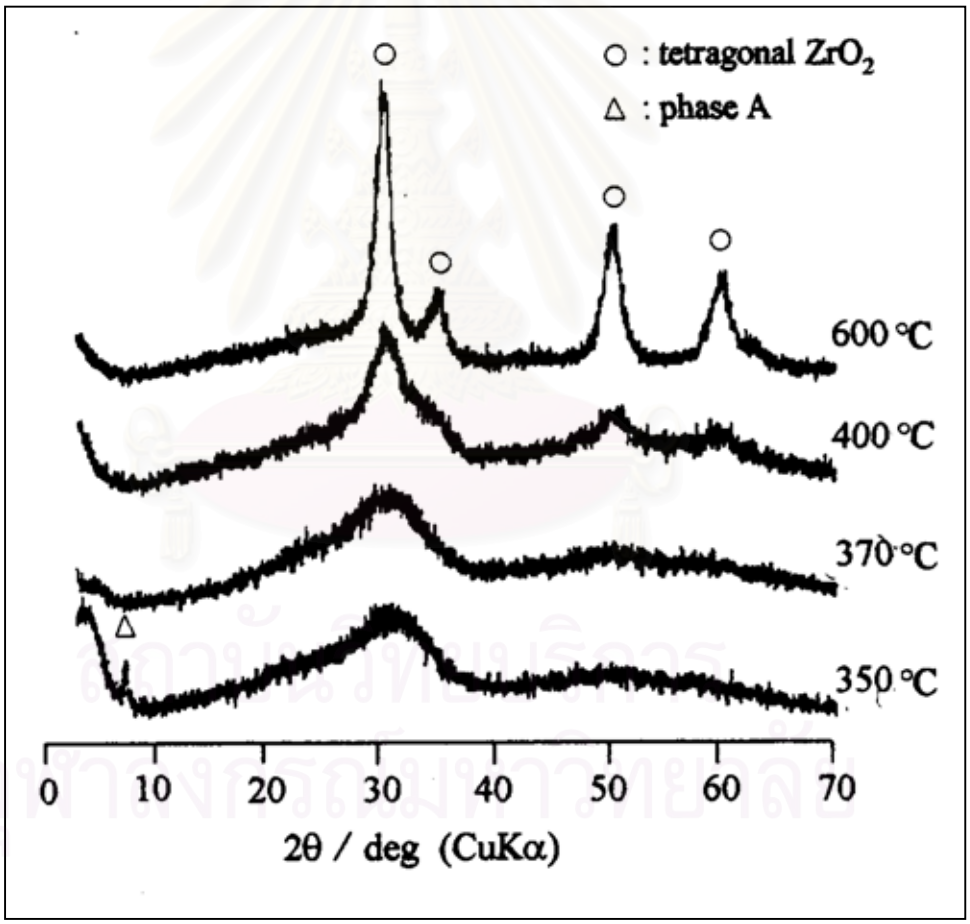

Figure 5.17 XRD patterns for the samples obtained by quenching at the temperature specified in the figure during the thermal analyses of Phase A. The original samples were obtained by the reaction of zirconium-*n* propoxide at 250^{o}C in 1,3-propanediol.

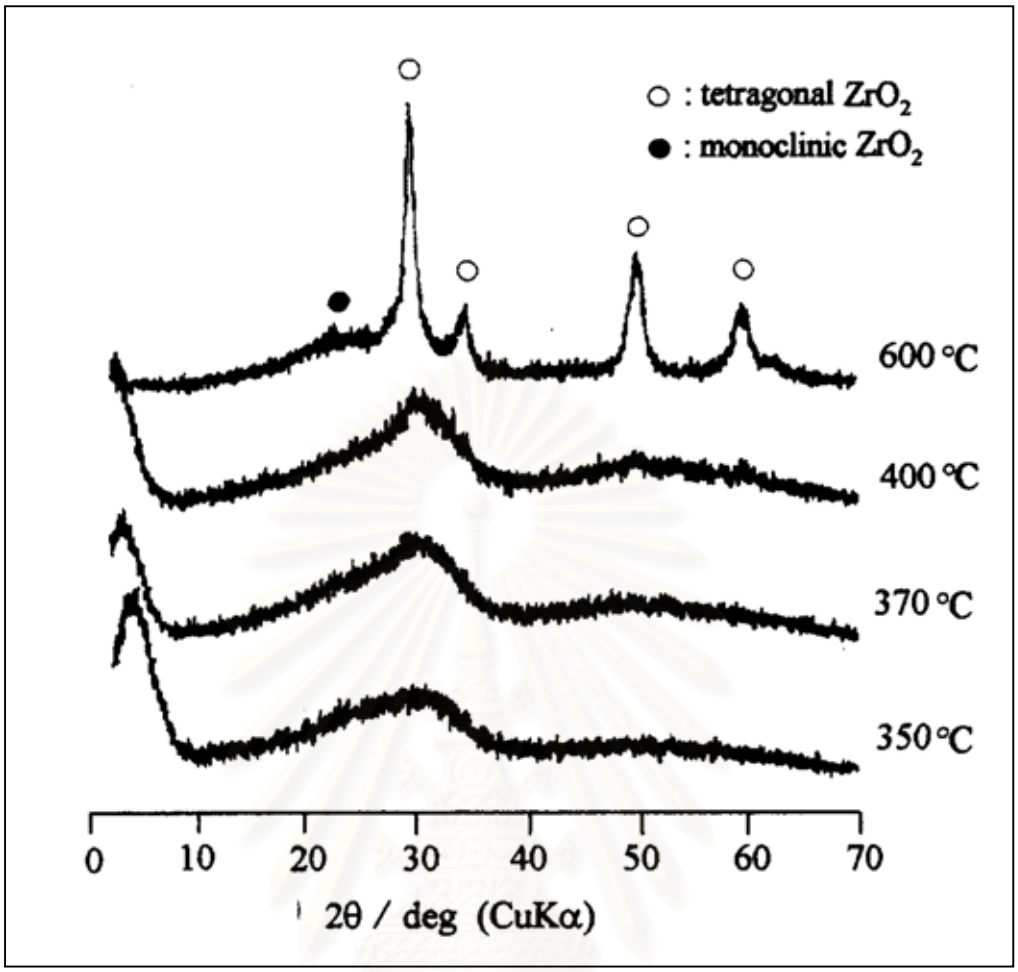

Figure 5.18 XRD patterns for the samples obtained by quenching at the temperature specified in the figure during the thermal analyses of Phase A. The originating samples were obtained by the reaction of zirconium-*n* propoxide at 250°C in 1,4-butanediol

SEM micrographs of phase A are shown in Figures 5.7 and 5.8. The Phase A product obtained in 1,4-BG was composed of large crystals. Calcination of this product gave pseudomorphs of Phase A. However, shrinkage took place, yielding cracks in the pseudomorphous particles. Pseudomorphous particles were also observed even after formation of tetragonal zirconia. On the other hand, the phase A product obtained in 1,3-PG comprised of agglomerates of smaller particles and calcination of this product did not alter the essential feature of the morphology. These results explain the difference in thermal decomposition profiles of the phase A products obtained in 1,3-PG and 1,4-BG (Figure 5.13 and 5.14). Since the former product had smaller crystal size with a large pore system between the crystals, the

organic molecules formed from phase A can easily diffuse out from the agglomerate of the smaller particles and combust in the gas phase giving the flames. On the other hand, the organic molecules formed from the phase A product obtained in 1,4-BG hardly diffuse out from the large pseudomorphous particles. Therefore, further decomposition of organic molecules took place remaining carbonaceous materials inside the particles while smaller hydrogen and water molecules diffused out from the particles. Since shrinkage of the particles takes place by the thermal decomposition of phase A because of the difference in true densities of phase A and zirconia, the pores should be formed in the pseudomorphous particles of phase A. However these pores should be so small that oxygen molecules cannot diffuse into the pore system. Therefore, the carbonaceous material cannot combust until sintering of zirconia particles takes place enlarging the pore size. In accordance with this argument, the elemental analysis of phase A calcined at 400^{o}C showed that the sample obtained in 1,4-BG contained much larger amount of carbon than that obtained in 1,3-PG (Table 5.3). Therefore, the weight-loss peak of the former sample at 540^{o}C was due to the combustion of the carbonaceous species remaining in micropore system of the large pseudomorphous particles.

Table 5.3 Elemental analysis of the phase A calcined at 400^{o}C.

Glycol	sample[a]	
	%C	%H
1,3-propanediol	1.59	0.42
1,4-butanediol	6.43	0.83

[a]Samples were obtained from the reaction of zirconium *n*-propoxide in glycol at 250^{o}C for 2 h and calcined in air at 400^{o}C for 1 h.

It should be noted that the experiments in section 5.3 and 5.4 are performed in Thailand. The differences of the synthesis parameters for the experiments in Thailand and in Japan are described in Experimental section.

In section 5.2, we found that the crystallization mechanism and the morphologies of zirconia prepared in 1,4-butanediol and in 1,5-pentanediol are different, therefore in this section we will examine the effect of synthesis conditions on the properties of zirconia obtained in both glycols

5.3 The effect of synthesis conditions on the properties of ZrO_2

5.3.1 Effect of drying condition

To examine the effect of drying conditions on zirconia powder, instead of washing the product with methanol followed by drying at room temperature, the glycol was removed from the autoclave by flashing at reaction temperature after 2 h reaction time. Thus, dried powders were obtained directly.

The morphologies of the powders obtained by the reaction of ZNP in 1,4-BG and 1,5-PeG with the drying by flashing off glycol are shown in Figures 5.19(b) and 5.20(b), respectively. For comparison, the SEM images of products dried in air after washing with methanol are given in Figures 5.19(a) and 5.20(a). When powders prepared in 1,5-PeG were dried by the former method, the as-prepared zirconia powder consists of fine particles and seems highly porous. However, morphology of powder obtained in 1,4-BG is not affected by the drying condition as seen in Figures 5.19(a) and 5.19(b). These results suggest that, for the case of zirconia prepared in 1,5-PeG, aggregation of particles occurred during the drying stage driven by the surface tension of the liquid between the particles (Iwamoto *et al.*, 2000). The size of the particles obtained by removal of the glycol at reaction temperature was apparently smaller than that obtained by the ordinary method. On the other hand, in 1,4-BG aggregation of particles took place during the reaction resulting in the formation of dense aggregates, which were difficult to break down in the drying stage.

The isotherm of zirconia powder prepared in 1,4-BG was of type IV, characteristic of a mesoporous texture (Figure 5.21). Drying by flashing did not alter the isotherm and pore size distributions. These results correspond well with our discussions of SEM images mentioned above that aggregation of these powders occurred during reaction rather than during drying. Apparently, the pore structure of the powders prepared in 1,4-BG cannot be altered by drying conditions.

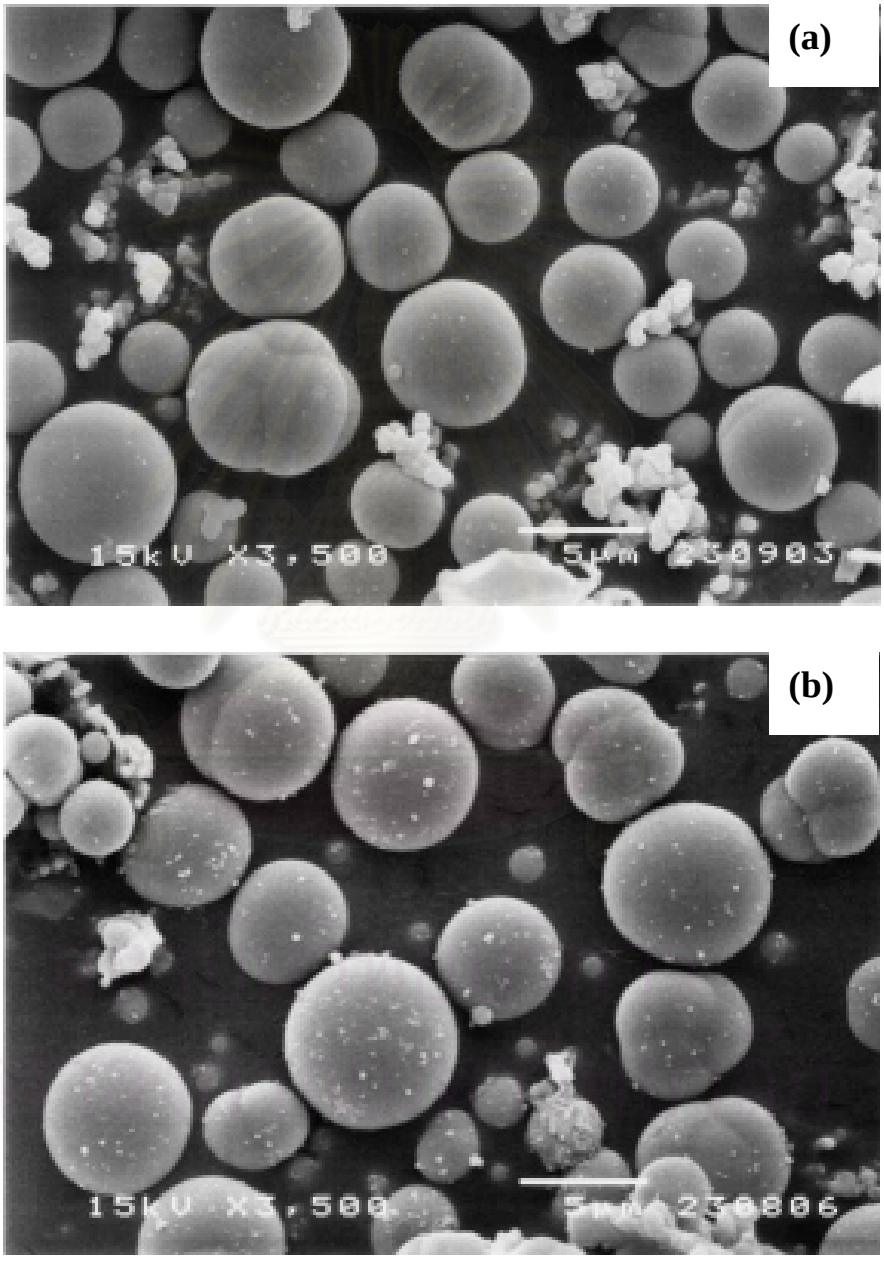

Figure 5.19 Scanning electron micrographs of powders obtained in 1,4-butanediol; (a) the product was dried in air after washing with methanol, (b) the product was dried by flash evaporation of the solvent from the autoclave at 300^{o}C after the reaction for 2 h.

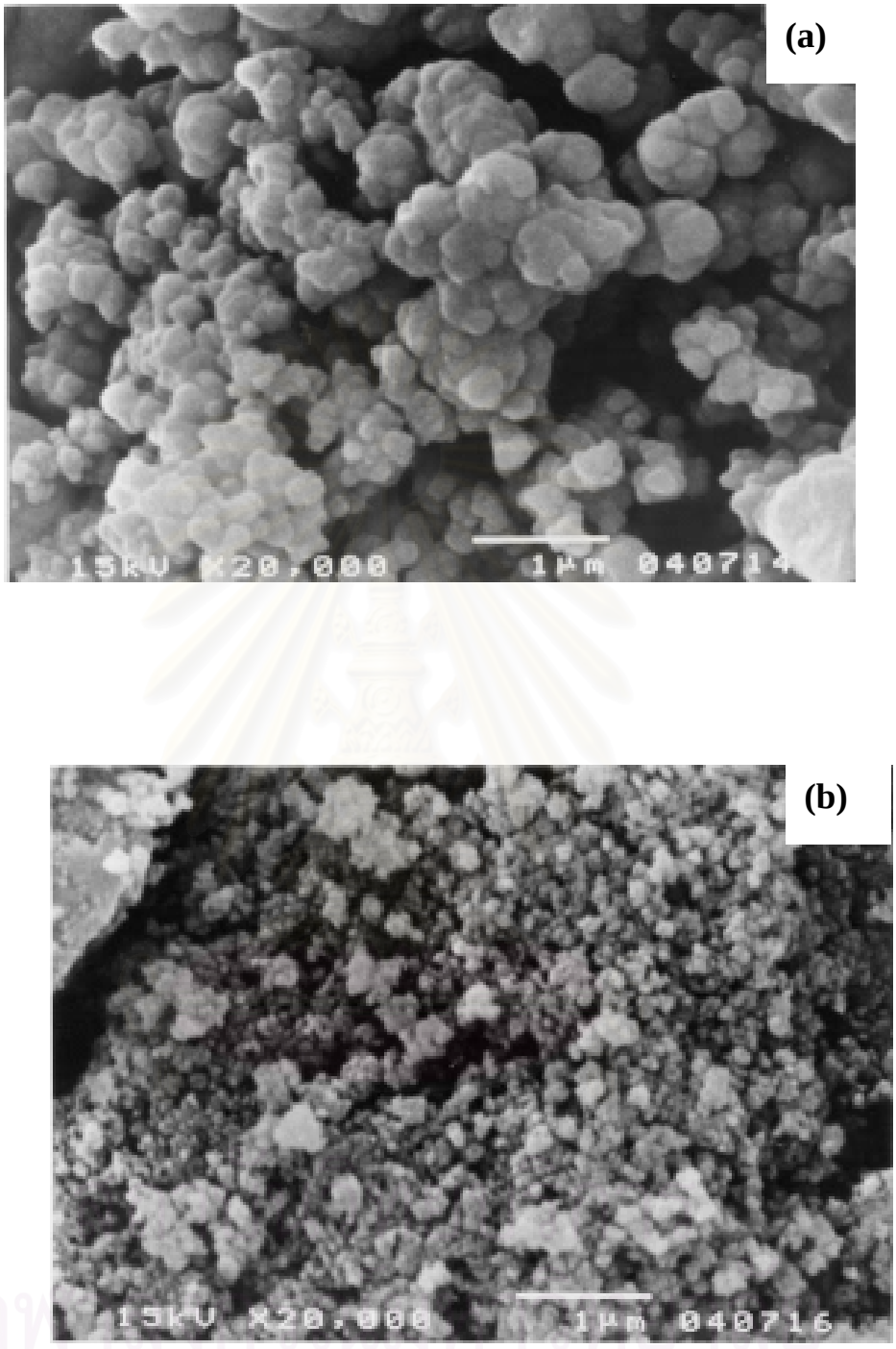

Figure 5.20 Scanning electron micrographs of powders obtained in 1,5-pentanediol; (a) the product was dried in air after washing with methanol, (b) the product was dried by flash evaporation of the solvent from the autoclave at 300^{o}C after the reaction for 2 h.

Typical adsorption/desorption isotherms of zirconia powders obtained in 1,5-PeG with different drying conditions are depicted in Figure 5.22, which shows that the type of isotherm and hysteresis loop changed dramatically with the drying condition. When powders were dried by removal of the glycol at reaction temperature instead of washing in methanol and air-drying, the isotherm of the powder changed from type I to type IV (BDDT classification) (Gregg and Sing, 1982) with the emergence of a hysteresis loop. The overlap of adsorption and desorption curves (Figure 5.22(a)) in the isotherm for the product washed in methanol and air-dried indicates the existence of many very narrow micropores in the powder (see Figure 5.21(c)). No hysteresis loop was observed in this product because the formation of a hysteresis loop is due to capillary condensation in mesopores.

As seen in Figure 5.22(d), the type IV isotherm with a type-H1 hysteresis loop (IUPAC nomenclature) (Gregg and Sing, 1982) is appropriate to powders with both mesopores and macropores. This change corresponds to an increase of modal pore diameter to around 3 nm for the powder dried by removal of the glycol at reaction temperature. These results suggest that the pore system of zirconia prepared in 1,5-PeG is improved when the glycol was evaporated and removed at reaction temperature because aggregation during drying is prevented.

Figure 5.23 shows the TEM micropraghs of zirconia obtained in 1,5-PeG at 300^{o}C for 2 h and the products were dried by ordinary method. Although SEM image (Figure 5.20 (a)) shows the apparently irregularly-shaped aggregation. TEM micrographs clearly showed that tiny primary particles form spherical aggregate with an average diameter of 50 nm, and that micropores are formed inside the secondary particles. Therefore, irregularly-shaped particles observed by SEM are agglomerate of microspheres, and mesopore system is formed between the secondary particles. The micropore system cannot be modified but the mesopore system can be altered by evaporation of the organic solvent at the reaction temperature. Therefore, the increase of pore diameter in this product after drying by flashing is attributed to the improvement of only mesopores formed between spherical secondary particles and micropore system still remained in the products.

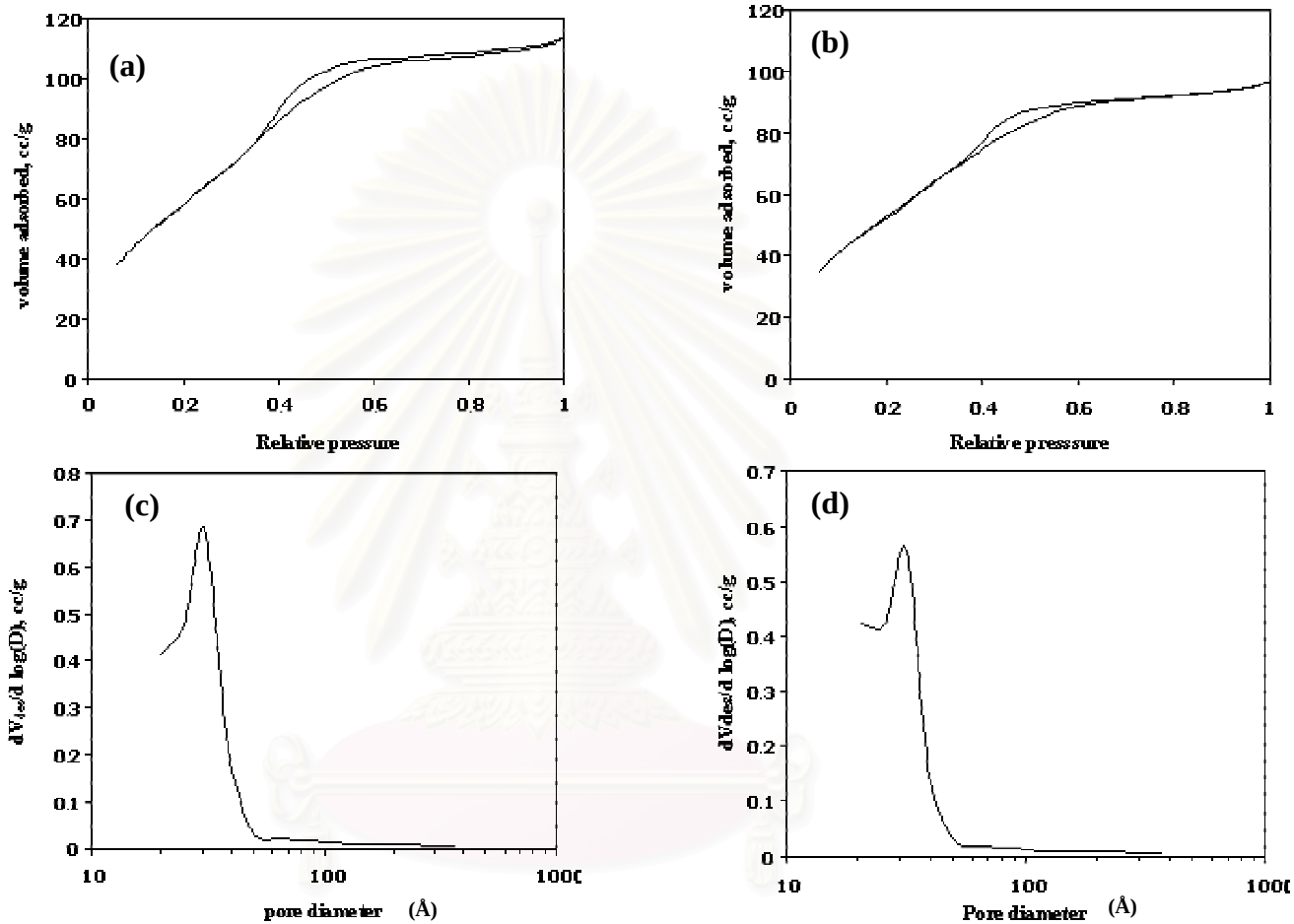

Figure 5.21 Typical adsorption/desorption isotherms and pore size distributions of as-synthesized zirconia prepared in 1,4-butanediol; (a) and (c): the product was dried in air after washing with methanol, (b) and (d): the product was dried by flash evaporation in autoclave after the reaction for 2 h.

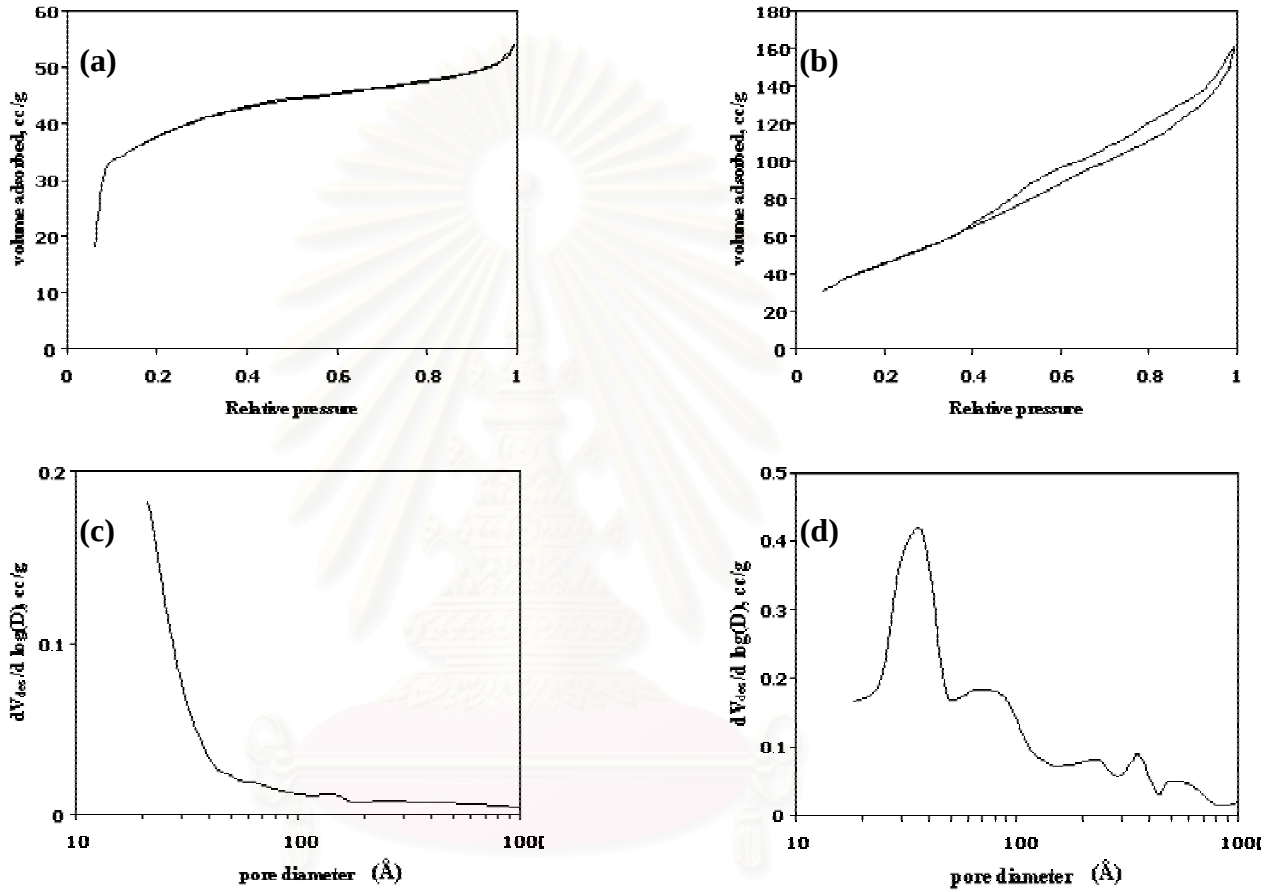

Figure 5.22 Typical adsorption/desorption isotherms and pore size distributions of as-synthesized zirconia prepared in 1,5-pentanediol; (a) and (c): the product was dried in air after washing with methanol, (b) and (d): the product was dried by flash evaporation in autoclave after the reaction for 2 h.

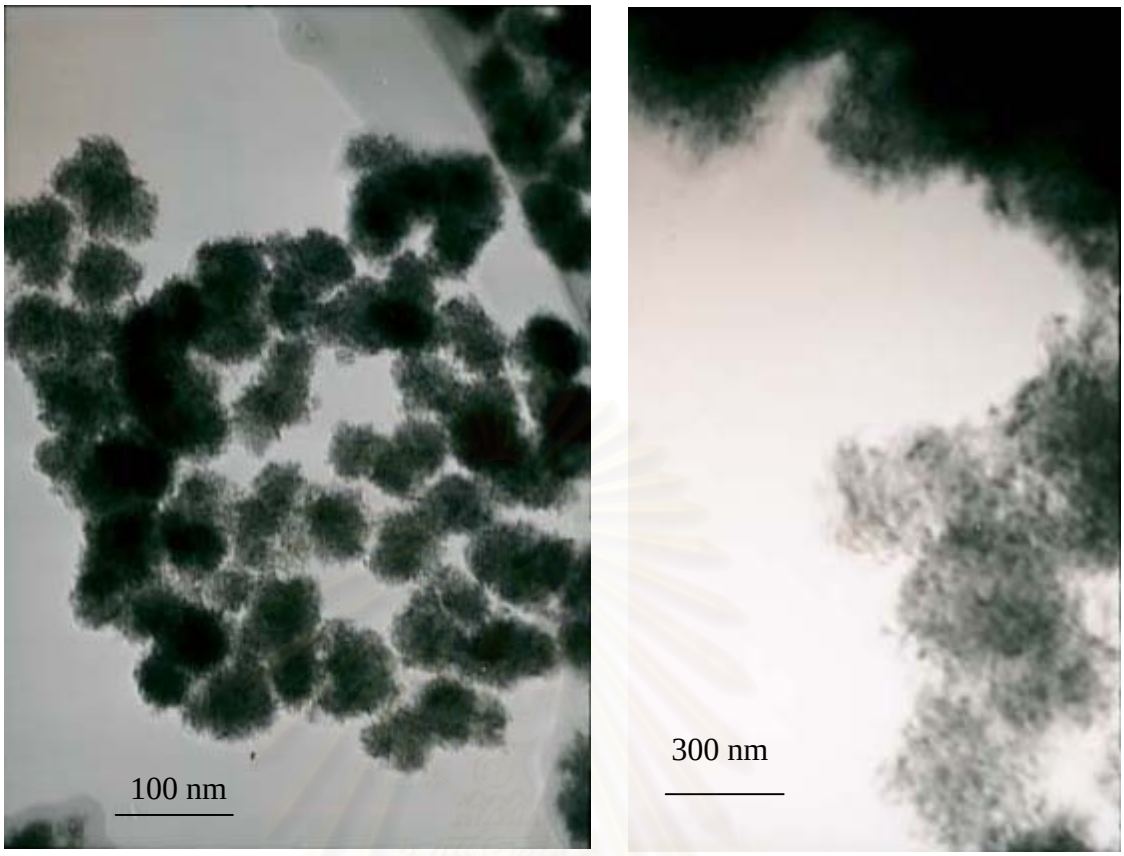

Figure 5.23 Transmission electron micrographs of powders obtained in 1,5-pentanediol at 300^{o}C for 2 h and the products were dried in air after washing with methanol

5.3.2 Effect of zirconium *n*-propoxide (ZNP) concentration in the mother liquor

To examine the effect of ZNP concentration, the amount of glycol used in the reaction was fixed and the amount of ZNP was varied from 7g to 25g. ZrO_2 powders obtained at 300^{o}C for 2 h in 1,4-BG and 1,5-PeG are white. Figures 5.24 and 5.25 show the XRD patterns for the powders prepared from both the glycols using different ZNP concentrations. The XRD patterns indicate tetragonal zirconia for all the as-synthesized products and no other crystal phases were observed. These results contradict those in section 5.1 which showed the formation of a mixture of tetragonal and monoclinic phases for the use of 1,5-PeG. As explained in the experimental section, the geometries of autoclave reactor and some synthesis parameters between the experiments in Japan and in Thailand are different. Therefore, these seem to be the primary reason of the different phases in the products. The dependence of crystallite size on ZNP concentration is given in Figure 5.26. The crystallite size of zirconia prepared in 1,4-BG was slightly increased by increasing the ZNP concentration whereas the crystallite size of the product obtained in 1,5-PeG was independent of ZNP concentration. From the experiment described in section 5.2, we found that crystallization and crystal growth of zirconia in 1,5-PeG proceeds by precipitation from the glycoxide. Thus, one of the possible explanation for the independence of zirconia crystallite size on ZNP concentration is that nucleation in 1,5-PeG is rapid leading to an excess of nuclei and thereby reducing the glycoxide concentration that is required for crystal growth. Therefore, increasing ZNP concentration, only increase the numbers of nuclei present.

Typical SEM images for the products prepared in 1,4-BG using different ZNP concentrations are shown in Figure 5.27. The powders have a spherical shape and dense mass and seem to be formed by aggregation of primary particles. The SEM photograph shows these secondary particles as separate microspheres. Interestingly, the lower the initial ZNP concentration, the smaller the size of the secondary particle. Increasing ZNP concentration increased mean microsphere diameter and reduced sharply the number of small microspheres. It must be noted that essentially monodispersed particles were obtained for the ZNP concentration of 0.21 mol/dm^3. This observation means that production of zirconia microspheres with various sizes is

possible by the use of 1,4-BG for synthesis. In section 5.2, we found that the secondary spherical particles were formed from the amorphous phase by solid-state transformation mechanism. Thus, one possible explanation is that low concentration of the starting materials yielded the amorphous phase with a lower density (high specific volume) because of incorporation of a large number of organic solvent molecules. Larger difference in specific volume between the amorphous phase and tetragonal zirconia would give smaller secondary particles. In contrast, the morphologies of zirconia prepared in 1,5-PeG was independent of ZNP concentration, as can be seen in Figure 5.28.

Figure 5.29 shows the XRD patterns of zirconia obtained in 1,4-BG with various ZNP concentrations after calcination at 600^{o}C. The product prepared with a low ZNP concentration essentially maintained the tetragonal phase and phase transformation was more obvious with increasing the ZNP concentration. As shown in Table 5.4, crystallite size of calcined samples slightly increased as the ZNP concentration was enhanced.

Table 5.4. Crystallite size of zirconia prepared in 1,4-butanediol and 1,5-pentanediol and then calcined in air at 600^{o}C for 2 h.

ZNP concentration (mol/dm^3)	Crystallite size[a] (nm)	
	1,4-butanediol	1,5-pentanediol
0.21	11.8	13.7
0.3	12.6	11.9
0.4	14.2	12.4
0.62	13.7	12.4

[a]Crystallite size calculated from 111 diffraction peak of tetragonal phase by Scherrer equation

The nitrogen adsorption isotherms of the calcined products of the reaction in 1,4-BG with various amounts of ZNP in solution are shown in Figure 5.30. With increasing ZNP concentration, the shape of isotherms gradually changed from one resembling type I to type IV with the appearance of a hysteresis loop. The corresponding pore size distributions are shown in Figure 5.31. For the products with

high concentrations of ZNP in the mother liquor, mesopore peaks can be seen (curve (c) and (d)). However, no mesopore peaks are found for the zirconia produced with relatively low ZNP concentrations (0.21 and 0.3 mol/dm^3) due to the presence of micropore system (curves (a) and (b) in Figure 5.31).

The specific surface areas and pore volumes of the as-synthesized products obtained in 1,4-BG and the calcined samples, prepared with different ZNP concentrations, are given in Table 5.5. As expected, the BET surface area and pore volume increased slightly with increasing ZNP concentration. According to the above results, it is clear that secondary particle size, BET surface area and pore system of zirconia prepared in 1,4-BG depended on the ZNP concentration. Therefore, it is possible to control the properties of zirconia particles by adjusting the amount of ZNP in the starting solution.

Table 5.5. Effects of ZNP concentration on the BET surface area and pore volume for zirconia synthesized in 1,4-butanediol at 300^{o}C for 2 h.

ZNP concentration (mol/dm^3)	BET surface area (m^2/g)		pore volume[c] (cc/g)	
	As-syn[a]	600^{o}C[b]	As-syn[a]	600^{o}C[b]
0.21	147	8.5	0.05	0.01
0.3	196	11	0.10	0.02
0.4	225	37	0.19	0.10
0.62	205	54	0.22	0.14

[a] The as-synthesized powders obtained by the glycothermal method.

[b] Powders were obtained by glycothermal method and then were calcined at 600^{o}C for 1 h.

[c] Average pore volume.

The above results are completely contradicting to generally observed tendency that the sample that preserve the tetragonal phase maintain larger surface area than the sample that transforms into the monoclinic phase. It is possible that after calcination particle shrinkage took place for the smaller particles yielding only micropores formed between primary particles. In the case of large particle, primary particles also tightly coagulated but larger particles cannot shrink because of limitation of the

distance of mass-transfer and therefore smaller aggregates were formed by sintering, yielding mesopore system in the spherical particles. However, this observation should be investigated further in detail in the future.

The XRD patterns of products obtained in 1,5-pentanediol after calcination at 600°C are given in Figure 5.32. Zirconia prepared with all ZNP concentrations showed the similar extent of phase transformation into monoclinic phase. In addition, the crystallite size of calcined samples were not different with varying of ZNP concentrations as shown in Table 5.4.

The isotherms and pore size distributions of products prepared in 1,5-PeG with various concentrations of ZNP are shown in Figures 5.33 and 5.34, respectively. The results indicate the presence of micropore system in the samples except for sample obtained with ZNP concentration of 0.21 mol/dm^3.

The results of BET analysis of products prepared in 1,5-pentanediol are given in Table 5.6. The specific surface area of zirconia was only slightly affected by ZNP concentration except the product obtained with ZNP concentration of 0.62 mol/dm^3, which had a relatively low surface area. However, the surface area and pore volume after calcination were essentially similar for all the powders prepared from the ZNP concentration of 0.21-0.62 mol/dm^3.

Table 5.6. Effects of ZNP concentration on the BET surface area and pore volume for zirconia synthesized in 1,5-pentanediol at 300°C for 2 h.

ZNP concentration (mol/dm^3)	BET surface area (m^2/g)		pore volume[c] (cc/g)	
	As-syn[a]	600°C[b]	As-syn[a]	600°C[b]
0.21	144	10.1	0.09	0.02
0.3	123	9.3	0.08	0.02
0.4	165	10.2	0.08	0.02
0.62	91	7.1	0.06	0.01

[a] The as-synthesized powders obtained by the glycothermal method.
[b] Powders were obtained by glycothermal method and then were calcined at 600°C for 1 h.
[c] Average pore volume.

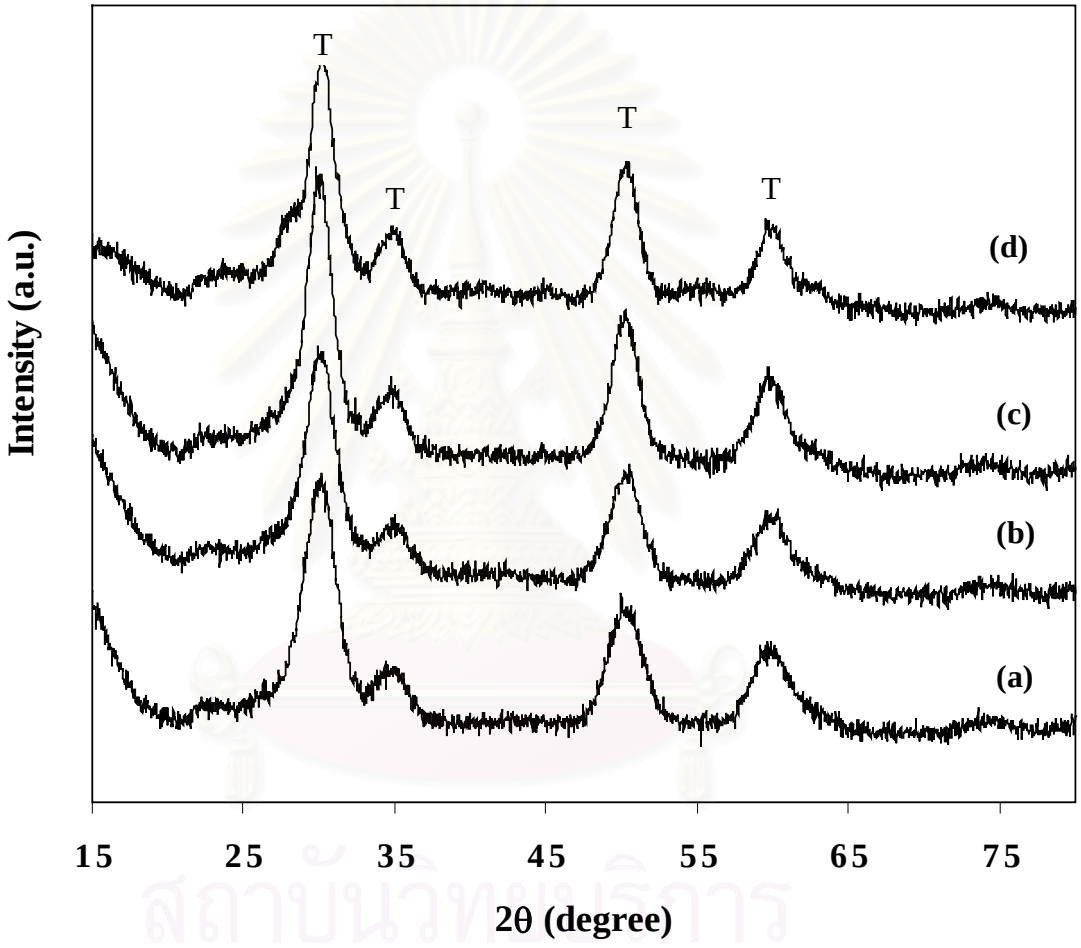

Figure 5.24 XRD patterns of the powders obtained by the reaction of zirconium tetra *n*-propoxide (ZNP) in 1,4-butanediol at 300^{o}C for 2 h by using ZNP concentration of (a) 0.21 mol/dm^3 (b) 0.3 mol/ dm^3 (c) 0.4 mol/dm^3 and (d) 0.62 mol/dm^3.

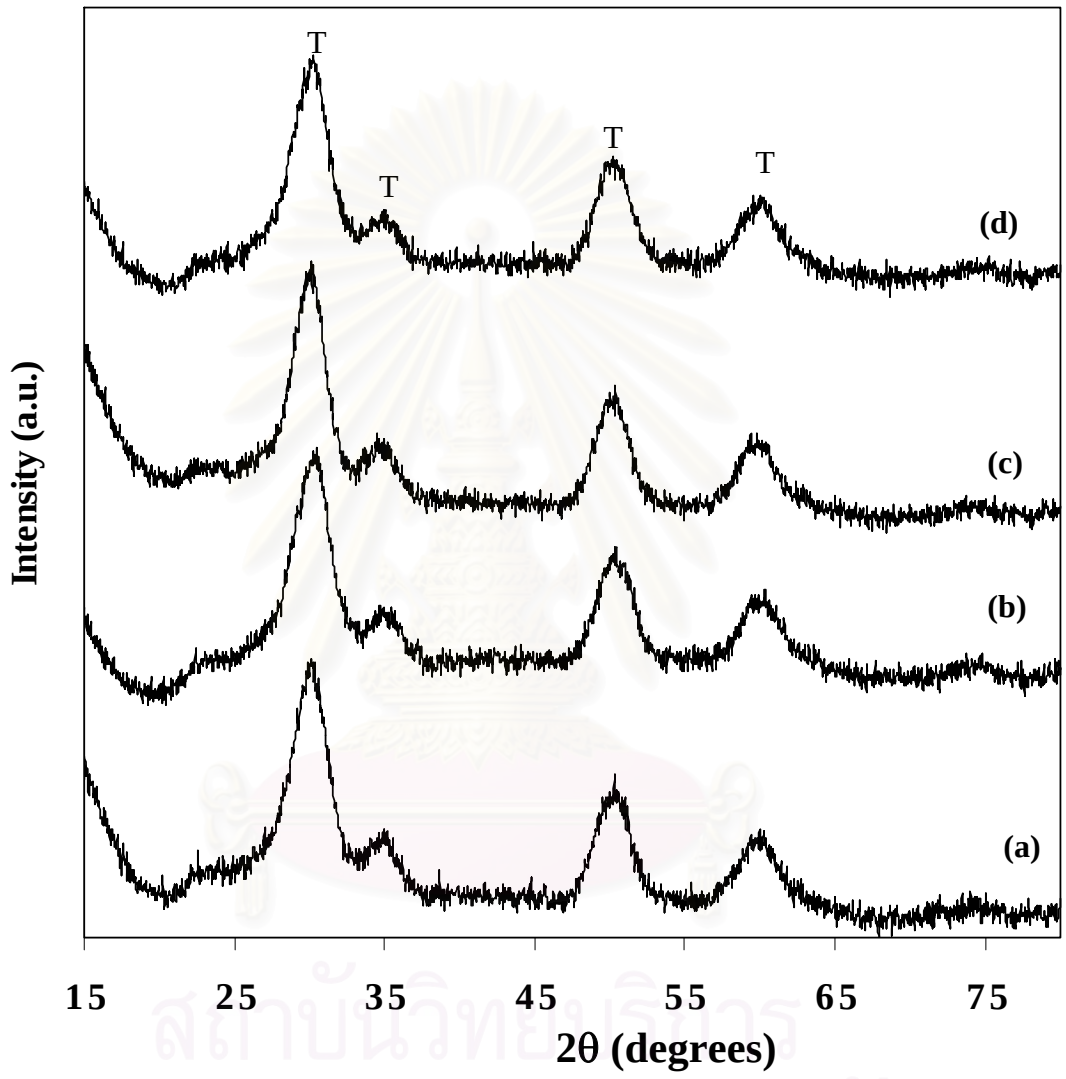

Figure 5.25 XRD patterns of the powders obtained by the reaction of zirconium tetra *n*-propoxide (ZNP) in 1,5-pentanediol at 300^{o}C for 2 h by using ZNP concentration of (a) 0.21 mol/dm^3 (b) 0.3 mol/ dm^3 (c) 0.4 mol/dm^3 and (d) 0.62 mol/dm^3.

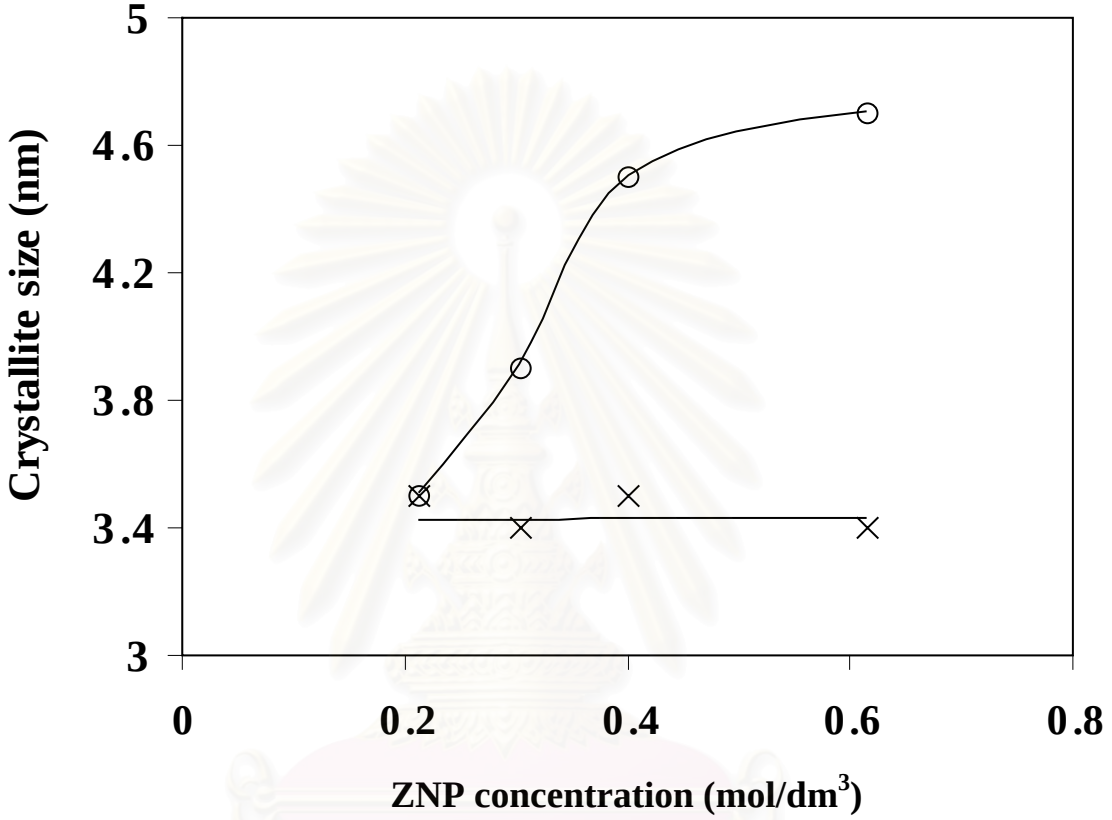

Figure 5.26 Dependence of the crystallite size of zirconia particles prepared in (o) 1,4-butanediol and (×) 1,5-pentanediol on the zirconium tetra *n*-propoxide concentration

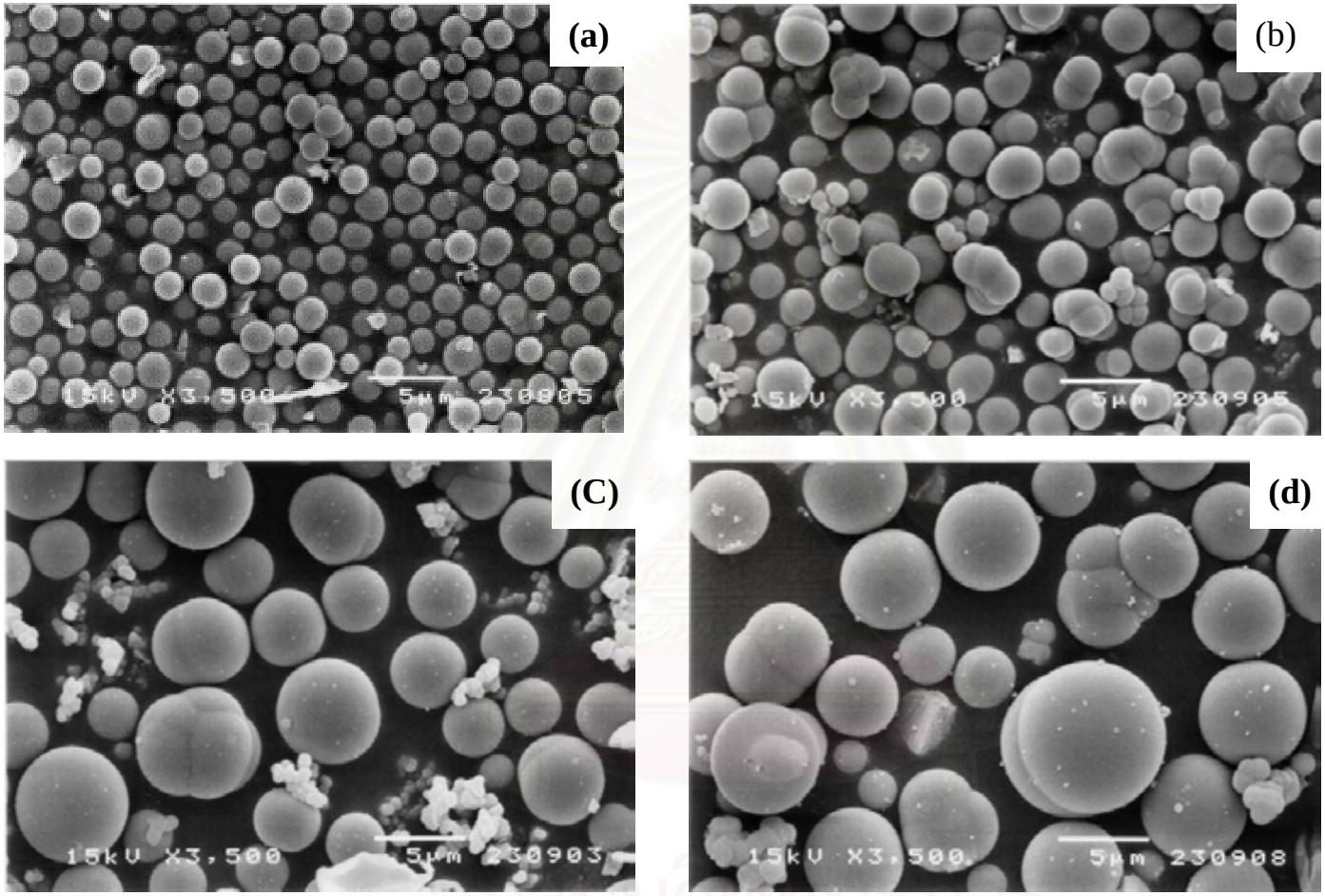

Figure 5.27 Scanning electron micrographs of the powders prepared by the reaction of zirconium tetra *n*-propoxide in 1,4-butanediol at 300°C for 2 h by using ZNP concentration of (a) 0.21 mol/dm^3 (b) 0.3 mol/ dm^3 (c) 0.4 mol/dm^3 and (d) 0.62 mol/dm^3.

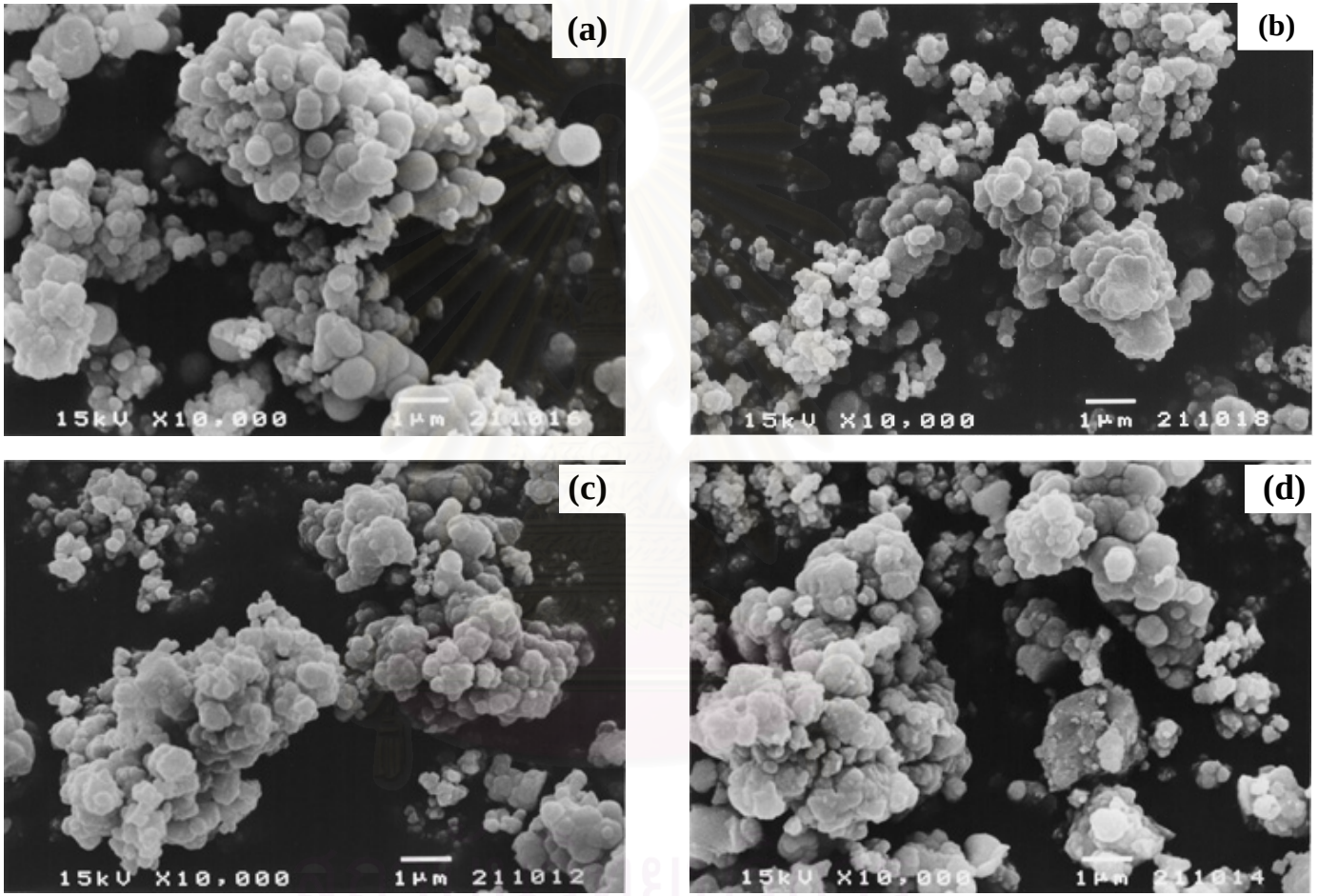

Figure 5.28 Scanning electron micrographs of the powders prepared by the reaction of zirconium tetra *n*-propoxide in 1,5-pentanediol at 300^{o}C for 2 h by using ZNP concentration of (a) 0.21 mol/dm^3 (b) 0.3 mol/ dm^3 (c) 0.4 mol/dm^3 and (d) 0.62 mol/dm^3.

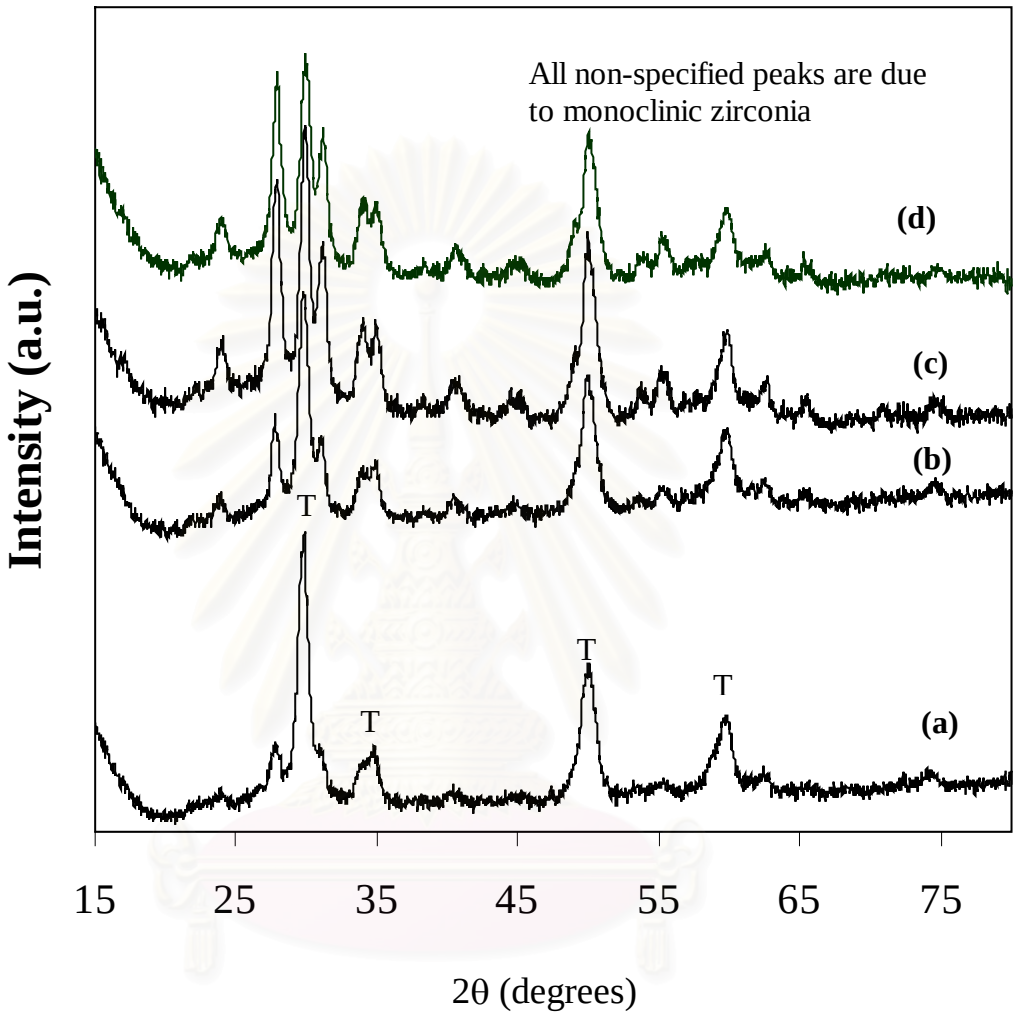

Figure 5.29 XRD patterns of the powders obtained by the reaction of zirconium tetra *n*-propoxide (ZNP) in 1,4-butanediol at 300^{o}C for 2 h by using ZNP concentration of (a) 0.21 mol/dm^{3} (b) 0.3 mol/ dm^{3} (c) 0.4 mol/dm^{3} and (d) 0.62 mol/dm^{3}. All the samples were calcined in air at 600^{o}C for 1 h.

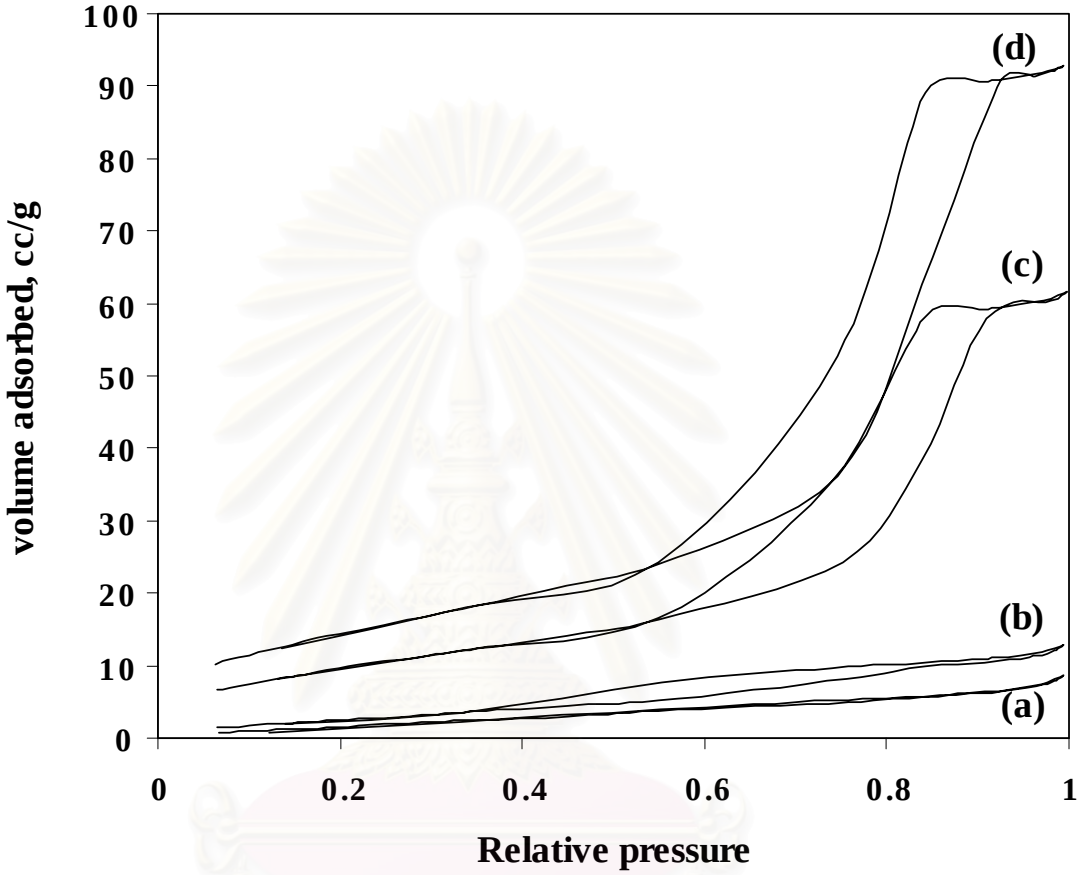

Figure 5.30 Adsorption isotherms of the zirconia prepared in 1,4-butanediol by using ZNP concentration of (a) 0.21 mol/dm^3 (b) 0.3 mol/ dm^3 (c) 0.4 mol/dm^3 and (d) 0.62 mol/dm^3. All the samples were calcined in air at 600^{o}C for 1 h.

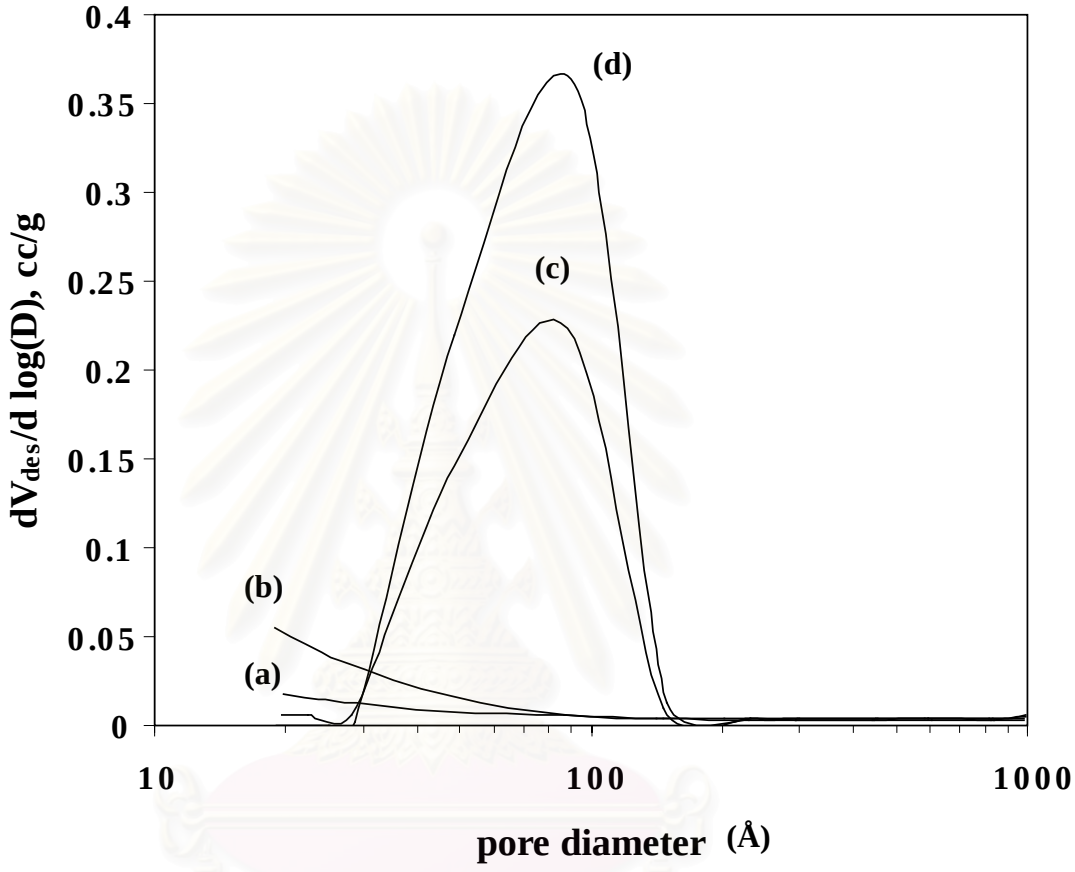

Figure 5.31 Pore size distributions of the zirconia samples prepared in 1,4-butanediol by using ZNP concentration of (a) 0.21 mol/dm^3 (b) 0.3 mol/ dm^3 (c) 0.4 mol/dm^3 and (d) 0.62 mol/dm^3. All the samples were calcined in air at 600^{o}C for 1 h.

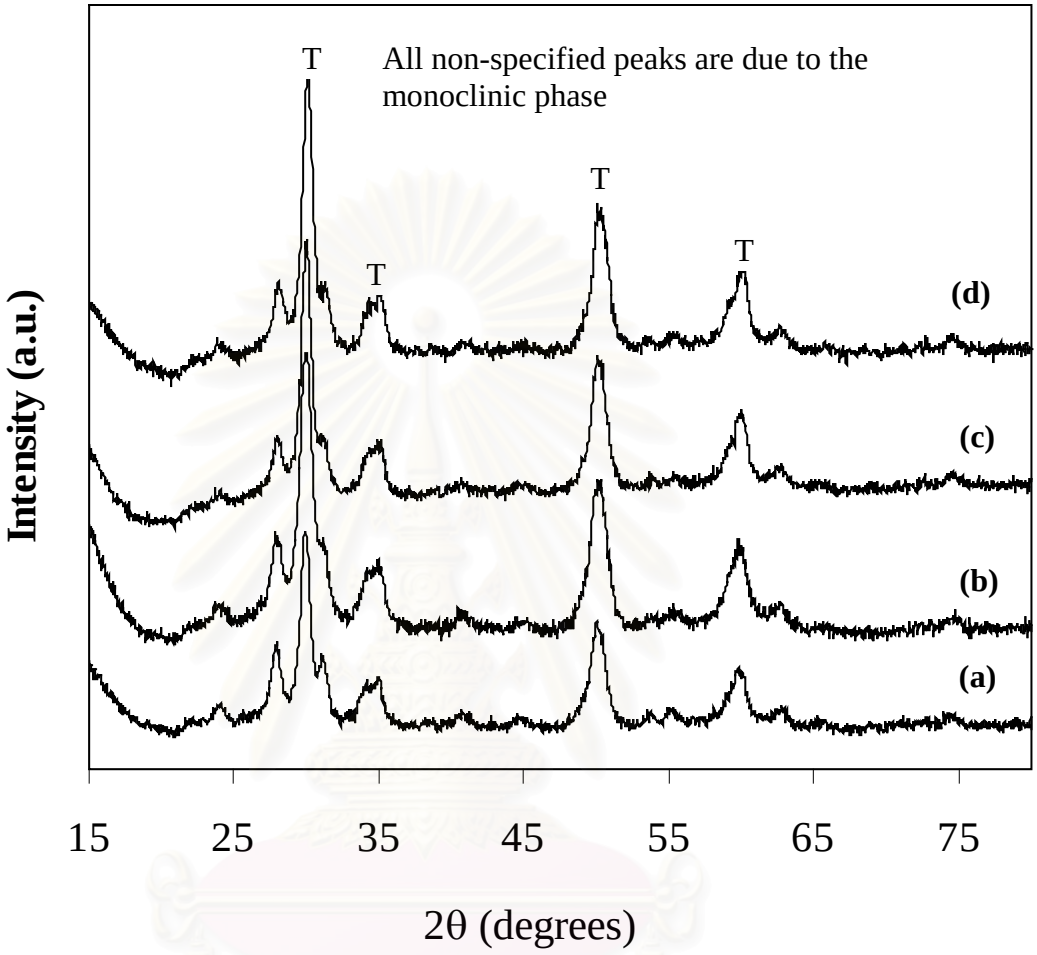

Figure 5.32 XRD patterns of the powders obtained by the reaction of zirconium tetra *n*-propoxide (ZNP) in 1,5-pentanediol at 300^{o}C for 2 h by using ZNP concentration of (a) 0.21 mol/dm^{3} (b) 0.3 mol/ dm^{3} (c) 0.4 mol/dm^{3} and (d) 0.62 mol/dm^{3}. All the samples were calcined in air at 600^{o}C for 1 h.

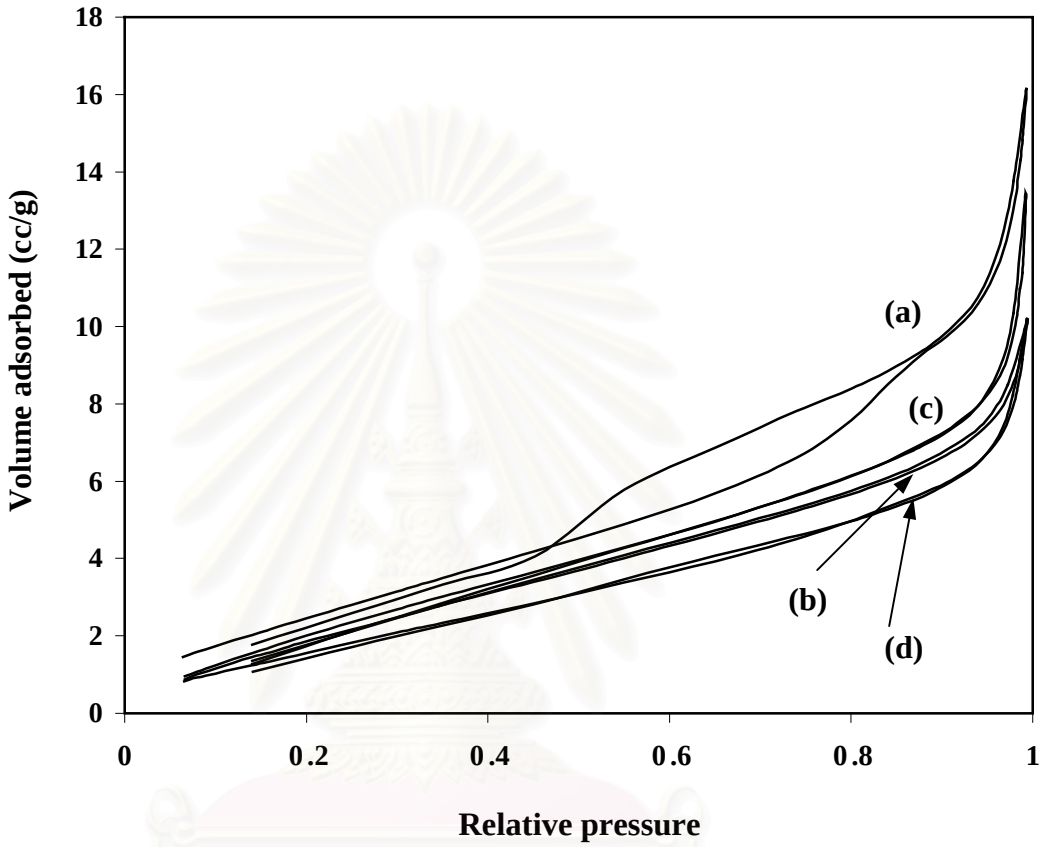

Figure 5.33 Adsorption isotherms of the zirconia samples prepared in 1,5-pentanediol by using ZNP concentration of (a) 0.21 mol/dm^3 (b) 0.3 mol/ dm^3 (c) 0.4 mol/dm^3 and (d) 0.62 mol/dm^3. All the samples were calcined in air at 600^{o}C for 1 h.

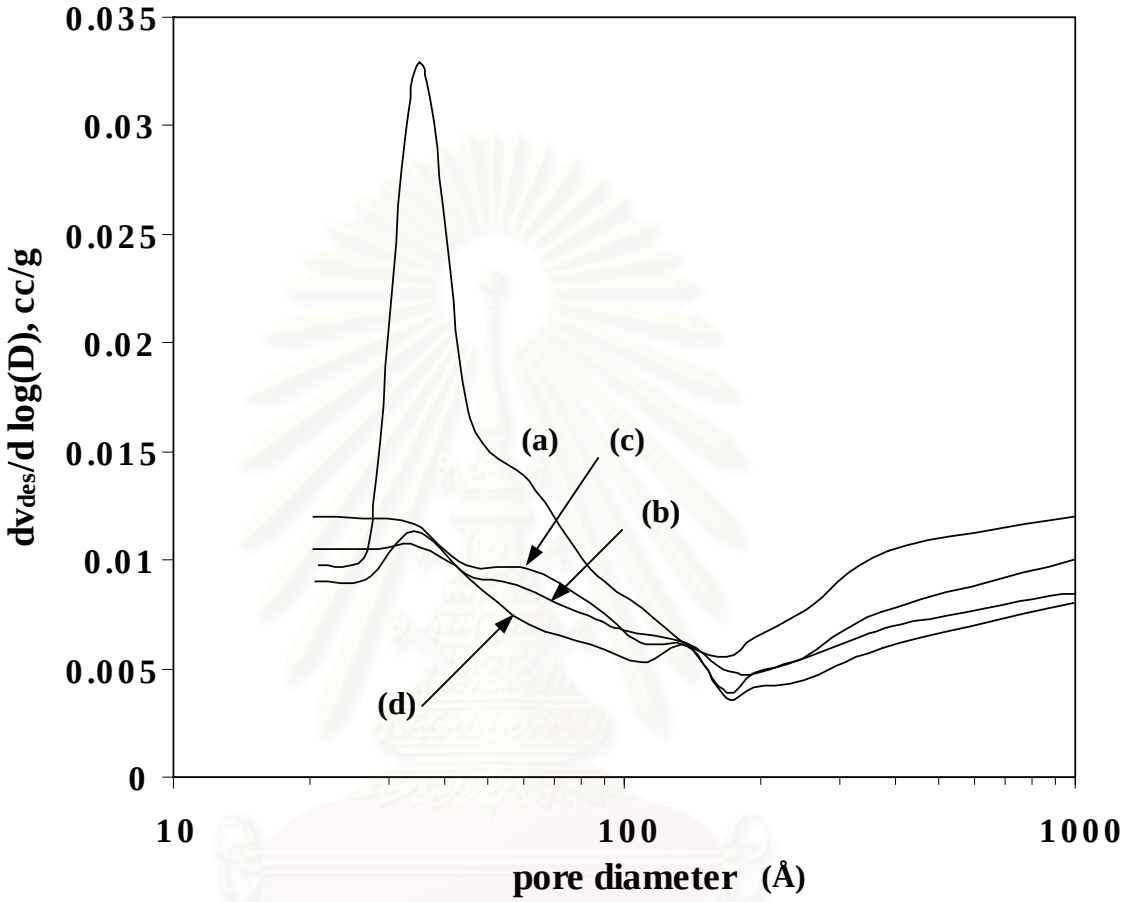

Figure 5.34 Pore size distributions of the zirconia samples prepared in 1,5-pentanediol by using ZNP concentration of (a) 0.21 mol/dm^3 (b) 0.3 mol/ dm^3 (c) 0.4 mol/dm^3 and (d) 0.62 mol/dm^3. All the samples were calcined in air at 600^{o}C for 1 h.

Since the BET surface area and thermal stability of zirconia after calcination is quite low, therefore we try to improve the thermal stability and BET surface area of the products by addition of silica.

5.4 The synthesis of silica-modified zirconia

The XRD patterns of the products obtained in 1,4-BG at 300^{o}C for 2 h with addition of TEOS at Si/Zr ratios of 0, 0.02, 0.04, 0.08 and 0.15 were shown in Figures 5.35, 5.36, 5.37, 5.38 and 5.39 respectively. Tetragonal zirconia was formed for all the products with the Si/Zr ratio of 0-0.15. The peak intensities were not altered with increasing TEOS content, suggesting that the crystallinity of samples prepared by the glycothermal method was not affected by increasing of the Si ratio. This result shows a sharp contrast against silica-zirconia samples prepared by other methods which generally exhibit decreased crystallinity with increasing silica content (Meijers *et al.*, 1991 and Aguilar *et al.*, 2000).

The tetragonal to monoclinic phase transformation temperature shifted toward higher temperatures with the increase in the amount of TEOS added to the reaction. Table 5.7 shows phase detected in the products and the samples after calcination. A small amount of Si ratio in the product resulted in the partial transformation to monoclinic phase at high temperature. However, the products with high Si/Zr ratios preserved the tetragonal phase after calcination at high temperatures. The product at Si/Zr ratio of 0.15 maintained the tetragonal phase even after calcination at 1000^{o}C, while the unmodified tetragonal zirconia began to transform to the monoclinic phase after calcination at 500^{o}C.

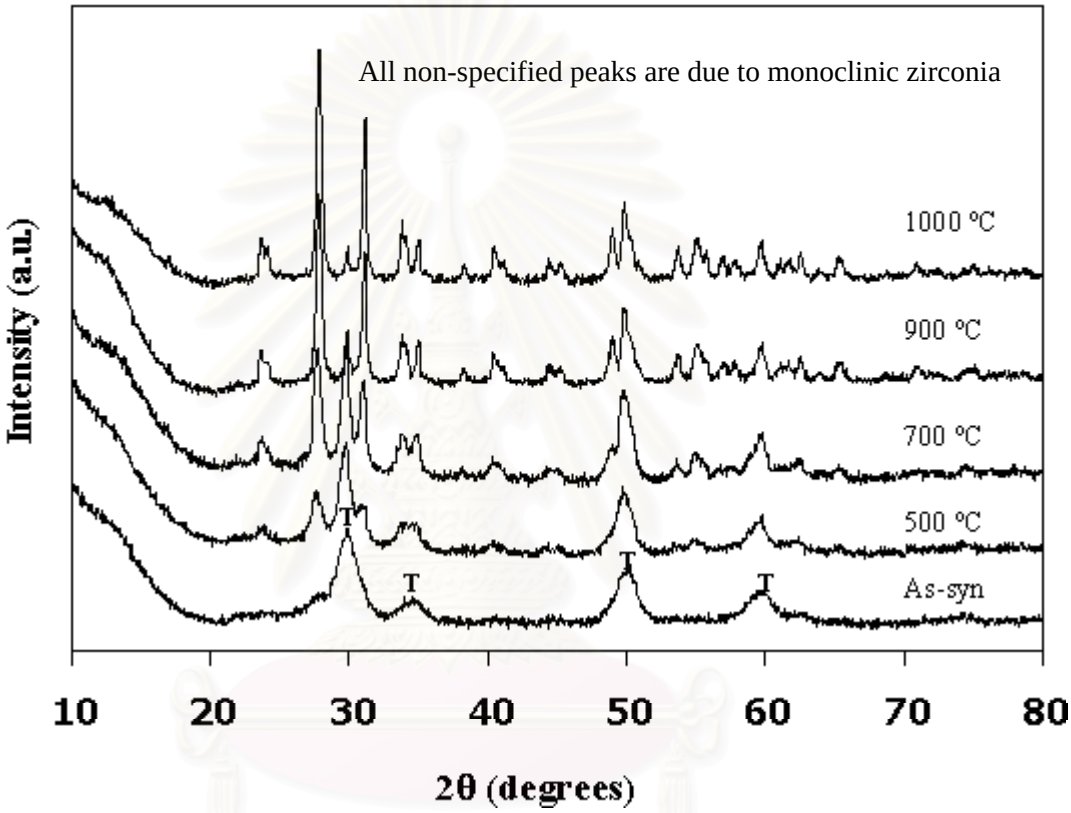

Figure 5.35 The XRD patterns of products obtained by the reaction of zirconium *n*-propoxide in 1,4-butanediol with the Si/Zr ratio of 0 and the samples obtained by calcination thereof at temperature specified in the figure.

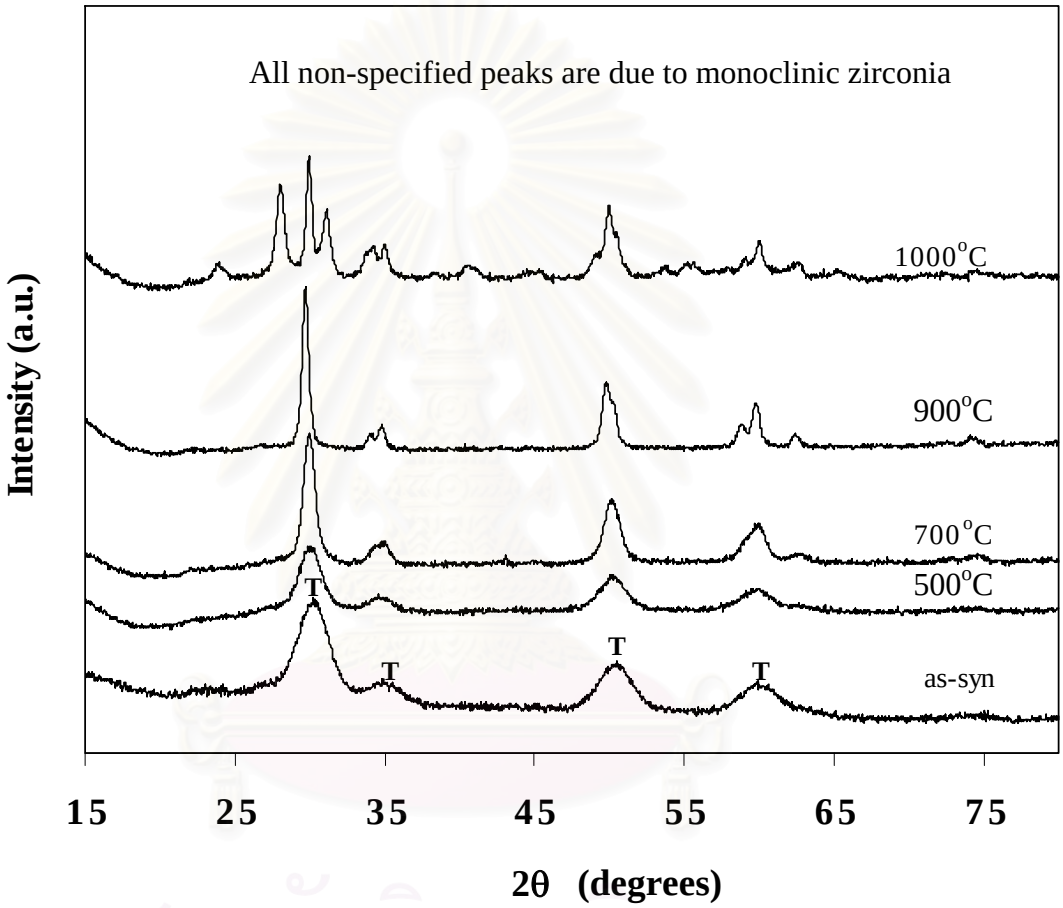

Figure 5.36 The XRD patterns of products obtained by the reaction of zirconium *n*-propoxide and TEOS in 1,4-butanediol with the Si/Zr ratio of 0.02 and the samples obtained by calcination thereof at temperature specified in the figure.

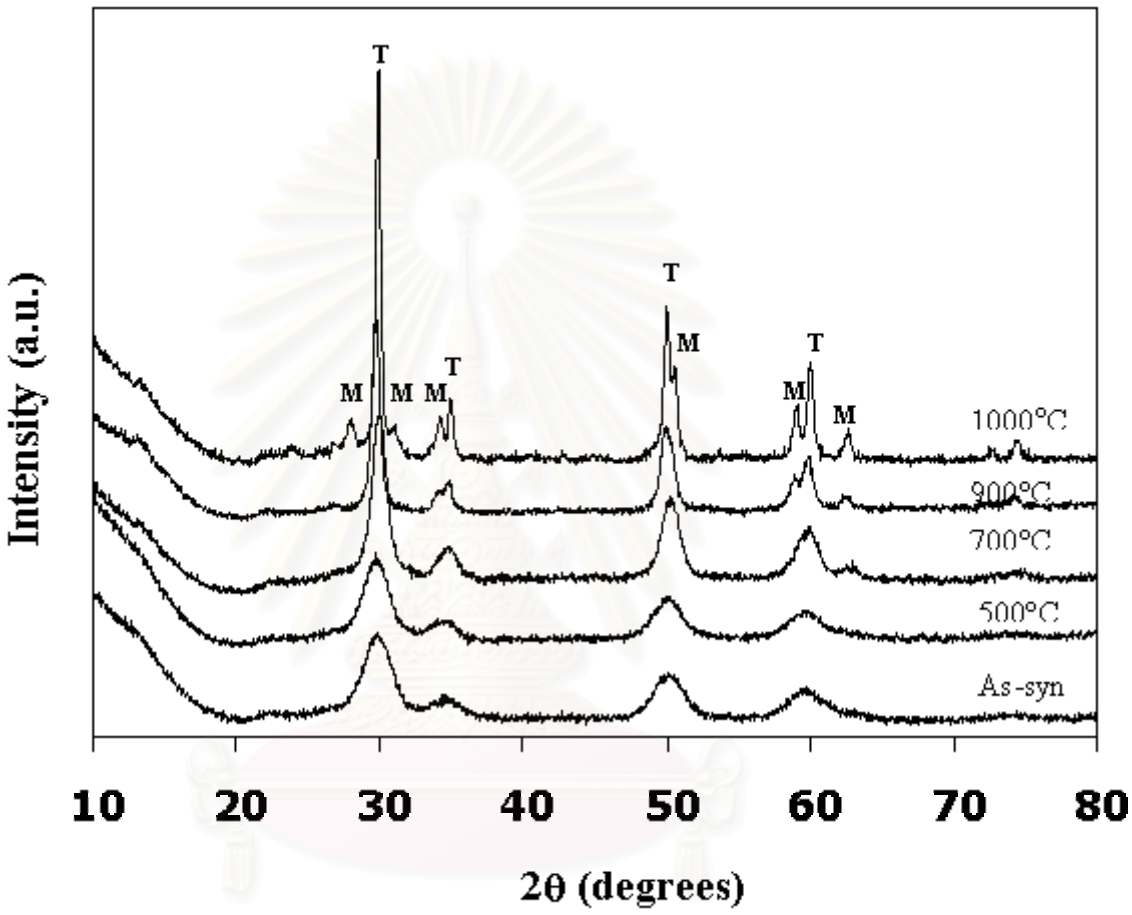

Figure 5.37 The XRD patterns of products obtained by the reaction of zirconium *n*-propoxide and TEOS in 1,4-butanediol with the Si/Zr ratio of 0.04 and the samples obtained by calcination thereof at temperature specified in the figure

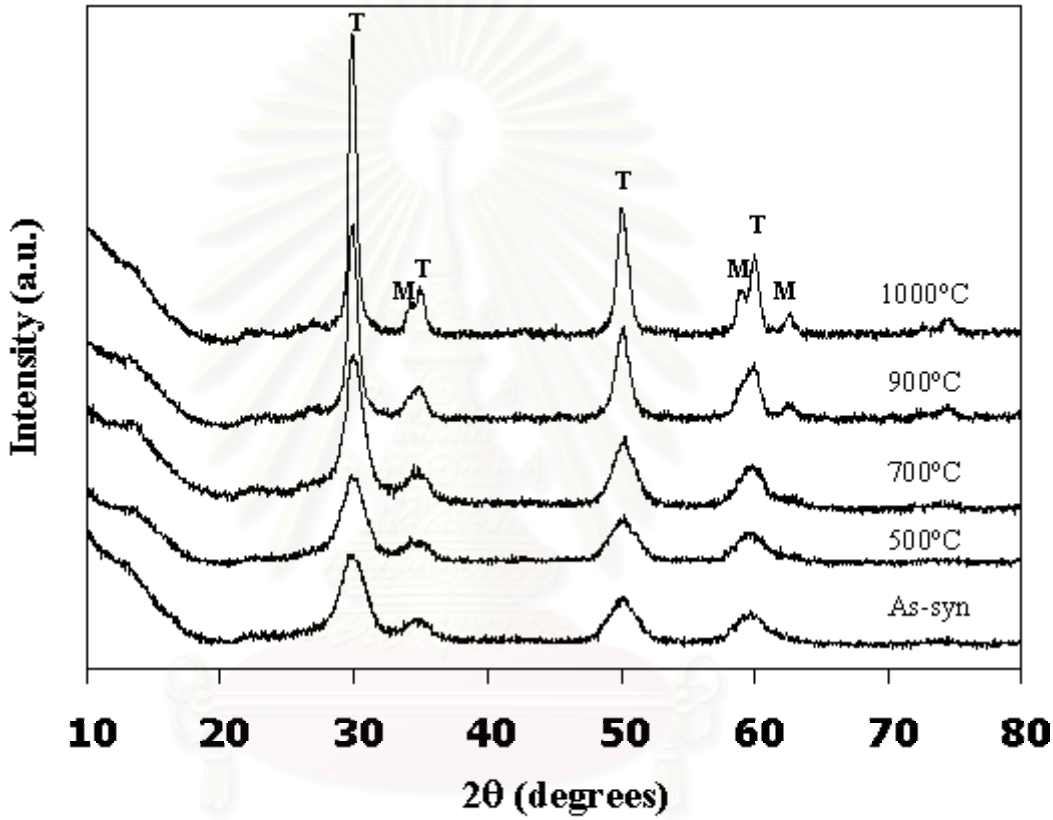

Figure 5.38 The XRD patterns of products obtained by the reaction of zirconium *n*-propoxide and TEOS in 1,4-butanediol with the Si/Zr ratio of 0.08 and the samples obtained by calcination thereof at temperature specified in the figure.

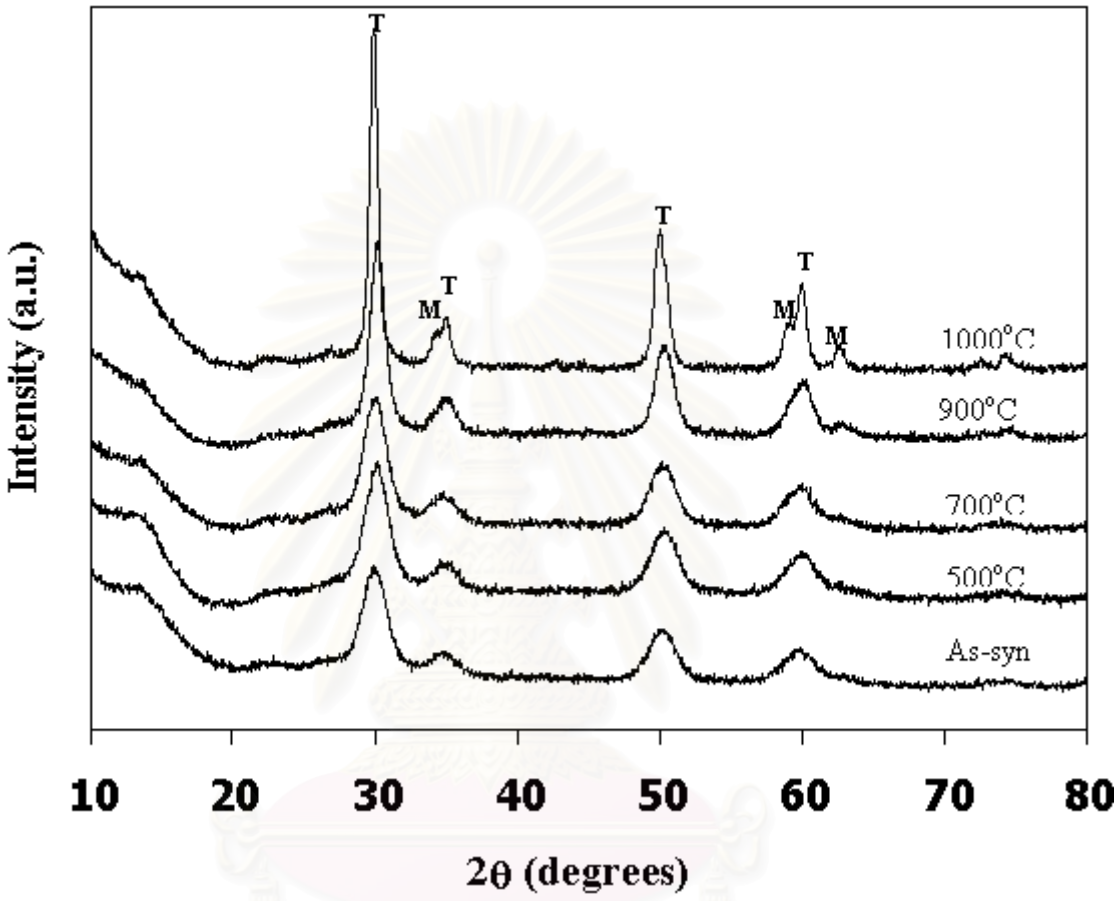

Figure 5.39 The XRD patterns of products obtained by the reaction of zirconium *n*-propoxide and TEOS in 1,4-butanediol with the Si/Zr ratio of 0.15 and the samples obtained by calcination thereof at temperature specified in the figure.

Table 5.7 Phases present in the products and samples obtained by calcination at various temperatures for 1 h.

Si/Zr ratio	As-syn	500 °C	600 °C	700 °C	800 °C	1000 °C
0	T	T, M	T, M	T, M	M	M
0.01	T	T, M	T, M	T, M	T,M	M
0.02	T	T	T	T	T, M	M
0.04	T	T	T	T	T, M	T, M
0.06	T	T	T	T	T	T, M
0.08	T	T	T	T	T	T, M
0.15	T	T	T	T	T	T, M

Table 5.8 includes the crystallite size and BET surface area of the products. The presence of Si in the products seems to decelerate the crystallite growth of tetragonal phase. A small amount of TEOS charged to the reaction resulted in an increase of surface area. The BET surface area drastically increased with increasing the amount of TEOS added. The present product with the Si/Zr ratio of 0.15 maintained the BET surface area of 214 and 126 m^2/g even after calcination at 500^oC and 800^oC, respectively. Soled and Mavicker (1992) reported that the surface area of bulk-substitued SiO_2-ZrO_2 at SiO_2 content of 25 mol% is at most 150 m^2/g after calcination at 500^oC. The silica-zirconia mixed oxides prepared by the sol-gel method (hydrolysis of alkoxides) had the surface area of 141 m^2/g at 25 mol% Si. Compared to the previous works, the present product with a small ratio of silica showed the larger surface area after calcination at higher calcination temperatures. The crystallite size of all the as-synthesized products aligned in the range of 3-5 nm. This suggested that the nucleation frequency of product is scarcely affected by TEOS content added to the reaction.

Figure 5.40 shows the scanning electron micrographs of the products obtained in 1,4-butanediol with the Si/Zr ratio of 0-0.08. All the products were composed of spherical particles. The product obtained without addition of TEOS had narrow particle size distribution, whereas the particle size of the products containing silica distributed in wide range. When TEOS was added to the reaction, the spherical particles formed aggromerates.

Table 5.8 Crystallite size and BET surface area of products prepared in 1,4-butanediol and the samples calcined at various temperatures for 1 h

Si/Zr ratio	As-syn		500 °C		600 °C		700 °C		800 °C		900 °C		1000 °C	
	d_{202}	S_{BET}	d_{202}	S_{BET}	d_{202}	S_{BET}	d_{202}	S_{BET}	d_{202}	S_{BET}	d_{202}	S_{BET}	d_{202}	S_{BET}
0	5.1	91	6.7	42	8.6	27	15.6	23	19.9	13	19.9	ND[†]	ND[††]	ND[†]
0.01	4.2	157	5.9	70	7.2	40	8.2	38	9.3	16	9.3	9	17.5	ND[†]
0.02	3.3	157	4.4	81	5.9	35	7.1	21	7.4	11	7.4	3	15.7	ND[†]
0.04	3.6	204	4.0	122	5.4	91	6.1	59	7.2	24	7.2	12	10.7	ND[†]
0.06	3.9	192	4.0	142	5	114	5.5	76	6.1	41	6.6	22	9.6	6.5
0.08	3.9	211	4.0	146	4.7	122	4.9	118	5.9	65	5.9	33	8.9	13
0.15	4.1	226	4.2	214	4.4	168	4.5	179	4.6	126	4.6	79	8.5	11

d_{202}, crystallite size calculated from 202 diffraction peak of tetragonal phase (nm)

S_{BET}, surface area measured from BET single point method (m^2/g)

[†] Cannot be accurately measured by BET single point method

[††] Cannot be accurately determined by XRD data

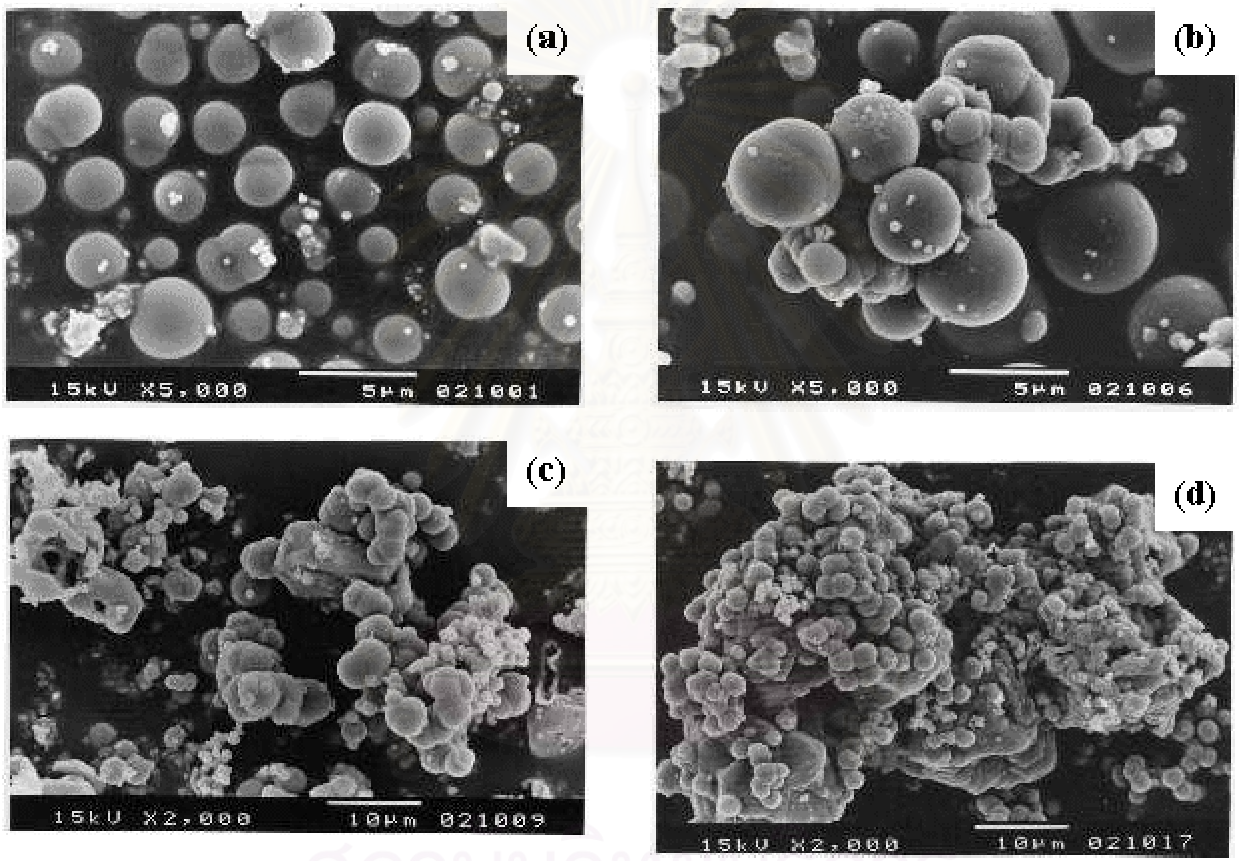

Figure 5.40 Scanning electron micrographs of the products obtained by the reaction of zirconium *n*-propoxide and tetraethyl orthosilicate with the ratio of (a) Si/Zr = 0, (b) Si/Zr = 0.02, (c) Si/Zr = 0.04, (d) Si/Zr = 0.08 in 1,4-butanediol at 300^{o}C for 2 h.

Figures 5.41, 5.42, 5.43 and 5.44 show the FT-IR spectra of the samples as-synthesized and calcined at various temperatures at the Si/Zr ratio of 0.02, 0.04, 0.08 and 0.15, respectively. The band at 1630 cm^{-1} was attributed to the adsorbed water (Wang *et al.*, 1996). All the as-synthesized samples exhibited bands at around 1560 cm^{-1}, 1460 cm^{-1} and 1420 cm^{-1} which were assigned to the glycol moieties occluded in the samples because peak positions are in good agreement with those of liquid 1,4-butanediol. These bands completely disappeared when the samples were calcined. The two bands at around 510 cm^{-1} and 600 cm^{-1} were found in all as-synthesized samples and they disappeared after calcination at certain temperature. The temperature at which such two bands disappeared increased with increasing the Si/Zr ratio and corresponded to the temperature of phase transformation into monoclinic phase. It was reported that the tetragonal zirconia phase vibrates at the frequently ~600 cm^{-1} and tetragonal zirconia also possesses a characteristic band at 480 cm^{-1}(Liu *et al.*,1988 and Lee *et al.*, 1988). Therefore, the bands at around 510 cm^{-1} and 600 cm^{-1} in the present samples can be assigned to the tetragonal phase.

The IR band at around 975-980 cm^{-1} is generally assigned to Si-O-Zr linkages (Lee and Condrate, 1988, Bosman *et al.*, 1994, Anderson and Fergusson, 1999). Therefore the bands located around 992 cm^{-1}, 995 cm^{-1}, 1015 cm^{-1} and 1025 cm^{-1} are assigned to Si-O-Zr bonds of the as-synthesized samples at the Si/Zr ratio of 0.02, 0.04, 0.08 and 0.15, respectively. The characteristic band of Si-O-Zr bonds shifted to higher frequencies when the silica content increased. This suggested that the extent of silica incorporated into the lattice of zirconia depended on the amount of TEOS added to the reaction. In addition, this peak shift indicated the high degree of homogeneities of the present samples.

The characteristic band of the Si-O-Zr of as-synthesized sample and 500^{o}C-calcined sample appeared at the same frequency for the sample of Si/Zr ratio of 0.02 and 0.04 as shown in Figures 5.41 and 5.42 and this band is stable up to 700^{o}C for the samples with higher silica contents (Si/Zr ratio of 0.08 and 0.15), as shown in Figures 5.43 and 5.44. This indicated that the Si-O-Zr bonds were formed by the reaction rather than during the calcination and that the stability of the Si-O-Zr bonds was enhanced with increasing the amount of TEOS charged. Since the inherent strength of

the Si-O-Zr bond should not be affected by surroundings, it is possible that an increase of stability of the Si-O-Zr bonds with an increase of TEOS charged is due to the stability of the tetragonal phase.

As the calcination temperature increased, the characteristic band of Si-O-Zr gradually shifted toward higher frequencies and approached 1100 cm^{-1}. It has been reported that pure silica absorbs infrared light at near 1100 cm^{-1} with a shoulder at near 1200 cm^{-1} due to Si-O bond stretching vibration and at 800 cm^{-1} and 470 cm^{-1} due to a ring structure of Si-O bonds (Fontana *et al*., 1997). The results suggested that the Si-O-Zr bonds were broken by calcination at high temperatures, leading to the formation of Si-O-Si bonds or phase segregation of ZrO_2 and SiO_2. The two characteristic bands of ring structure of Si-O bonds at 800 cm^{-1} and 470 cm^{-1} were not found in the present samples. Zhan and Zeng (1999) reported that the ring-structural Si-O bands at 800 and 470 cm^{-1} were destroyed when the Zr content was higher than 50 mol% due to the complete insertion of Zr atoms, indicating a high degree of mixing between SiO_2 and ZrO_2.

From these results, the silica-modified zirconia prepared by the glycothermal method exhibited a high degree of homogeneities for the range of Si/Zr ratio of 0.02-0.15.

The relative crystallite size of the zirconia (the ratio of the crystallite size of calcined sample to that of as-synthesized sample) at Si/Zr ratio ranged from 0-0.15 is plotted in Figure 5.45 as a function of calcination temperature. For the pure zirconia, the crystallite size increased rapidly with an increase in the calcination temperature accompanying with the phase transformation into the monoclinic phase. For silica-modified zirconia, the crystallite size slightly increased up to a certain temperature depending on the ratio of TEOS charged (see Figure 5.45). The presence of Si-O-Zr bonds in the samples retarded the crystal growth up to certain calcination temperature, and above this temperature the Si-O-Zr bonds were broken and the Si-O-Si bonds were formed, leading to the rapid crystal growth. From the XRD results, the phase transformation temperature into monoclinic phase was higher for silica-modified

zirconia compared to pure zirconia due to the relatively slow crystal growth of silica-modified zirconia.

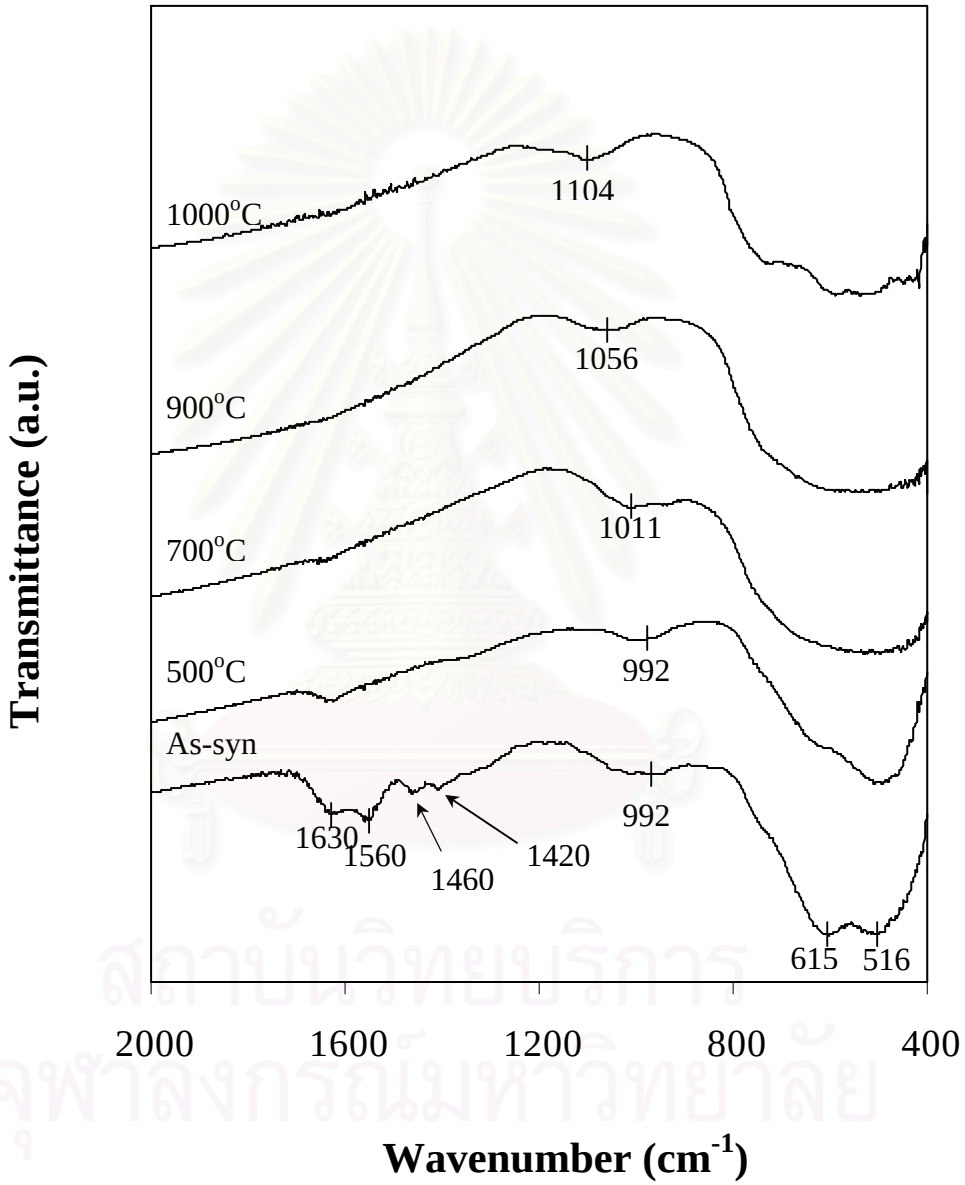

Figure 5.41 FTIR spectra of the product obtained by the reaction of zirconium *n*-propoxide and TEOS in 1,4-butanediol with the Si/Zr ratio of 0.02 and the samples obtained by calcination thereof at temperature specified in the figure.

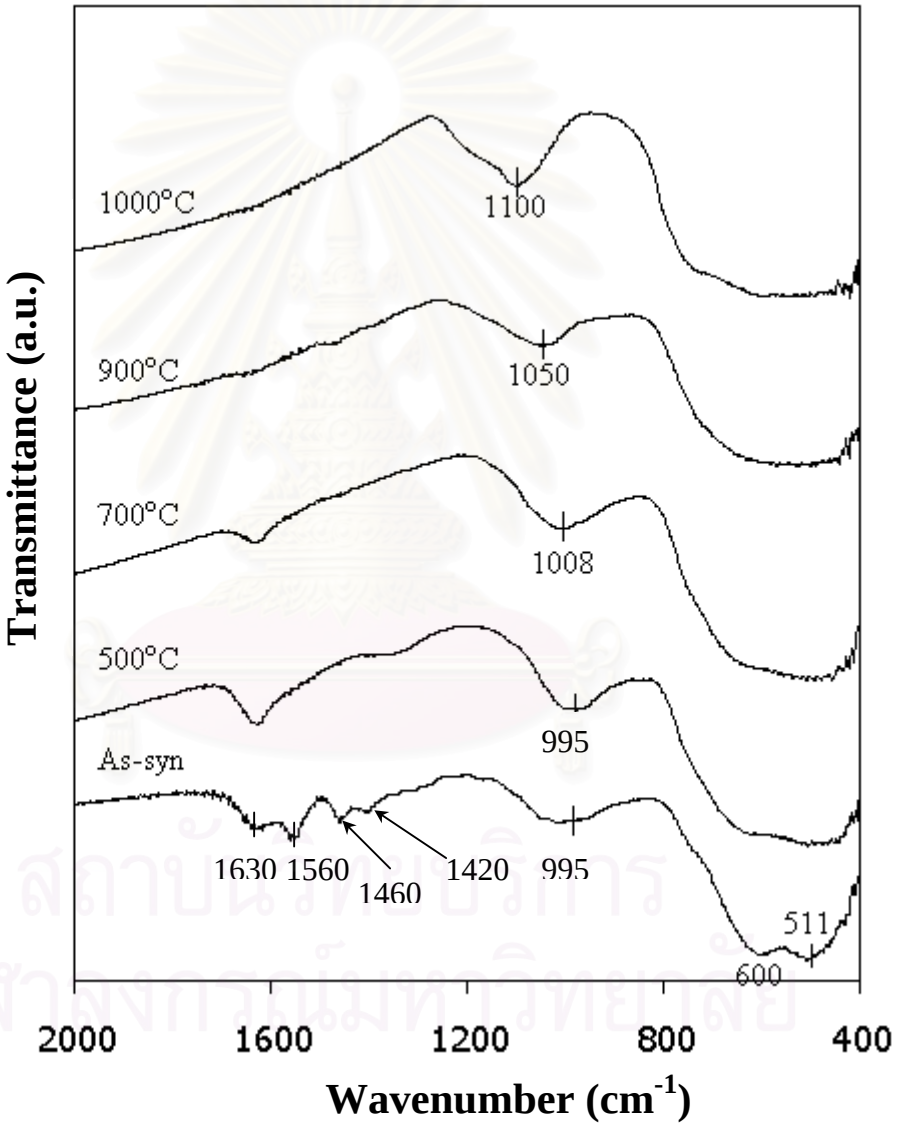

Figure 5.42 FTIR spectra of the product obtained by the reaction of zirconium *n*-propoxide and TEOS in 1,4-butanediol with the Si/Zr ratio of 0.04 and the samples obtained by calcination thereof at temperature specified in the figure.

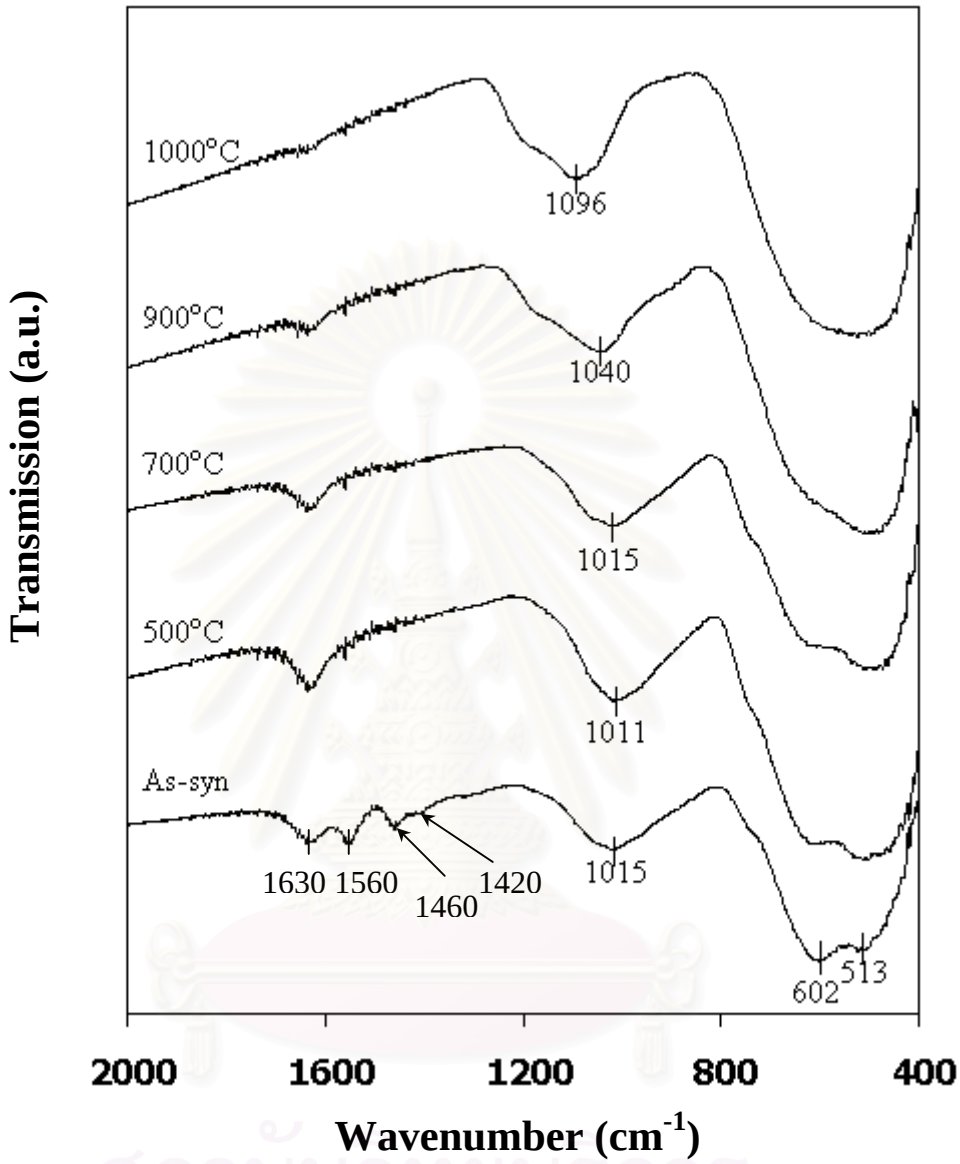

Figure 5.43 FTIR spectra of the products obtained by the reaction of zirconium *n*-propoxide and TEOS in 1,4-butanediol with the Si/Zr ratio 0.08 and the samples obtained by calcination thereof at temperature specified in the figure.

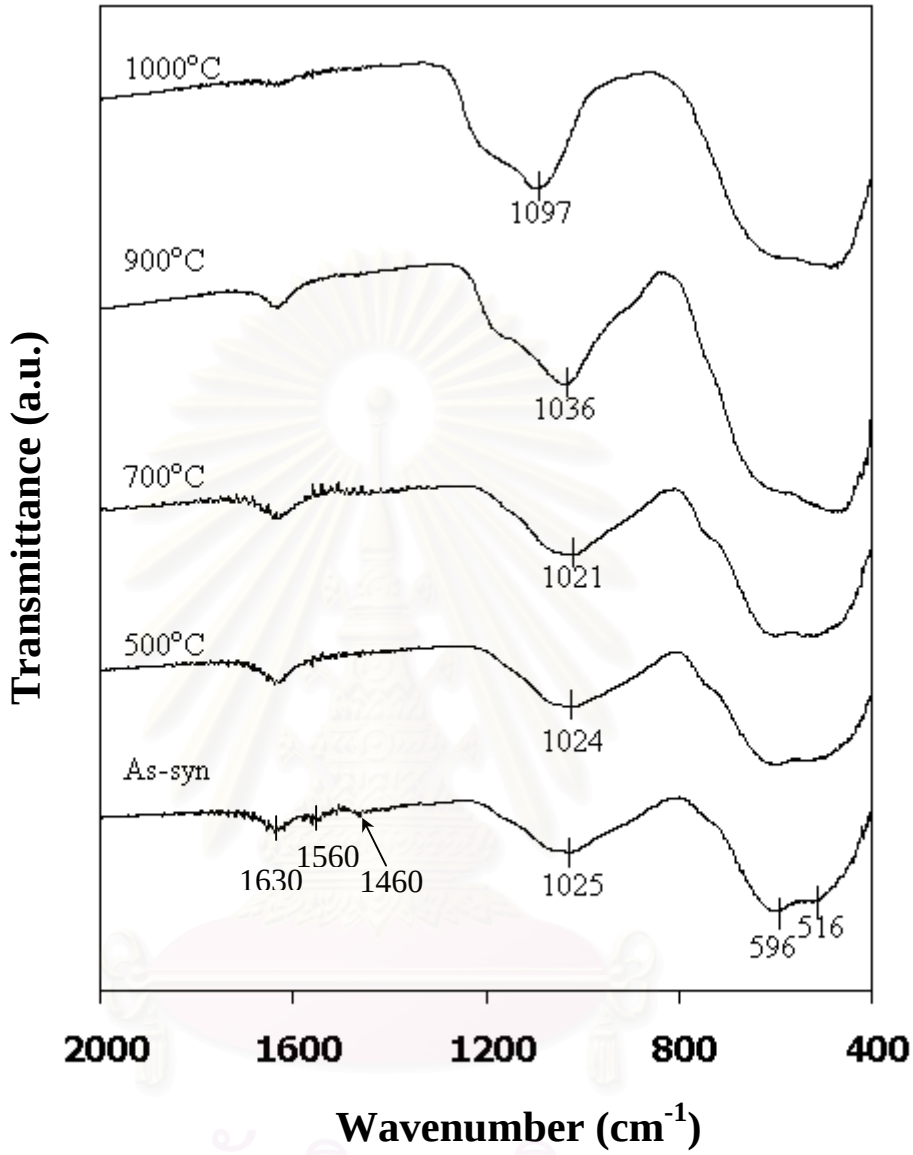

Figure 5.44 FTIR spectra of the products obtained by the reaction of zirconium *n*-propoxide and TEOS in 1,4-butanediol with the Si/Zr ratio 0.15 and the samples obtained by calcination thereof at temperature specified in the figure.

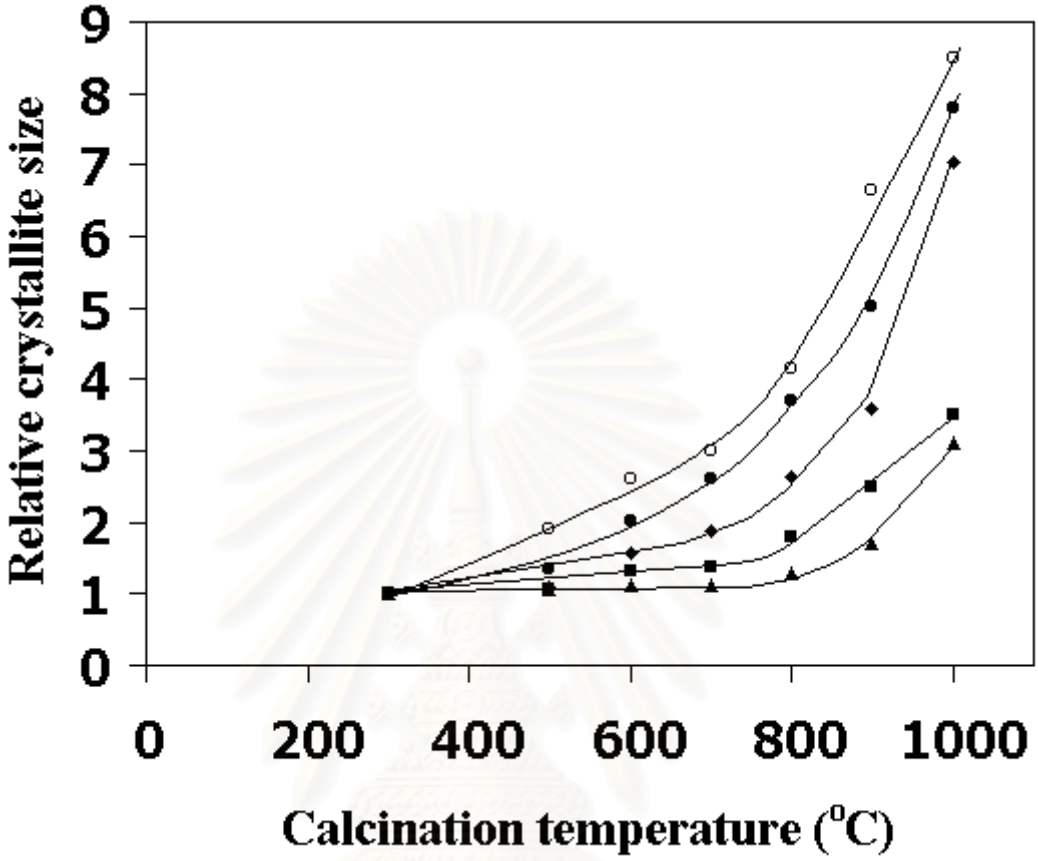

Figure 5.45 The variation of the relative crystallite size (the ratio of the crystallite size of the calcined sample to that of the as-synthesized sample) with the calcination temperature for the samples of (○) Si/Zr = 0, (●) Si/Zr = 0.02, (◆) Si/Zr = 0.04, (■) Si/Zr = 0.08, (▲) Si/Zr = 0.15

CHAPTER VI

CONCLUSIONS AND RECOMMENDATION

6.1 Conclusions

The reaction of zirconium tetra *n*-propoxide (ZNP) in glycols took place via several intermediate phases. Alkoxyl exchange reaction of ZNP with the glycol occurred at lower temperature yielding zirconium glycoxide. The reaction behavior depended on the carbon number (n) of the glycol; amorphous product (n = 2), crystalline glycol complex and subsequent transformation into tetragonal zirconia (n = 3 and 4) and directly zirconia (n = 5 and 6). Thermal decomposition of the crystalline glycol complex (phase A) took place yielding spherical particles of zirconia, while the zirconia directly crystallized from zirconium glycoxide was composed of irregularly-shaped particles. Based on the inductive effect (i.e., electron withdrawing effect) of the hydroxyl group, the formation of zirconia proceeds more easily with increasing carbon number of glycol because less unstable carbocation was formed when the carbon number of glycol increased. For the case of n = 4 and 5, neighboring group participation is predominant yielding oxonium ions which are more stable than primary carbocation.

Alkoxyl exchange reaction of ZNP with the amino alcohol took place at lower temperature yielding zirconium 2-aminoethoxide. High coordinating ability of the amino group with zirconium atom and inductive effect of the amino group inhibits the cleavage of C-O bonds so that the crystalline zirconia was not formed in 2-aminoethanol. Substitution of hydrogen of the NH_2 group of ethanol amine with the alkyl or hydroxyalkyl group decreases both the inductive effect and coordination ability of the amino group. Therefore, the cleavage of C-O bonds of these species took place yielding crystalline zirconia.

Synthesis conditions, i.e., ZNP concentration and drying method, affected the physical properties of zirconia. The use of 1,4-butanediol yielded the microspherical

secondary particle. The crystallite size, secondary particle size and BET surface area increased with increasing the ZNP concentration. Glycol removal at reaction temperature did not change the pore system of the powder because the aggregation of primary particles probably occurred during the reaction process. On the other hand, crystallite size, secondary particle size and BET surface area of zirconia obtained in 1,5-pentanediol were not affected by ZNP concentration, whereas the pore size of the powders was enlarged when the glycol was removed from autoclave by flash evaporation due to the reduction of aggregation among the ultrafine particles during drying by the ordinary method. The independence of zirconia crystallite size on ZNP concentration is due to the rapid nucleation in 1,5-PeG leading to an excess of nuclei and thereby reducing the glycoxide concentration that is required for crystal growth. Therefore, increasing ZNP concentration only increases the numbers of nuclei present.

The modification of zirconia with silica was found to increase the BET surface area and thermal stability of zirconia. Tetragonal to monoclinic transformation temperature shifted toward higher temperatures. Moreover, the crystallite growth rate during calcination was decreased with an increase of the Si content. This is due to the formation of Si-O-Zr bonds in the samples during the glycothermal reaction.

6.2 Recommendation for future study

From the previous conclusions, the following recommendations for future studies are proposed.

1. In some experiments i.e., the reaction of ZNP in 1,5-pentanediol and in *N*-methylethanolamine, the monoclinic zirconia was formed in addition to tetragonal phase. This should be investigated further in detail to find the reason of the monoclinic phase formation.

2. In this work, we found that the unidentified crystalline phase was the crystalline glycol complex. However, the chemical structure of this phase has not been clarified. Therefore, this should be studied for the future work.

3. The needle-like particles were found in the samples obtained in 1,4-BG at 280^{o}C for 0 h and 1 h, it should be examined how these particles participate in the crystallization mechanism of zirconia.

4. Zirconia prepared with a low ZNP concentration in 1,4-BG preserved tetragonal phase after calcination but the BET surface area is lower than the product obtained in relatively high concentration, which transformed to the monoclinic phase. It should be examined the reason for preservation of surface area in the smaller particles prepared with low ZNP concentration.

5. For the silica-modified zirconia samples, investigation of ^{29}Si NMR should be done to study silicon environments in the samples.

6. Prepare the silica-modified zirconia in 1,5-PeG

REFERENCES

Afanasiev, P.; Geantet, C.; Breysse, M. Role of oxoanions in the stabilization of tetragonal zirconia. J. Mater. Chem. 4 (1994): 1653-1657.

Aguilar, D. H., Torres-Gonzalez, L. C.; Torres-Martinez, L. M.; Lopez, T.; Quintana, P. A study of the crystallization of ZrO_2 in the sol-gel system: ZrO_2-SiO_2. J. Solid State Chem. 158 (2000): 349-357.

Amenomiya, Y. Methanol syntheses from CO_2+H_2. 2. copper-based binary and ternary catalysts. Appl. Catal. 30 (1987): 57-68.

Anderson, J. A.; Fergusson, C. A. Surface and bulk properties of silica-zirconia mixed-oxides: acid vs base catalysed condensation. J. Non-Cryst. Solids 246 (1999): 177-188.

Aronne, A.; Marotta, A.; Pernice, P.; Catanro, M.; Sol-gel processing and crystallization of yttria-doped zirconia. Thermochim. Acta 275 (1996): 75-82.

Beck, H. P.; Kabila, C. The solubility of Fe, Cr and Nb in ZrO_2 and its effect on thermal dialtion and polymorphic transition. Mater. Res. Bull. 25 (1990): 1161-1168.

Bedio, A. F.; Klabunde K. J. Synthesis of high surface area zirconia aerogels using high temperature supercritical drying. Nanostruc. Mater. 8 (1997): 119-135.

Beghi, M.; Chiurlo P.; Costa, L.; Palladino, M.; Pirini, M. F. Structural investigation of the silica titania gel glass-transition. J. Non-Cryst. Solids 145 (1992): 175-179.

Bitter, J. H.; Sechan K.; Lercher, J. A. The state of zirconia-supported platinum catalysts for CO_2/CH_4 reforming. J. Catal. 171 (1997): 279-286.

Bosman, H. J. M.; Kruissink, E. C.; Van der Spoel, J.; Van der Brink, F. J. Characterization of the acid strength of SiO_2-ZrO_2 mixed oxides. J. Catal. 148 (1994): 660-672.

Brodsky, C. J.; Ko, E. I. Effect of supercritical drying temperature on the properties of zirconia, niobia and titania-silica aerogels. J. Non-Cryst. Solids 186 (1995): 88-95.

Bruce, L.; Mathews, J. F. The Fischer-Tropsch activity of nickel-zirconia. Appl. Catal. 4 (1982): 353-369.

Bucko M. M.; Haberko, K. Crystallization of zirconia under glycothermal conditions. J. Am. Ceram. Soc. 78 (1995): 3397-3400.

Centi, G.; Cerrato, G.; Angelo, S. D.; Finardi, U.; Giamello, E.; Morterra, C.; Perathoner, S. Catalytic behavior and nature of active sites in copper-on-zirconia catalysts for the decomposition of N_2O. Catal. Today 27 (1996): 265-270.

Chang, H. L.; Shady, P.; Effect of sodium on crystallite size and surface area of zirconia powders at elevated temperatures. J. Am. Ceram. Soc. 83 (2000): 2055-2061.

Cheng, H. M.; Wu, L. J.; Ma, J. M.; Zhang, Z. Y.; Qi, L. M. The effects of pH and alkaline earth ions on the formation of nanosized zirconia phases under hydrothermal conditions. J. Europ. Ceram. Soc 19 (1999): 1675-1681.

Chuah, G. K.; Jaenicke, S.; Cheong S. A.; Chan K. S. The influence of preparation conditions on the surface area of zirconia. Appl. Catal. A: General 145(1996): 267-284.

Chuah, G. K.; Pong, B. K. The preparation of high-surface-area zirconia - II. Influence of precipitating agent and digestion on the morphology and microstructure of hydrous zirconia. J. Catal. 175 (1998): 80-92.

Chuah, G. K. An investigation into the preparation of high surface area zirconia. Catal. Today. 49 (1999): 131-139.

Contescu, C.; Popa, V. T.; Miller, J. B.; Ko, E. I.; Schwarz, J. A. Proton affinity distributions of TiO_2-SiO_2 and ZrO_2-SiO_2 mixed oxides and their relationship to catalyst activities for 1-butene isomerization. J. Catal. 157 (1995): 244-258.

Cormack, A.N.; Parker, S.C. Some observation on the role of dopants in phase-transition in zirconia from atomistic simulations. J. Am. Ceram. Soc. 73 (1990): 3220-3224.

Dell'Agli, G.; Colantuono, A.; Mascolo, G. The Effect of mineralizers on the crystallization of zirconia gel under hydrothermal conditions. Solid State Ionics 123 (1999): 87-94.

Dell'Agli, G.; Mascolo G. Low temperature hydrothermal synthesis of ZrO_2-CaO solid solutions. J. Mater. Sci. 35 (2000): 661-665.

del Monte, F. D.; Larsen, W.; Mackenzie, J. D. Chemical interactions promoting the ZrO_2 tetragonal stabilization in ZrO_2-SiO_2 binary oxides. J. Am. Ceram. Soc. 83 (2000): 1506-1512

del Monte, F. D.; Larsen, W.; Mackenzie, J. D. Stabilization of tetragonal ZrO_2 in ZrO_2-SiO_2 binary oxides. J. Am. Ceram. Soc., 83 (2000): 628-634.

Denkewicz, R. P.; TenHuisen, K. S.; Adair, J. H. Hydrothermal crystallization kinetics of meta-ZrO_2 and t-ZrO_2. J. Mater. Res. 5 (1990): 2698-2705.

Domen, K.; Kondo, J.; Maruya, K.; Onishi, T. Infrared studies of ethane hydrogenation over ZrO_2. Catal. Lett. 12 (1992): 127-138.

Dow, W. P.; Huang, T. J. Effect of oxygen vacancy of yttria-stabilized zirconia support on carbon monoxide oxidation over copper catalyst. J. Catal. 147 (1994): 322-332.

Feng, Z,; Postula, W. S.; Erkey C.; Phillip, C. V.; Akgerman, A.; Anthony. R. G. Selective formation of isobutane and isobutene from synthesis gas over zirconia catalysts prepared by a modified sol-gel method. J. Catal. 148 (1994): 84-90.

Fontana, A.; Moser, E.; Rossi, F. Campostrini, R.; Carturan, G. Structure and dynamics of hydrogenated silica xerogel by Raman and Brillouin scattering. J. Non-Cryst. Solids 212 (1997): 292-298.

Frankin, R.; Goulding, P.; Haviland, J.; Joyner, R. W.; McAlpine, I.; Moles, P.; Norman, C.; Norwell, T. Stabilization and catalytic properties of high surface area zirconia. Catal. Today 10 (1991): 405-407.

Fujii, H.; Mizuno, N.; Misono, M. Pronounced catalytic activity of LA_1-$XSRXCOO_3$ highly dispersed on ZrO_2 for complete oxidation of propane. Chem. Lett. 11 (1987): 2147-2150.

Gavalas, G. R.; Phichitkul, C.; Voecks, G. E. Structure and activity of NiO/alpha-Al_2O_3 and NiO/ZrO_2 calcined at high-temperatures.1. Structure. J. Catal. 88 (1984): 54-64.

Garvie, R. C. Stabilization of tetragonal structure in zirconia microcrystals J. Phys. Chem. 82 (1978): 218-224.

Gopalan, R.; Chang, C. H.; Lin, Y. S. Thermal stability improvement on pore and phase structure of sol-gel derived zirconia. J. Mater. Sci. 30 (1995): 3075-3081.

Gregg, S. J.; Sing, K. S. W. Adsorption, surface area and porosity, 2nd ed., Academic Press, London, 1982.

Heuer, A. H. Transformation Toughening in ZrO_2-containing Ceramics. J. Am. Ceram. Soc. 70 (1987): 689-98.

He, M.Y.; Ekerdt, J.G. Infrared studies of the adsorption of synthesis gas on zirconium dioxide. J. Catal. 87 (1984): 381-388.

Inoue, M.; Tanino, H.; Kondo, Y.; Inui, T. Formation of microcrystalline alpha-alumina by glycothermal treatment of gibbsite. J. Am. Ceram. Soc. 72 (1989): 352-353.

Inoue, M.; Otsu, H.; Kominami, H.; Inui, T. Synthesis of yttrium-aluminum-garnet by the glycothermal method. J. Am. Ceram Soc. 74 (1991): 1452-1454.

Inoue, M.; Kominami, H.; Inui, T. Novel synthetic method for the catalytic use of thermally stable zirconia. thermal-decomposition of zirconium alkoxides in organic media. Appl. Catal. A: General 97 (1993): L25-L30.

Inoue, M.; Kominami, H.; Inui T. Novel synthesis method for thermally stable monoclinic zirconia: hydrolysis of zirconium alkoxides at high-temperatures with a limited amount of water dissolved in inert organic-solvent from the gas-phase. Appl. Catal A: General 121 (1995): L1-L5.

Inoue, M.; Otsu, H.; Kominami, H.; Inui, T. Glycothermal synthesis of rare-earth aluminum garnets. J. Alloys Comp. 226 (1995): 146-151.

Inoue, M.; Nishikawa, T.; Otsu, H.; Kominami, H.; Inui, T. Synthesis of rare-earth gallium garnets by the glycothermal method. J. Am. Ceram. Soc. 81 (1998) 1173-1183.

Inoue, M. Mechanisms for the glycothermal syntheis of mixed oxides. Adv. Sci. Technol. 29 (2000): 855-862.

Inoue, M.; Sato, K.; Nakamura, T.; Inui, T. Glycothermal synthesis of zirconia-rare earth oxide solid solutions. Cat. Lett. 65 (2000): 79-83.

Iwamoto, S.; Tanakulrungsank, W.; Inoue, M.; Kagawa, K.; Praserthdam, P. Synthesis of large-surface area silica-modified titania ultrfine particles by the glycothermal method. J. Mater. Sci. Lett. 19 (2000): 1439 –1443.

Jackson, N. B.; Ekerdt, J. G. Isotope studies of the effect of acid sites on the reactions of C-3 intermediates during isosynthesis over zirconium dioxide and modified zirconium dioxide. J. Catal. 126 (1990): 46-56.

Lee, S. W.; Condrate R. A. The infrared and Raman spectra of SiO_2-ZrO_2 glasses prepared by a sol-gel process. J. Mater. Res. 23 (1988): 2951-2959.

Li, P.; Chen, I. W.; Effect of dopants on zirconia stabilization- An X-ray absorption study: I, Trivalent dopants. J. Am. Ceram. Soc. 77 (1994) 118-128.

Lide, D. R. Handbook of Chemistry and Physics, 81st ed., CRC Press, New York, 2000-2001.

Lin, J. D.; Duh, J. G. Coprecipitation and hydrothermal synthesis of ultrafine 5.5 mol% CeO_2-2 mol% $YO_{1.5}$-ZrO_2 powders. J. Am. Ceram. Soc. 80 (1997): 92-98

Liu, D. W.; Perry, C. H.; Ingel, R. P. Infrared-spectra in nonstoichiometric yttria-stabilized zirconia mixed-crystals at elevated-temperature. J. Appl. Phys. 64 (1988): 1413-1417.

Livage, J.; Doi, K.; Mazieres, C. Nature and thermal evolution of amorphous hydrated zirconium oxide. J. Am. Ceram. Soc. 51 (1968): 349-53.

Matsui, K.; Ohgai, M. Formation mechanism of hydrous-zirconia particles produced by hydrolysis of $ZrOCl_2$ solutions: I. J. Am. Ceram. Soc. 80 (1997): 1949-1956.

Matsui, K.; Ohgai, M. Formation mechanism of hydrous-zirconia particles produced by hydrolysis of $ZrOCl_2$ solutions: II. J. Am. Ceram. Soc. 83 (2000): 1386-1392.

Meijer, A. C. Q. M.; Jong, A. M. D.; Gruijthuijsen, L. M. P.; Niemantsverdriet, J. W. Preparation of zirconium-oxide on silica and characterization by X-ray photoelectron-spectroscopy, secondary ion mass-spectrometry, temperature programmed oxidation and infrared-spectroscopy. Appl. Catal. 70 (1991): 53-71.

Mercera, P. D. L.; Van Ommen, J. G.; Doesburg, E. B. M.; Burggraaf, A. J.; Ross, J.R.H. Zirconia as a support for catalysts: Evoluation of the texture and structure on calcination in air, Appl. Catal. 57 (1990): 127-148.

Mercera, P. D. L.; Van Ommen, J. G.; Doesburg, E. B. M.; Burgraaf, A. J.; Ross, J. R. H. Zirconia as a support for catalysts: Influence of additives on the thermal stability of the porous texture of monoclinic zirconia. Appl. Catal. 71 (1991): 363-391.

Mercera, P. D. L.; Van Ommen, J. G.; Doesburg, E. B. M.; Burgraaf, A. J.; Ross, J. R. H. Stabilized tetragonal zirconium oxide as a support for catalysts. Appl. Catal. 78 (1991): 79-96.

Miller, J. B.; Rankin, S. E.; Ko, E. I. Strategies in controlling the homogeneity of zirconia silica-aerogels-effect of preparation on textural and catalytic properties. J. Catal. 148 (1994): 673-682.

Miller, T. M.; Grassian, V. H. Environmental catalysis-adsorption and decomposition of nitrous-oxide on zirconia. J. Am. Chem. Soc. 117 (1995): 10969-10975.

Mitsuhashi, T.; Ichihara, M.; Tatsuke, U. Characterization and stabilization of metastable ZrO_2. J. Am. Ceram. Soc. 57 (1974): 97-101.

Morrison and Boyd, Organic Chemistry, Prentice-Hall, New Jersey, 1992.

Morterra, C.; Gerrato, G.; Ferroni, L.; Montararo, L. Surface characterization of yttria-stabilized tetragonal ZrO_2 .1. Structural, morphological, and surface hydration features. Mater. Chem. Phys. 37 (1994): 243-257.

Mottet, B.; Pichavant, M.; Beny, J. M.; Alary, J. A. Morphology of zirconia synthesized hydrothermally from zirconium oxychloride. J. Am. Ceram. Soc. 75 (1992): 2515-2519.

Nakano, Y.; Yamaguchi, T.; Tanabe, K. Hydrogenation of conjugated dienes over ZrO_2 by H_2 and cyclohexadiene. J. Catal. 80 (1983): 307-312.

Nishizawa, H.; Yamasaki, N.; Matsuoka, K. Crystallization and transformation of zirconia under hydrothermal conditions. J. Am. Ceram. Soc. 65 (1982): 343-346.

Norman, C. J.; Goulding, P. A.; McAlpine, I. Role of anions in the surface-area stabilization of zirconia. Catal. Today 20 (1994): 313-322.

Osendi, M. I.; Moya, J. S.; Sena, C. J.; Soria, J. Metastability of tetragonal zirconia powders. J. Am. Ceram. Soc. 68 (1985): 135-39.

Othmer, K., Encyclopedia of Chemical technology, 3rd ed., Wiley-interscience Publication, John Wiley & Sons (1978)

Prokhorenko, E. V.; Pavlenko, N. V.; Golodets, G. I. Effect of the nature of the support on the catalytic properties of cobalt and nickel-catalysis in the reaction of hydrogenation of carbon-monoxide. Kinet. Catal. (English Trans). 29 (1988): 702-706.

Pyda, W.; Haberko, K.; Bucko, M. M. Hydrothermal crystallization of zirconia and zirconia solid solutions. J. Am. Ceram. Soc. 74 (1991): 2622-2629.

Sato, S.; Takahashi, R.; Sodesawa, T.; Tanaka, S.; Oguma, K.; Ogura, K. High-surface-area SiO_2-ZrO_2 prepared by depositing silica on zirconia in aqueous ammonia solution. J. Catal. 196 (2000): 190-194.

Smith, M. B.; March, J. MARCH'S Advanced organic chemistry: reaction, mechanisms, and structure, John Wiley&Sons, Toronto (2001).

Sohn J. R.; Jang H. J. Characterization of ZrO_2-SiO_2 unmodified or modified with H_2SO_4 and acid catalysis. J. Mol. Catal. 64 (1991) 349-360.

Soled, S.; McVicker, G. B. Acidity of silica-substituted zirconia. Catal. Today 14 (1992): 189-194.

Srinivasan, R.; Harris, M. B.; Simpson, S. F.; De Angelis, R. J.; Davis, B. H. Zirconium-oxide crystal phase - The role of the pH and time to attain the final pH for precipitation of the hydrous zirconia. J. Mater. Res. 3 (1988): 787-797.

Srinivasan, R.; De Angelis, R. J.; Ice, G.; Davis, B. H. Critical particle-size and phase transformation in zirconia - Transmission-electron microscopy and X-ray-diffraction studies. J. Am. Ceram. Soc., 73 (1990): 3528-3530.

Srinivasan, R.; Taulbee, D.; Davis, B. H. The effect of sulfate on the crystal-structure of zirconia. Catal. Lett. 9 (1991): 1-8.

Tanabe, K. Surface and catalytic properties of ZrO_2. Mater. Chem. Phys. 13 (1985): 347-364.

Tani, E.; Yoshimura, M.; Somiya, S. Hydrothermal preparation of ultrafine monoclinic ZrO_2 powder. J. Am. Ceram. Soc. 64 (1981): C-181.

Tani, E.; Yoshimura, M.; Somiya, S. Formation of ultrafine tetragonal ZrO_2 powder under hydrothermal conditions. J. Am. Ceram. Soc. 66 (1982): 11-14.

Tijburg, I. I. M.; Geus, J. W.; Zandbergen, H. W. Application of lanthanum to pseudo-boehmite and gamma-Al_2O_3. J. Mater. Sci. 26 (1991): 6479-6486.

Valigi, M.; Gazzoli, D.; Dragone, R.; Marucci, A.; Mattei, G. Manganese oxide zirconium oxide solid solutions. An X-ray diffraction, Raman spectroscopy, thermogravimetry and magnetic study. J. Mater. Chem. 6 (1996): 403-408.

Wang, S. W.; Huang, X. X.; Guo, J. K. Wet chemical synthesis of ZrO_2-SiO_2 composite powders. J. Europ. Ceram. Soc. 16 (1996): 1057-1061.

West, A. R.; Solid State Chemistry and its Application, John Wiley&Sons, Brisbane, 1997.

Yoshimura, M.; Somiya, S. Hydrothermal synthesis of crystallized nano-particles of rare earth-doped zirconia and hafnia. Mater. Chem. Phys.61 (1999): 1-8.

Zhan, Z. Q.; Zeng, H. C. A catalyst-free approach for sol-gel synthesis of highly mixed ZrO_2-SiO_2 oxides. J. Non-Cryst. Solids 243 (1999): 26-38.

Zhang, L.; Weijie, J.; Dong, L.; Chen, Y. Effect of supported Na^+ ions on the texture properties of ZrO_2. J. Solid State Chem. 138 (1998): 41-46.

Zhu, W. Z.; Yan, H. Stability of tetragonal in ZrO_2 (2 mol % Y_2O_3) ceramics sintered in reducing atmosphere. J. Mater. Sci. lett. 16 (1997): 1540-1543.

APPENDICES

APPENDIX A

CALCULATION OF THE AMOUNT OF THE REAGENT REQUIRED FOR THE REACTION

In this study, silica-modified zirconia with various molar ratios were prepared using 1,4-butanediol as the solvent, and therefore detailed calculation procedure is given here.

Calculation of the amount of TEOS for silica-modified zirconia preparation

Zirconium tetra *n*-propoxide (ZNP) and tetraethyl orthosilicate (TEOS) are used as the reactants to prepare silica-modified zirconia.

1. Zirconium *n*-propoxide [$Zr(OC_3H_7)_4$] has a molecular weight of 327.57 g/mol.
   Zirconium, Zr, has an atomic weight of 91.22 g/mol.
2. Tetraethyl orthosilicate [$(C_2H_5O)_4Si$] has a molecular weight of 208.33 g/mol
   Silicon, Si, has an atomic weight of 28.0855 g/mol.

Example: Calculation of preparation of silica-modified zirconia with the molar ratio Si/Zr of 0.08 are as follows:

Fifteen gram of zirconium *n*-propoxide was used for the preparation of silica-modified zirconia with a molar ratio Si/Zr of 0.08.

Zirconium *n*-propoxide 15 g was consisted of zirconium equal to:

Zirconium = 15/327.57 = 0.0458 mol

To get the product with molar ratio Si/Zr of 0.08;

Silicon = 0.08 x 0.0458 mol = 0.00366 mol

Tetraethyl orthosilicate reqired is equal to: 208.33 x 0.00366 = 0.7633 g

APPENDIX B

CALCULATION OF THE CRYSTALLITE SIZE

Calculation of the crystallite size by Debye-Scherrer equation

The crystallite size was calculated from the half-height width of the diffraction peak of XRD pattern using the Debye-Scherrer equation.

From Scherrer equation:

$$D = \frac{K\lambda}{\beta \cos \theta} \qquad \text{(B.1)}$$

where D = Crystallite size, Å

K = Crystallite-shape factor = 0.9

λ = X-ray wavelength, 1.5418 Å for CuKα

θ = Observed peak angle, degree

β = X-ray diffraction broadening, radian

The X-ray diffraction broadening (β) is the pure width of a powder diffraction free from all broadening due to the experimental equipment. α-Alumina is used as a standard sample to observe the instrumental broadening since its crystallite size is larger than 2000 Å. The X-ray diffraction broadening (β) can be obtained by using Warren's formula.

From Warren's formula:

$$\beta = \sqrt{B_M^2 - B_S^2} \qquad \text{(B.2)}$$

Where B_M = The measured peak width in radians at half peak height.

B_S = The corresponding width of the standard material.

Example: Calculation of the crystallite size of zirconia

The half-height width of 111 diffraction peak = 1.83^o (from the figure B.1)

= $(2\pi x180)/360$

= 0.0319 radian

The corresponding half-height width of peak of α-alumina (from the Bs value at the 2θ of 30.3^o in figure B.2) = 0.0043 radian

The pure width, $\beta = \sqrt{B_M^2 - B_S^2}$

$= \sqrt{0.0319^2 - 0.0043^2}$

= 0.0316 radian

B = 0.0316 radian

2θ = 30.3^o

θ = 15.15^o

λ = 1.5418 Å

The crystallite size = $\frac{0.9x\ 1.5418}{0.0316\ \cos 15.15}$ = 45.49 Å

= 4.5 nm

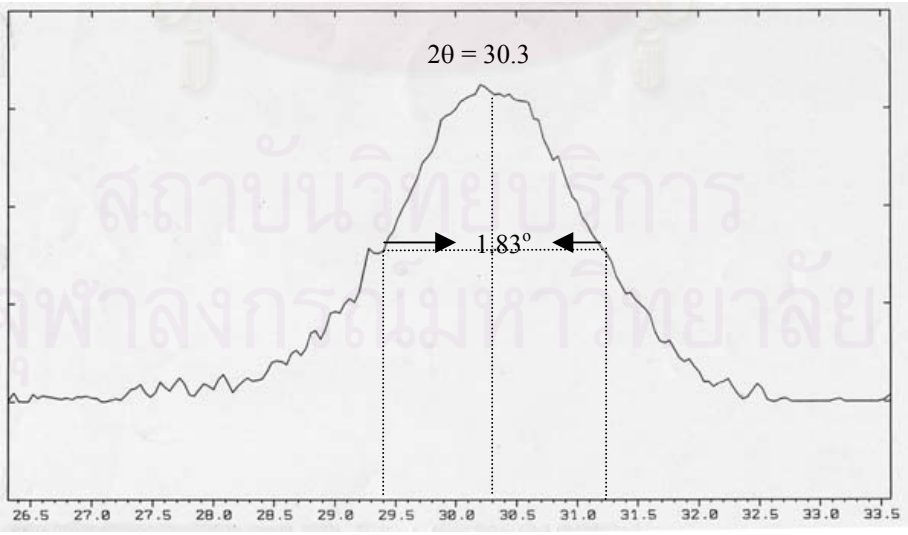

Figure B.1 The 111 diffraction peak of zirconia for calculation of the crystallite size

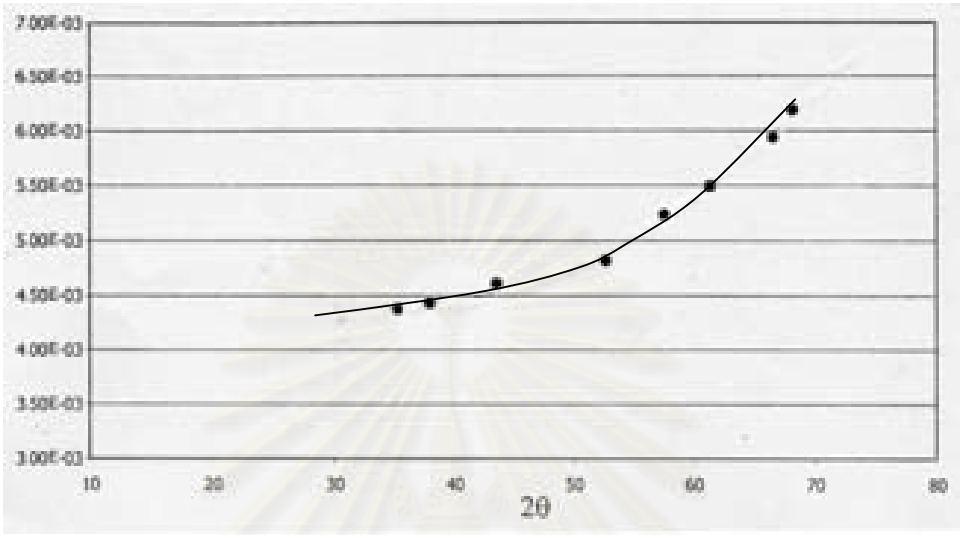

Figure B.2 The plot indicating the value of line broadening due to the equipment. The data were obtained by using α-alumina as a standard

APPENDIX C

CALCULATION OF BET SURFACE AREA BY THE SINGLE POINT METHOD

From Brunauer-Emmett-Teller (BET) equation:

$$\frac{X}{V(1-X)} = \frac{1}{VmC} + \frac{(C-1)X}{VmC} \qquad (C.1)$$

Where: X = relative partial pressure of N_2, P/P_o

P_o = saturated vapor pressure of N_2 (or adsorbed gas) at the experimental temperature

P = equilibrium vapor pressure of N_2

V = volume of gas adsorbed at a pressure P; ml at the NTP/ g of sample

V_m = volume of gas adsorbed at monolayer, ml. at the NTP / g of sample

C = constant

Assume $C \rightarrow \infty$, then

$$\frac{X}{V(1-X)} = \frac{X}{Vm} \qquad (C.2)$$

$$Vm = V(1-P/P_o)$$

From the gas law,

$$\frac{P_bV}{273} = \frac{P_tV}{T} \qquad (C.3)$$

Where: V = constant volume

P_b = pressure at 0 ^oC

P_t = pressure at t ^oC

$T = 273.15 + t, K$

$P_t = 1$ atm and thus, $P_b = (273.15 / T)$

Partial pressure of Nitrogen:

$$P = \frac{[\text{Flow of } (He+N_2) - \text{Flow of } He]}{\text{Flow of } (He+N_2)} \quad (C.4)$$

$$= 0.3 \text{ atm}$$

N_2 saturated vapor pressure, $P_o = 1.1$ atm

$$p = P / P_o = P / 1.1 = 0.3/1.1 = 0.2727$$

How to measure V

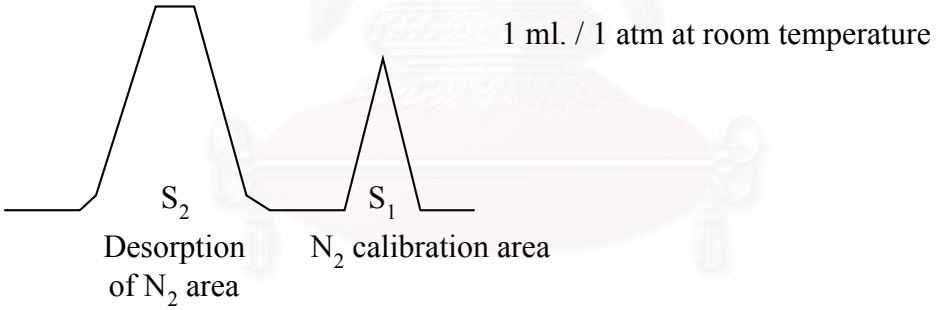

$$V = \frac{S_2}{S_1} \times \frac{1}{W} \times \frac{273.15}{T} \text{ ml. / g of catalyst} \quad (C.5)$$

Where, S_1 = Nitrogen 1 ml/1 atm of room temperature area

S_2 = Desorption of nitrogen area

W = Weight of the sample (g)

T = Room temperature (K)

Therefore,

$$Vm = \frac{S_2}{S_1} \times \frac{1}{W} \times \frac{273.15}{T} \times (1\text{-}p)$$

$$Vm = \frac{S_2}{S_1} \times \frac{1}{W} \times \frac{273.15}{T} \times 0.7273 \qquad (C.6)$$

Surface area of catalyst:

$$S = \frac{N\sigma V_m}{M}$$

Where, N = Avogadro number $= 6.02 \times 10^{23}$

σ = area occupied by one molecule of adsorbed nitrogen $= 16.2 \times 10^{-20}$

M = volume of one mole nitrogen = 22410 cm^3/mol

Then,

$$S = 4.352\ Vm$$

$$S = \frac{S_2}{S_1} \times \frac{1}{W} \times \frac{273.15}{T} \times 0.7273 \times 4.352$$

$$S = \frac{S_2}{S_1} \times \frac{1}{W} \times \frac{273.15}{T} \times 3.1582 \qquad (C.7)$$

APPENDIX D

LIST OF PUBLICATIONS

1. Sirarat Kongwudthiti, Piyasan Praserthdam, Waraporn Tanakulrungsank, Masashi Inoue, Synthesis of large-surface area silica-modified zirconia by the glycothermal method, Journal of Materials Science Letter 21 (2002): 1461-1464

2. Sirarat Kongwudthiti, Piyasan Praserthdam, Waraporn Tanakulrungsank, Masashi Inoue, The influence of Si-O-Zr bonds on the crystal-growth inhibition of zirconia prepared by the glycothermal method, Journal of Materials Processsing Technology 6737 (2003): 1-4

VITA

Miss Sirarat Kongwudthiti was born on October 29, 1978 in Bangkok, Thailand. She received the second-class honors of the Bachelor Degree of Chemical Engineering from Faculty of Engineering, Chulalongkorn University in March 1999. Then, she has continued study in Doctoral degree of Chemical Engineering at Chulalongkorn University since June 1999.